# Characteristics of Cloudiness over Indian Subcontinent and Adjoining Oceanic Region as revealed through Satellite Observations

Thesis Submitted to the
Cochin University of Science and Technology

in partial fulfillment of the requirements
for the award of the degree of

**DOCTOR OF PHILOSOPHY**
in
**Atmospheric Science**

By
**VIJAYKUMAR P**


**Department of Atmospheric Sciences**
**Cochin University of Science and Technology**
**COCHIN - 682 016**

*MARCH -2018*

# Certificate

This is to certify that the thesis entitled **"Characteristics of Cloudiness over Indian Subcontinent and Adjoining Oceanic Region as revealed through Satellite Observations"** is an authentic record of the research work carried out by **Mr. Vijaykumar P** under my supervision and guidance in the Department of Atmospheric Sciences, Cochin University of Science and Technology, in partial fulfilment of the requirements for the award of the degree of **Doctor of Philosophy in Atmospheric Science** and that no part of this work has previously formed the basis for the award of any degree, diploma or associateship in any University.

Kochi-682016
28th March 2018

**Dr. Santosh K.R**

# Declaration of Authorship

I hereby do declare that the thesis entitled "**Characteristics of Cloudiness over Indian Subcontinent and Adjoining Oceanic Region as revealed through Satellite Observations"** is a genuine record of research work done by me under the supervision and guidance of Dr. Santosh K R, Associate Professor, Department of Atmospheric Sciences, Cochin University of Science and Technology, in partial fulfilment of the requirements for the award of the degree of **Doctor of Philosophy in Atmospheric Science** and that no part of this work has previously formed the basis for the award of any degree, diploma or associateship in any University.

Kochi-682016

28h March 2018 **Vijaykumar P**

# Acknowledgements

First and foremost I express my sincere and deepest gratitude to my research guide Dr. Santosh K R for his motivation, moral support, and continuous encouragement throughout the course of this thesis work.

I am very much thankful to Sri. Baby Chakrapani, Head, Department of Atmospheric Sciences, for his valuable help and support. He allowed me to use all the facilities available in the department without any constraints.

I thank Prof. K Mohankumar, Director, Advanced Centre for Atmospheric Radar Research, CUSAT, who is also my doctoral committee member for providing all the encouragements and valuable suggestions throughout my research period.

I express my heartfelt gratitude and indebtedness to Dr. Abhilash S, Asst. Professor, Department of Atmospheric Sciences for providing me unconditional support and day to day guidance without which, this thesis may not have been possible. Above the feelings of gratitude, for reinstalling my faith in destiny, I owe to him.

I am thankful to Prof. Rammohan (Former Dean, Faculty of Marine Sciences) for his valuable suggestions, motivation and encouragements. I express my thankfulness to Prof. C A Babu (Former Head), Department of Atmospheric Sciences for providing all the necessary facilities, encouragement, support, and suggestions throughout the period of research.

I am grateful to Prof. C. K Rajan and Prof. P V Joseph for valuable suggestions and encouragements. I extend my thanks to Prof. A.N. Balchand, Dean, faculty of Marine Sciences, Dr. V Madhu, Dr. Ignetius Kunjumon, Dr. Satheeshan K, Dr. Lekshmi P.R and Dr. Midhun M, Department of Atmospheric

Sciences, Dr. R. Sajeev and Sri. P.K Saji, Department of Physical Oceanography, Dr. Padmakumar, Department of Marine Biology, Microbiology and Biochemistry, Dr. K.R Baiju and Dr. Ajayakumar P, Department of marine Geology and Geophysics and Dr. Sajeevan T P, NCAAH.

I am grateful to Prof. B.E. Mapes, University of Miami, USA for his valuable suggestions and critical corrections. I also extend my gratitude to C. Suvarchal Kumar and I-Kuan Hu, University of Miami, USA for co-authoring.

Many thanks are due to Dr. Sreedevi M G, for her support and encouragements at all occasions. I thank administrative staff of Dept. of Atmospheric Sciences, Sri. Rajesh B, Smt.Saraswathy NirmalaVarrier, Smt. Shila M and Sri.Selvakumar K K for providing me helps from time to time.

I thank my lab-mates, Dr. Anu Simon, Dr. Aype Thomas, Dr. Sabin T P, Dr. Johnson Zaccharia, Dr. Sivaprasad, Dr. Nithin Viswambharan, Dr. Jayakrishnan P R, Dr. Abheesh, Dr. Reshmi, Dr. Anila, Smt. Asha S Phillip, Dr. Smitha A, Smt. Smitha John and Sri. Baburaj for their company and cooperation.

I am grateful to the Research Scholars and M Sc. Students of Dept. of Atmospheric Sciences for their support and encouragements from time to time.

I extent my special thanks to Dr. Harisankar H.S for his lovely company and critical proof reading of this thesis. I thank my friends Sri. Sandeep V M, Dr. K KBaiju, Dr. Abhilash K R, Sri. Sumesh N V, Dr. Sandeepan B. S, Sri. Najeem Shajahan, Sri. Prasanth Varavoor, Sri. Amal Dev, Sri Sinaj Mani, Sri. Sajesh S, Sri. Reghunathan, Sri. Sajan K P, Dr. Prabhakaran M P, Sri. Satheesh T, Sri. Shinto Roose, Sri. Sherin Hassan and Dr. Liby Thomas, for their enormous support. My thanks are also due to Dr. Shaiju P, Dr. Gireeshkumar T R, Dr. Deepulal and Dr. Jayesh Puthumana.

I thankfully remember the love and care I received from *Late* Sri. Mathew Chettan in this occasion.

I thank Dr. Mridula G, Dr. T N Venkitesh and Dr. Arshad Shameem, National Aerospace Laboratory, Bangalore, Dr. K Rajeev, Space Physics Laboratory, VSSC, Dr. M R Ramesh Kumar and Dr. Syam Sankar, NIO Goa, for helping me during the starting stages of my research.

I thank Dr. Soma Senroy, India Meteorological Department, New Delhi who provided me training to process INSAT data sets.

I wish to thank Sri. V V Pushpangadan, Sri. Ashok Kumar Thekkan, Sri. S Sivaprasad, Sri. S K Suresh CEOs, Vegetable and Fruit Promotion Council Keralam where I worked as Project Associate for providing me permission and facilities for continuing my studies. My thanks are also due to Sri. Noushad P M, Sri. Sivakumar P J, Smt. Rani George, Smt. Kavitha S Nair, Smt. Sheena Rajagopal, Smt. Pavithra Sebastian, Smt. Beena G Menon, Smt. Sephy Joseph, Smt. Bindu P D and Dr. Susha, VFPCK, Kakkanad for encouragements and assistance.

My deepest gratitude goes to my achan, amma and two brothers and their families for their love and support throughout my life. I thank my *Late* grandparents for their prayers and love. Words fail to express my appreciation to my dear wife Dr. Dhanya K C and my two loving daughters for their love, care and support. I extend my heartfelt thanks to all my family members especially my sisters in law, brother in law and parents in law.

I express my sincere gratitude to Cochin University of Science and Technology for providing facilities for carrying out this work. The financial support from University Grants Commission of India is thankfully acknowledged.

INSAT data for the study is obtained from Satmet Division of India Meteorological Department, New Delhi and the Meteorological and Oceanographic Satellite Data Archival Centre (MOSDAC) of Indian Space Research Organization (ISRO).Gridded daily Rainfall data is obtained from India Meteorological Department. TRMM data sets have been provided by National Aeronautics and Space Administration (NASA), NCEP Reanalysis Derived data was provided by the NOAA/OAR/ESRL PSD, Boulder, Colorado, USA. I thank all these institutions.

Above all, I bow my head before God almighty for keeping in me the hope to complete the work successfully.

*Dedicated to my Family, Teachers and God almighty....*

# *CONTENTS*

**Chapter-2**

**Data and Methods**



**Chapter-3**

**Distribution of Cloudiness and Categorization of Rainfall Types**

## ABBREVIATIONS

| | |
|---|---|
| AIRS | Atmospheric Infrared Sounder |
| AVHRR | Advanced Very High resolution Radiometer |
| BT | Brightness Temperature |
| CERES | Clouds & Earths Radiant Energy System |
| CH | Cloud High |
| CILR | Central Indian Land Region |
| CL | Cloud Low |
| CM | Cloud Medium |
| CSH-LH | Convective and Stratiform Latent Heating |
| CTBT | Cloud Top Brightness Temperature |
| CTT | Cloud Top Temperature |
| DMSP | Defence Meteorological Satellite Program |
| DV | Diurnal Variation |
| EASWCI | Eastern Arabian Sea and West Coast of India |
| ECZ | Enhanced Cloud Zone |
| ENSO | El Niño-Southern Oscillation |
| ESA | European Space Agency |
| FRC | Fraction of Rain Contributed |
| GMS | Geostationary Meteorological Satellites |
| GMT | Greenwich Mean Time |

| | |
|---|---|
| GOES | Geostationary Operational Environmental Satellite system |
| GOES-E | Geostationary Operational Environmental Satellite system East |
| GOES-W | Geostationary Operational Environmental Satellite system West |
| GOMS | Geostationary Operational Meteorological Satellite |
| GPM | Global Precipitation Measurement Mission |
| GSM | Geostationary Meteorological Satellite |
| HBOB | Head Bay of Bengal |
| IMD | India Meteorological Department |
| IMERG | Integrated Multi SatellitE Retrievals for GPM |
| INSAT | Indian National Satellite |
| INSAT VHRR IR | Indian National Satellite Very high resolution radiometer Infra Red |
| IR | Infra Red |
| IRBT | Infra Red Brightness Temperature |
| ISCCP | International Satellite Cloud Climatology Project |
| ISMR | Indian Summer Monsoon Rainfall |
| ISO's | Intra Seasonal Oscillations |

| | |
|---|---|
| ISRO | Indian Space Research Organisation |
| ITCZ | Inter Tropical Convergence Zone |
| JAXA | Japan Aerospace Exploration Agency |
| JJAS | June July August September |
| LH | Latent Heat |
| LHR | Latent heating rate |
| LPA | Long period average |
| LSI | Lightning Imaging Sensor |
| LST | Local Standard Time |
| MAM | March April May |
| MCZ | Maximum Cloud Zone |
| MODIS | Moderate Resolution Imaging Spectroradiometer |
| MOSDAC | Meteorological and Oceanographic Satellite Data Archival Centre |
| MTC | Mid Tropospheric Cyclones |
| MTSAT | Multifunctional Transport Satellites |
| NASDA | National Space Development Agency of Japan |
| NCAR | National Centre for Atmospheric Research |
| NCEP | National Centers for Environmental Prediction |
| NOAA | National Oceanic and Atmospheric Administration |

| | |
|---|---|
| NOAA-POES | National Oceanic and Atmospheric Administration Polar Orbiting Environmental Satellites Series |
| OLR | Outgoing Long Wave radiation |
| OND | October November December |
| ONI | Oceanic Niño Index |
| PR | Precipitation Radar |
| QPE | Quantitative precipitation estimates |
| Rfrq | Frequency of Occurrence of Extreme Rainfall Events |
| RMS | Root Mean Square |
| SAC | Space Application Centre |
| SEIO | Southeast Indian Ocean |
| SSM/I | Special Sensor Microwave Imager |
| SSMIS | Special Sensor Microwave Imager Sounder |
| SST | Sea Surface Temperature |
| SWIO | South West Indian Ocean |
| TCI | TRMM Combined Instrument |
| TIROS | Television and Infrared Satellite |
| TMI | TRMM Microwave Imager |
| TPRR | TRMM PR Rain Rate |
| TPW | Total Precipitable Water |

| | |
|---|---|
| TRMM | Tropical Rainfall Measuring Mission |
| TT | Temperature Threshold |
| TTL | Tropical Tropopause Layer |
| VHRR | Very High Resolution Radiometer |
| VIRS | Visible Infrared Scanner |
| VIS | Visible Wavelength |
| WCRP | World Climate Research Program |
| WMO | World Meteorological Organization |
| WV | Water Vapour |
| YOTC | Year of Tropical Convection |

# *Preface*

Clouds are condensed form of water in the atmosphere appearing in numerous varieties and shapes. Understanding the characteristics of clouds is highly significant because clouds produce precipitation and it plays a prominent role in modulating the climate by directly influencing the energy distributions within the earth's atmospheric system. Clouds can be better watched using satellites placed in outer space. Indian geostationary satellites have continuously monitored the sky for nearly three and a half decades but the INSAT data sets are yet to be explored in its full potential. Previous studies on cloud features over Indian region have mostly utilised coarse resolution outgoing long wave radiation (OLR) or rainfall data sets alone to quantify convection. This study extensively investigates the features of cloudiness over the Asian monsoon region using the rarely utilised high resolution hourly INSAT infrared brightness temperature (IRBT) data sets for 5 years.

The Thesis is divided into 7 Chapters. General introduction to the clouds, satellite observations, Indian summer monsoons and cloudiness over the Indian region is provided briefly in Chapter-1.Details of Data used and the general methods adopted for the analyses are provided in chapter-2. In Chapter-3, details of a primary work carried out using 2 years of 3 hourly IR-BT data sets for the purpose of deciphering the relation between rain types and cloud top temperature is provided. Regional differences in cloud-rain relationship are explored.The seasonal and intraseasonal relations of rainfall and associated cloudiness are examined in details in chapter-4. Heavy rainfall events during the Indian monsoon period form an insightful portion of the present study. Heavy rainfall events contribute more than 15% of the total

rainfall over the Northwest and central Indian region during monsoon season. The features of cloudiness during the Active and Break phases of monsoon and the spatio-temporal evolution of clouds during these phases are studied. This is perhaps the first study of its kind using infrared brightness temperature data. In this chapter, role of different types of clouds on the northward propagating Monsoon Intraseasonal Oscillations (MISO) is examined. Deep clouds mostly contribute to the north westward mode and shallow to high clouds show clear northward propagation features and both of them together determine the active and break phases of MISO over Central Indian region.

In Chapter-5, the diurnal variation of cloudiness over the Indian monsoon region during pre, summer and post monsoon season is investigated using hourly INSAT data for 5 years. Regional differences in diurnal patterns and associated cloud type distribution are analysed. This chapter mainly examined the role of different types of clouds and rain intensity classes in determining the amplitude and phases of the diurnal cycle of rainfall over many representative regions over South Asia. In chapter-6, an attempt has been made to examine the complex relationship between different phases of ElNino Southern Oscillation (ENSO) and cloud characteristics during Indian summer monsoon by using TRMM satellite derived multilevel products and hydrometeor profiles. This analysis reveals the distinct regional response of ESNO phases on the structure of heating and hydrometeor profiles. The summary and major conclusions of the thesis are presented in Chapter-7.

# *List of Figures*

# *List of Tables*

## Chapter -1

# Introduction

### 1.1 General introduction to clouds and importance of studying cloud features

Clouds are a visible mass of condensed water vapour floating in the atmosphere, typically high above the general level of the ground. Some clouds are found only at high elevations, whereas others nearly touch the ground. Clouds can be thick or thin, big or little – they exist in seemingly endless varieties of forms. They are a crucial part of the global hydrological cycle, redistributing water to earth's surface in the form of precipitation (e.g., Rogers and Yau, 1979; Pruppacher and Klett, 1980; Ramanathan *et al.,* 1989; Kiehl and Trenberth, 1997; Trenberth *et al.,* 2009). In addition, they are a key element for the global energy budget since they interact with both shortwave (solar) and long wave (terrestrial) radiation. These so-called cloud–radiation interactions depend strongly on the type of cloud. Clearly clouds affect the global climate and thus understanding clouds is an important factor for future climate projections. The effects on Earth's energy budget and on the hydrological cycle both depend on processes on the microphysical scale, encompassing the formation of cloud droplets, ice crystals, raindrops, snowflakes, graupel and hailstones.

At any given time, there exist three broad bands where Earth's skies are mostly cloudy: one narrow strip near to the equator and two wider strips in the mid-latitudes. The band near to the equator is a function of the large scale circulation patterns or Hadley cells present in the tropics. Hadley cells are

defined by cool air sinking near the 30 degree latitude line north and south of the equator and warm air rising from the lower levels from the equatorial region where winds from northern and southern hemispheric Hadley components converge. The warm, moist air that converges at lower altitudes near the equator cools when lifted upwards and become less efficient in holding the moisture. Consequently, water vapor condenses into cloud particles and produces a reliable band of thunderstorms in an area known as the Inter Tropical Convergence Zone (ITCZ). The location of the ITCZ has an annual cycle that follows the position of the Sun's zenith but is modulated largely by the distribution of land masses.

The other two bands of clouds are present in the middle latitudes 60 degrees north and south of the equator. This is the belt where the edges of polar and mid-latitude (or Ferrel) circulation cells collide and push air upward, fuelling the formation of the large-scale frontal systems that dominate weather patterns in the mid-latitudes. While clouds form where air rises as part of the atmospheric circulation patterns, descending air inhibits cloud formation. Since air descends between about 15 and 30 degrees north and south of the equator, clouds are rare and deserts are common over these latitudes.

Decades of satellite observations and astronaut photographs show that clouds dominate space-based views of Earth. There are several global cloud climatologies derived from satellite data available, known as satellite retrievals. One study (King *et al.,* 2013) based on nearly a decade of satellite data estimated that about 67% of Earth's surface is typically covered by clouds. According to Stubenrauch *et al.,* 2009, in the global annual average, roughly 70% of Earth's surface is covered with clouds. The cloud cover is 5%–15% higher over oceans than over land.

Clouds play a key role in regulating the planet's average temperature. Some clouds contribute to cooling by reflecting part of the Sun's incident energy or shortwave radiation back to space. Other clouds contribute to warming by acting like a blanket that traps energy emitted by Earth's surface and lower atmosphere (thermal energy or long wave radiation). Cloud systems also deals with evenly spreading the Sun's energy over the Earth's surface. Storms move across the planet and carry out the job of transporting energy from warm areas near the equator to cold areas near the poles. Even small changes in the abundance or location of clouds could produce changes in the climate much more significantly than the anticipated changes caused by greenhouse gases, human-produced aerosols, or other factors associated with global change.

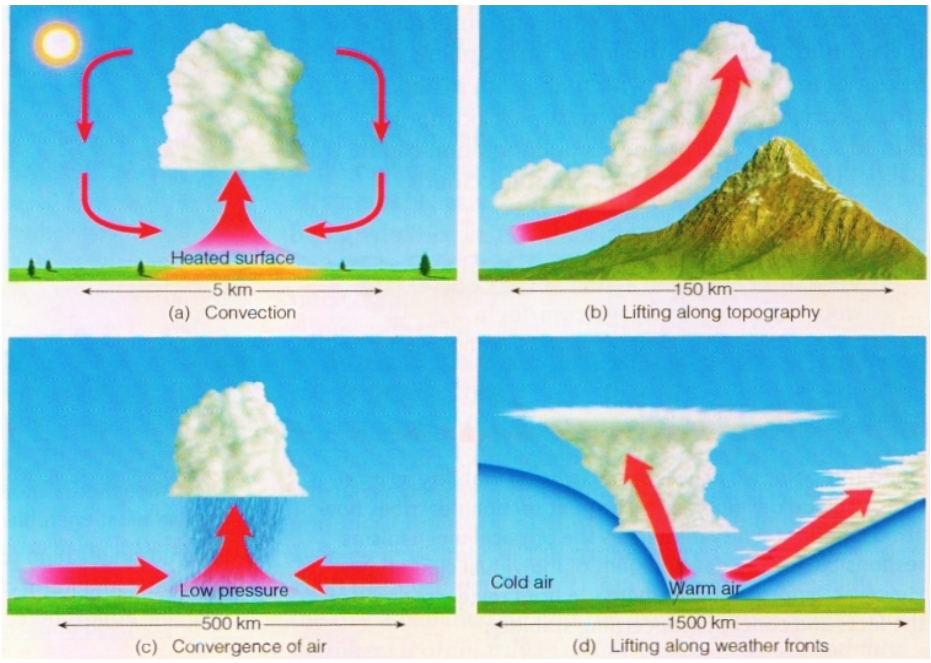


Figure 1.1. Primary mechanisms for the formation of clouds. Figure from Ahrens C Donald *Essentials of Meteorology An invitation to the Atmosphere (6th edition),* Brooks/Cole, Cengage Learning, 2008.

There are four primary of mechanisms for the formation of clouds, (a) surface heating and convection (b) convergence of surface air (c) forced lifting by topography and (d) lifting resulted by frontal interactions as illustrated in Figure 1.1.

## 1.2 Classification of clouds

Clouds are ever changing and appear in an infinite variety of forms. The classification of clouds is based on a book written by Luke Howard, a London pharmacist and amateur meteorologist, in 1803. His book, The Modifications of Clouds, named the various cloud structures he had studied. The terms he used were readily accepted by the meteorological community and are still used across the world today. The World Meteorological Organization (WMO) has extended Luke Howard's classifications to make 10 main groups of clouds, called *genera*. These are divided into three levels - cloud low (0 to ~2 km, CL), cloud medium ((~2 to ~8 km in the tropics, ~2 to ~7 km in the mid latitudes and ~2 to ~4 km in the high latitudes, CM) and cloud high (~8 to ~18 km in tropics, ~7 to ~13 km in mid-latitudes and ~4 to 8 km in high latitudes, CH) - according to the part of the atmosphere in which they are usually found. High clouds are named as Cirrus, Cirrocumulus and Cirrostratus, medium clouds are named as Altocumulus, Altostratus and Nimbostratus and the low clouds are named as Stratocumulus, Stratus, Cumulus and Cumulonimbus. These clouds are further subdivided to *species* and *varieties*. Among the above listed clouds, cumulonimbus clouds are regarded as vertically developing clouds (~500 m to the upper troposphere) which have a lower cloud base but under favourable conditions (like moisture availability, lower-level convergence, upper level divergence, atmospheric instability, and high value of convective available potential energy) they grow

to become giant clouds. The deep convective clouds are generally mixed phase clouds with lower part (below 5km in tropics) in liquid phase, middle part composed of a mixture of super cooled water droplets and ice crystals and the upper part (>8 km) almost completely in ice phase. These clouds play a crucial role in the transport of energy and moisture from the lower atmosphere to the upper troposphere and heating of the atmosphere through release of latent heat. They lead to the lifting of convective tropopause and largely modulate the characteristics of the tropical tropopause layer (TTL). These clouds play a major role in the global electrical circuit (Singh *et al.,* 2007) as well.

## 1.3 Satellite observations of clouds over the globe

Continuous synoptic survey of the state of the atmosphere over the entire globe can be achieved only by satellite observations. Operational weather satellite sensors have supplied data records extending nearly 4 decades. Whereas polar-orbiting cross-track scanning sensors generally provide daily global coverage only at particular local times of day, geostationary satellites are placed at particular longitudes along the equator and permit higher-frequency temporal sampling (15-min to 3-h intervals). The relevant passive satellite sensors measure radiation scattered or emitted by Earth's surface and by Earth's atmosphere including clouds. Visible light can be used to sense clouds from satellites because they reflect more solar radiation than ice free ocean or snow free land. While thickly cloudy sky appear dark watched from below, they instead appear bright in visual imageries taken from space. Sensors on board satellites which are used to identify clouds are called imagers. Both the movement and the structure of cloud systems can be studied using imageries. While visible light and its reflective properties help observing the clouds only during the day time, cloud

observation is possible both day and night through Infra-Red (IR) and water vapour (WV) channels. To maximize the sensitivity to the presence of clouds and to determine key cloud properties, specific spectral domains are exploited for particular retrieval methods.

The conversion of the measured radiances into cloud properties involve two steps, (1) cloud detection and (2) cloud property retrieval, often based on forward radiative transfer model computations and employing ancillary data to isolate the cloud radiative contributions from surface and non-cloud atmospheric contributions. Compared to the earth's surface, clouds usually appear brighter and colder. Cloudy scenes exhibit larger spatial and temporal radiative variability than cloud-free or so-called clear-sky scenes. There are occasions when it became difficult to distinguish cloud from earth's surface. If the radiance contrast is small between the cloud and the underlying surface (situations like clouds appear over highly solar reflecting surfaces such as snow or ice, clouds with small thermal contrast to the surface below as for low-level clouds in humid boundary layers over ocean, or cloud edges) and when clear-sky scene variability is larger than usual (for instance, optically thin clouds over heterogeneous land areas or clouds over winter land areas), cloud detection becomes challenging. (Stubenrauch *et al.,* 2012)

The first successful weather satellite was TIROS-1, launched by NASA on April1, 1960. Among the payloads that TIROS-1 carried were infrared detectors to measure the amount of heat radiated by the earth's surface and the clouds**.** Since then, a number of satellites have been flown into the space with various missions. Syncom 2 was the first geosynchronous communications satellite, though with an orbit that was inclined rather than geostationary launched by NASA on July 26, 1963. During the following decades several

satellite systems with different sensors provided data for a wide range of atmospheric parameters that enhanced our understanding of Earth-atmosphere processes and dynamics. Smith *et al.,* (1986) and Kidder and Vonder Haar (1995) give an overview of Earth-atmosphere observing satellite systems. More recently, Kidd et al., (2009), Thies and Jorg Bendix (2011) and Yang et al., (2013) outlined the status of satellite based meteorological and climatological research.

A number of national agencies and international collaborations have successfully launched and operated satellites for various purposes among them weather observations have always been in prime place. The major series of geosynchronous satellites which have enabled the observation of earth from space include satellites developed and operated by the United States' National Oceanic and Atmospheric Administration (NOAA) Geostationary Operational Environmental Satellite system (GOES), the European Space Agency's (ESA) METEOSAT, the Japanese Multifunctional Transport Satellites (MTSAT) which replaced the Geostationary Meteorological Satellites (GMS), the Chinese FY-2 and FY-4 series, the Russian Geostationary Operational Meteorological Satellite (GOMS)/Elektro series and the Indian Space Research Organisation's (ISRO), INSAT series of satellites. All these satellites carry specialised instruments on board which are operated in various spectral bands of visible, IR and water vapour channels.

Among the polar orbiting satellites which have revolutionised our understanding of the global cloud distribution are the National Oceanic and Atmospheric Administration Polar Orbiting Environmental Satellites Series (NOAA-POES) which provides the longest set of global observations employing Advanced Very High resolution Radiometer (AVHRR) operated in

different channels of Visible (VIS) and Infrared (IR) wavelengths, Defence Meteorological Satellite Program (DMSP) satellites since 1987 which carry on board Special Sensor Microwave Imager (SSM/I) and the Special Sensor Microwave Imager Sounder (SSMIS), International collaboration missions like Terra and Aqua the satellites which operates Moderate Resolution Imaging Spectroradiometer (MODIS) and Atmospheric Infrared Sounder (AIRS). Perhaps a single most important mission which has pushed the scientific world's perspectives and knowledge of tropical precipitation and sea surface temperature (SST) to miles ahead is a joint mission of NASA and the Japan Aerospace Exploration Agency namely the Tropical Rainfall Measuring Mission (TRMM) which carried specialised instruments on board including TRMM Microwave Imager (TMI) and Precipitation Radar (PR). TRMM provided the first high-quality rainfall and space-time structures of Latent Heat (LH) over the global Tropics and subtropics (Tao et al., 1996). (Seasonal average LH profiles for Indian region are provided in Figure 1.2).

Regarding Cloud observation projects in particular, the International Satellite Cloud Climatology Project (ISCCP) was established in 1982 as part of the World Climate Research Program (WCRP), a collaboration involving 10 institutions in five countries that collect and analyze the measurements from the international constellation of weather satellites to collect weather satellite radiance measurements and to analyze them to infer the global distribution of clouds, their properties, and their diurnal, seasonal and interannual variations. The resulting datasets and analysis products are being used to study the role of clouds in climate, both their effects on radiative energy exchanges and their role in the global water cycle. The ISCCP cloud datasets provided first systematic global view of cloud behaviour of the space and time scales of the weather (Rossow and Duenas, 2004).

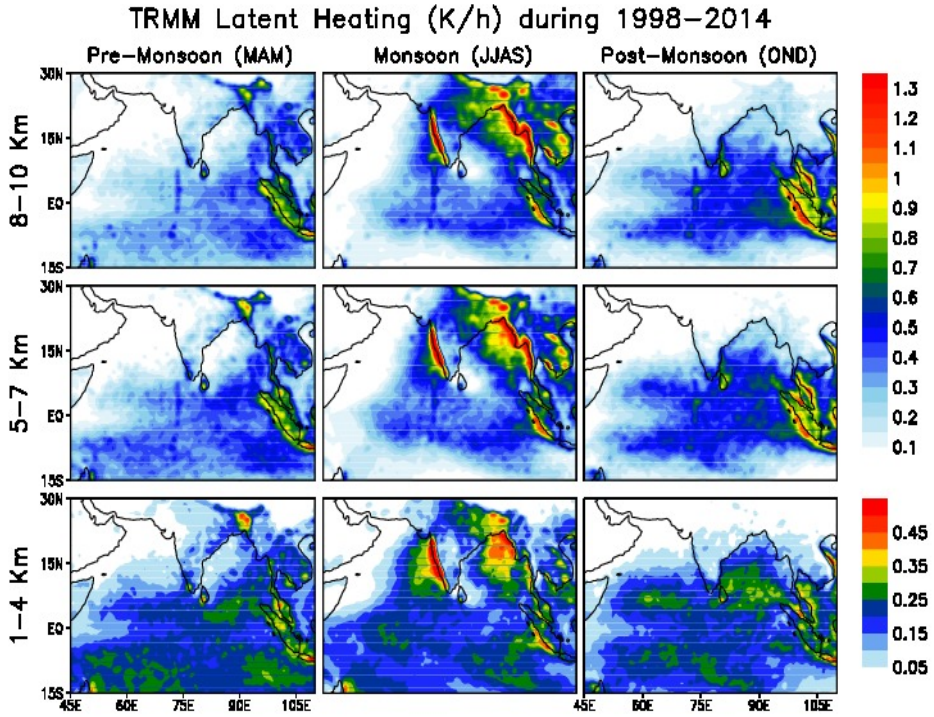


Figure 1.2 Seasonal variation of latent heating at different levels in atmosphere during pre monsoon, monsoon and post monsoon seasons.

## 1.4 Indian monsoon systems

Ramage (1971) defined the monsoon area based on a number of criteria like (i) the prevailing wind direction should shift by at least $120^{O}$ between January and July, (ii) average frequency of prevailing wind directions in January and July should exceed 40%, (iii) the mean resultant winds in at least one of the months should exceed 3 ms $^{-1}$ , and (iv) fewer than one cyclone – anticyclone alternation only should occur every two years in either month (January, July) in a $5^{O}$ latitude – longitude grid. The area between $35^{O}$N and $25^{O}$S and $30^{O}$W and $170^{O}$E satisfies this definition and India and the surrounding oceans are covered within the monsoon regime (Ramage, 1971, Rao, 1976). The cloud distribution over the monsoon region undergoes large

and systematic annual variations, with minimum cloudiness in winter and maximum in summer months (figure1.3).

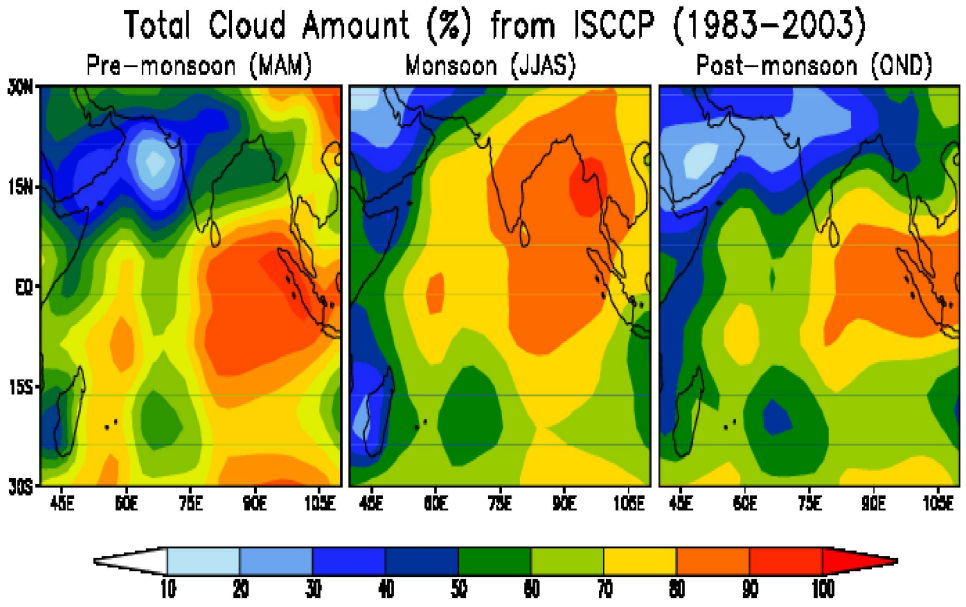


Figure 1.3 ISCCP Total cloud amount for pre, summer and post monsoon seasons

The fundamental mechanism that drives monsoon circulations is the cross-equatorial pressure gradient formed by the differential heating between the landmasses of the summer hemisphere and the oceans of the winter hemisphere. The spatial and temporal variability of monsoon precipitation is far more complicated than the one which could be expected from such a slowly varying cross-equatorial pressure gradient alone. In fact, the processes that produce the specific spatial distribution of even the long term mean precipitation is poorly understood. Different processes, phenomena, and geographic features have been suggested as modulators of monsoon precipitation, such as local and regional effects of orography (e.g., Grossman and Garcia 1990; Grossman and Durran 1984; Xie et al., 2006), propagation

characteristics of the monsoon intraseasonal oscillation (MISO) that involve both the ocean and the atmosphere (e.g., Lawrence and Webster 2002; Jiang *et al.,* 2004; Wang *et al.,* 2005), propagation of biweekly signals from the South China Sea (Annamalai and Slingo 2001), and land atmosphere feedbacks (e.g.,Webster 1983). All of these features of the monsoon in isolation or in combination appear as possible reason/s for the observed variability in spatial and temporal pattern of rainfall.

The emergence of weather satellites brought forth an ample opportunity to analyse the cloud properties in detail and led to leaping improvements in our understanding of the monsoon system.

## 1.5 Distribution, characteristics and variability of cloudiness over Indian region

During the pre satellite era, cloud observation was limited chiefly to manual recordings and though ground based radars. The major limitation of such observational methods was the limited spatial coverage and low frequency of recordings. Satellites have helped map the global clouds in near perfection. The International Satellite Cloud Climatology Project (ISCCP) provides the most comprehensive and long-term (July 1983 to December 2009) analysis of the satellite data on a global scale, which has immensely contributed to the present understanding of the global distribution and properties of clouds and their spatio-temporal variations (Rossow and Schiffer,1991, Rossow and Schiffer 1999; Rossow and Garder , 1993; Schiffer and Rossow ,1983).

The regional distribution of cloudiness over the India and adjacent oceans have extensively been studied using satellite data over many years

(e.g., Saha, 1971, 1972; Sikka and Gadgil., 1980, Grossman and Garcia, 1990; Bony *et al.,* 2000; Gambheer and Bhat, 2000, 2001; Roca and Ramanathan, 2000; Roca *et al.,* 2002; Zuidema, 2003; Sathiyamoorthy *et al.,* 2004; Puranik and Karekar , 2006; Meenu *et al.,* 2007, 2010, 2012; Haynes and Stephens, 2007; Srinivasan and Joshi , 2007; Devasthale and Grassl , 2009; Wonsick *et al.,* 2009; Sunilkumar *et al.,* 2010; Nair *et al.,* 2011; RameshKumar *et al.,* 2012; Sabin *et al.,* 2013; Rajeevan *et al.,* 2010, Vijaykumar *et al.,* 2017). The radiative impact of cloudiness have become subject to the many studies like Pai and Rajeevan, 1998; Rajeevan and Srinivasan, 2000; Patil and Yadav , 2005; Roca *et al.,* 2005; Samala and Krishnan, 2008, etc. The latent heating distributions in the atmosphere have also been examined by many researchers (eg., Magagi and Barros, 2004).

Several important aspects of the cloud distribution over the Indian region have been revealed through these studies, among them include the occurrence of the deepest convective clouds in the entire globe over the north Bay of Bengal during the Asian summer monsoon season, a double ITCZ over the Indian Ocean during November-December and April months and large spreading of cirrus clouds originating from the deep convective outflows in the Bay of Bengal over to the Indian region and the Arabian Sea during the summer monsoon season. It has also been understood that variations in the Hardley and Walker cells have a great influence on the monthly variations in the spatial distribution of total and high-altitude clouds. The minimum cloudiness (<15%) over the Indian region occurs during winter, when the descending limb of Hadley cell is located over the north-central Arabian Sea and Central Indian region. It has been understood that the clouds undergoes diurnal variations, phase of which varying with season (Wonsick *et al.,* 2009). Cloud features associated with the Active and Break phases of monsoon have

been studied by Devasthale and Grassl (2009) and observed the dominance of deep convective clouds with brightness temperature <233$^{O}$K during the active monsoon period and suppression of convective activity over the Arabian Sea and the west coast of India during break monsoon periods. Haynes and Stephens, 2007 and Rajeevan *et al.,* 2013 observed that the convective areas over the tropical Indian Ocean is rich of deep precipitating clouds with cloud top height >11 km during the summer monsoon period, leading the convective tropopause over the north Bay of Bengal remain lifted upwards to around 13 to 15 km altitude while the thickness of tropical tropopause layer (TTL) shrinks to <3 km during June to August period (Meenu *et al.,* 2010).

## 1.8 Scope and objectives of the present study

While many studies have revealed various aspects of cloudiness over the Indian region during different seasons using various satellite data sets, the India's own geostationary INSAT data remain comparatively less used. Either the difficulty to get access to the data or the unavailability of ready-to-use datasets have considerably lagged the studies using INSAT. The present study explores the potential of INSAT infrared data sets to reveal many elusive aspects of cloudiness over India and surrounding oceanic regions. High temporal and spatial resolution of INSAT-IR data set enables us to explore the characteristics of cloudiness over the Indian mainland and the adjoining oceanic region during different seasons.

**More precisely, the main objectives of this study are**

1. To understand the one to one relation between the infrared brightness temperature (IRBT) and rainfall amounts over different regions within the monsoon regime

2. Investigate the seasonal and intraseasonal variations of cloudiness using INSAT IRBT

3. Explore the BT associations to heavy rain events occurring during different seasons

4. Study the diurnal variation of cloudiness and rainfall over Indian region during different seasons

5. Assess the interannual variability in the latent heating and hydrometeor structure in association with different ENSO phases.

**Chapter-2**

# Data and Methods

## 2.1 Datasets

The primary weather parameters used in the present study are brightness temperature of cloud tops derived from INSAT infrared radiances, gridded rainfall amounts derived from rain guage observational network of India Meteorological Department and rainfall amounts quantified from space borne radars. The following subsections describe more on the different data sets used for the present study.

### 2.1.1 INSAT Kalpana-1 IR Brightness Temperature

Infrared brightness temperature (IRBT) provides approximate temperature of the emitting surface. The satellite Kalpana-1 (formerly METSAT-1) of the Indian National Satellite (INSAT) series was launched in 2002 with initial mission life of seven years. Stationed at 74°E, and the data are highly useful for meteorological applications over the Indian region (Kaila et al., 2002). The main instrument of Kalpana-1 is the Very High Resolution Radiometer (VHRR) for imaging in three spectral bands namely VIS (visible; 0.55– 0.75 μm), thermal IR (10.5–12.5 μm) and WV (water vapour; 5.7–7.1 μm). The nominal spatial resolution (i.e. pixel size) of images obtained by these three channels for a nadir-viewing scan position is 2, 8 and 8 km respectively. For the present study, we have used IR Brightness Temperature (IRBT) data. Data is available for half hour interval, we have used hourly data set for the present study.

### 2.1.1(a) Data for the period 2007 and 2008

During the initial period of the study, INSAT IR Brightness temperature (BT) data was not freely available. The primary analyses presented in chapter-3 of this thesis were carried out using limited data sets that the India Meteorological Department provided for exclusive purpose of this study. The data sets were obtained from the Satmet Division of India Meteorological Department (IMD), New Delhi in raw format. The Indian geostationary satellite Kalpana-1 very high resolution radiometer (VHRR) Infra Red (IR) pixel level radiance data having a temporal resolution of 3 hour for the period from 00:00 hr of 01st June to 21:00 hr of 30th September for the years 2007 and 2008 have been utilised in carrying out the preliminary analyses.

### 2.1.1(b) Processing of the data set (Jun-Sep of 2007&2008)

The spatial resolution of the raw data was 8×8 km at the nadir. The original INSAT VHRR IR radiance values were converted into equivalent Brightness Temperatures (BT) using the look up tables provided. Each data file was subjected to North-South and East-West spatial correction by applying correction factors obtained from IMD log book. Images of all the 3 hourly files were prepared and every single image was manually examined to identify the erroneous or partially scanned images if any. Some images which were found to be incomplete and inaccurate were removed. Nearly 13% of the total 976 such images in both the years had been abandoned. A single combined data file of good images was prepared to carry out all further analysis. The original resolution of the basic data file was varying from place to place as the number of data points available at the nadir being maximum and with the resolution decreasing on increasing distance from the nadir. A

spatial averaging of the original data was carried out in preparing a data set of 0.25×.25° resolution. The years for the analysis were chosen arbitrarily based on the availability of the INSAT data sets.

**2.1.1(c) Open access to the data and online availability**

Off late, half hourly INSAT data from 2009 to mid-September 2017 have been made available for download through the ftp portal of the Meteorological and Oceanographic Satellite Data Archival Centre (MOSDAC) of Indian Space Research Organisation (ISRO). The Brightness Temperature (BT) data sets from the Kalpana-1 satellite during the period from October 2012 to September 2017 is found to be almost continuous and uninterrupted. Thus data for this 5 year period is used for the analyses. There are a few random missing records which were filled with blank values for preparing the data set for the analyses.

**2.1.1(d) Processing of the data set (Oct 2012-Sep2017)**

The original resolution brightness temperature (BT) data is obtained from MOSDAC as values of pixels and their respective latitudes and longitudes. The original data is averaged and projected to a uniform 0.25x0.25 degree mesh for the region 30 S to 30 N and 40 E to 110 E. The term ‘pixel’ often used in chapters refers to 0.25x0.25 grid value.

**2.1.2 TRMM Data sets and Global Precipitation Mission**

The Topical Rainfall Measuring Mission (TRMM), a joint program between NASA and the National Space Development Agency of Japan (NASDA), launched in November 1997 in a low inclination orbit is designed to monitor the tropical and subtropical precipitation and energy (e.g., see Kummerow et al., 1998; Adler et al., 2000; Huffman et al.,2007). TRMM satellite produced over 17 years of valuable scientific data. The TRMM orbit

is near circular with an inclination of $35^{O}$ to the equator. The low satellite orbital inclination enable it to observe the tropical region more frequently compared to the polar orbiting satellites. The TRMM has five instruments on board: Precipitation Radar (PR), TRMM Microwave Imager (TMI), Visible Infrared Scanner (VIRS), Clouds & Earths Radiant Energy System (CERES) and Lightning Imaging Sensor (LSI). The Precipitation Radar is active microwave radar while all other payloads are passive instruments operating in the visible, near-IR, thermal IR and microwave bands.

The Precipitation Radar on board TRMM provided the first-ever estimate of the vertical profile of latent heat that is released by precipitating clouds. The Precipitation Radar (PR) is scanning radar operating at 13.8 GHz and employs an active phased array. It detects the altitude-resolved radar signal scattered/reflected from precipitating clouds, which in turn is used to derive the radar reflectivity of these clouds. The backscattering or reflection detected by PR occurs mainly from precipitation. The contribution of non-precipitating clouds on the TRMM-PR signal is negligible. This is because of the substantially longer wavelength of TRMM PR compared to the droplet size of non-precipitating clouds (typically 8-100 μm). The TRMM-PR has a horizontal resolution of 4.3 km at nadir, range resolution of 250 m and scanning swath width of 220 km. The radar reflectivity observed by TRMM-PR can define the layer depth of the precipitation in the atmosphere and provide information about the rainfall reaching the surface, which are essential to determining the latent heat input to the atmosphere.

Estimates of the rainfall (R) are carried out using the altitude profiles of radar reflectivity (Z) observed by the PR radar, employing the Z-R relationship (Tao et al., 2006). The data processing procedures were developed based on the application of rain gauge and disdrometer observations of rain

rate and droplet size distribution in conjunction with the radar measurements to provide the necessary calibration of the radar rain estimates (Tao et al., 2006). The technique was thoroughly tested and evaluated by the TRMM validation team during the pre-mission phase as well as using ground validations (Tao et al., 2006). The estimated rain rates are used to derive the altitude profiles of latent heating of the atmosphere by the convective and stratiform precipitating clouds.

The Global Precipitation Measurement (GPM) mission is an important new program designed for global satellite precipitation estimation based on an international satellite constellation, which provides precipitation measurements from space at a spatial resolution of 0.1° × 0.1° and a half-hourly temporal resolution (Hou et al., 2014). As the successor of the TRMM, the GPM mission provides four levels of products based on various algorithms. The algorithm for the Integrated Multi SatellitE Retrievals for GPM (IMERG) is intended to intercalibrate, merge and interpolate all satellite microwave precipitation estimates together with microwave calibrated infrared (IR) satellite estimates, precipitation gauge analysis, and potentially other precipitation estimators at fine time and space scales for the TRMM and GPM eras over the entire globe.

(http://pmm.nasa.gov/sites/default/files/document_files/IMERG_ATBD_V4.6.pdf.)

**2.1.2(a)TRMM PR 3B42 V7 rainfall**

Tropical Rainfall Monitoring Mission (TRMM) Precipitation Radar (PR) 3B42 V7 hourly Rain Rate (RR) having a temporal resolution of 3 hour and spatial resolution of 0.25°×°0.25° for the period 2007 & 2008 for which INSAT data is available is used for the analyses in chapter-1. This product

depends on input from both microwave and IR channels (Huffman et al., 2007). The algorithm consists of two separate steps. The first step uses the TRMM VIRS and TMI orbit data (TRMM products 1B01 and 2A12) and the monthly TMI/TRMM Combined Instrument (TCI) calibration parameters (from TRMM product 3B31) to produce monthly IR calibration parameters. The second step uses these derived monthly IR calibration parameters to adjust the merged-IR precipitation data, which consists of GMS, GOES-E, GOES-W, Meteosat-7, Meteosat-5 and NOAA-12 data. The final gridded, adjusted merged-IR precipitation (mm/hr) and RMS precipitation-error estimates have a daily temporal resolution and a 0.25-degree by 0.25-degree spatial resolution. Spatial coverage extends from 50° south to 50° north latitude.

### 2.1.2(b) TRMM-GPM 3B42RT Rainfall

Three hourly near real time precipitation rates known as TRMM 3B42RT data sets (Huffman, 2016) with a spatial resolution of 02.5x0.25 degree is used in the present study. The data for the same period as that of INSAT is used for the analyses. For the present analysis, a subset of data is prepared for the Indian region from the global data sets. The grid points of 3B42RT are so chosen as to coincide exactly with that of INSAT so as to use for pixel to pixel comparison between rain and corresponding cloud types.

### 2.1.2(c) TRMM Monthly multilevel Products

Methodologies for estimating latent heating based on precipitation rate profile retrievals from TRMM-PR measurements are described in Tao et al. (2006). The present study uses the TRMM-PR-Level-3 product on the monthly mean convective and stratiform latent heating (CSH-LH) to investigate the altitude variations of latent heating by precipitating clouds and its spatial

variations. This data set is provided with a spatial resolution of 0.5 ◦ × 0.5 ◦ at 19 vertical levels from the surface to a height of 18 km.

The CSH algorithm also uses surface precipitation rates, percentage of its stratiform and convective components, and location of the observed cloud system for deriving the latent heat profile. The inversion to derive latent heating rate (LHR) is based on a look-up table of LHR profiles derived from simulations using the Goddard Cumulus Ensemble model and diagnostic heating budgets (Tao et al., 2001). The main drawback of this data set is that the CSH algorithm does not estimate the LHR in the absence of surface rainfall. However, the net LHR in the absence of surface precipitation is generally very small (Zuluaga et al., 2009).

The data products used for the present study are 3H31 Latent heat profiles and 3B32 Hydrometeor profiles. Data for the period 1998 to 2014 has been utilised in the present study. Monthly Convective Stratiform Heating from Combined 3H31productis apparent heating profiles from surface convective and surface stratiform rainfall rate. This data sets provide Latent Heating profiles from 0.5 Km up to 18 Km at spatial resolution 0.5 º x 0.5 º latitude longitude grid. Monthly hydrometeor profile 3B31is a combined rainfall product which uses the high quality retrievals done for the narrow swath in 2B31 to calibrate the wide swath retrievals generated in 2A12. For each 0.5 degree box and each vertical layer, an adjustment ratio is calculated for the swath overlap region for one month. Only TMI pixels with 2A12 pixel Status equal to zero are included in monthly averages, which effectively remove sea ice. These data sets provide profiles of rainwater, snow and graupel for 0.5 Km up to 18 Km at spatial resolution 0.5 º x 0.5 º latitude longitude grid.

(https://storm.pps.uosdis.nasa.gov/storm/data/docs/filespec.TRMM.V7.pdf)

### 2.1.3. IMD 0.25x0.25 Gridded Rainfall Data

Gridded rainfall data of India Meteorological Department (IMD) are highly useful datasets available in multiple spatial resolutions. The present study utilises high resolution daily gridded data referred to as IMD4 (Pai *et al.,* 2010). Pai *et al.,* 2010 provides a detailed description of development of this data set. This data set is developed by using inverse distance weighted interpolation (IDW) scheme proposed by Shepard (1968) and has incorporated more number of gauge observations than that used in the previous versions (Rajeevan et al.2006, 2008, 2009 & 2010). For the present study, data for the period 1981-2017 is used. The spatial resolution of IMD4 daily data is 0.25 $^{o}$x 0.25 $^{o}$ latitude longitude grid.

### 2.1.4 NCEP-NCAR Reanalyses data

The National Center for Environmental Prediction and National Center for Atmospheric Research (NCEP/NCAR) reanalyses (Kalnay et al., 1996) are employed to represent the circulation field at standard pressure levels. Data for every 2.5 x 2.5 latitude-longitude grids are available at four times daily resolution from 1948 to till date. The reanalysis uses a frozen data assimilation model for the entire period which may eliminate spurious discontinuities that arise from changes in the assimilation. Monthly Vertical pressure velocity data is obtained from NCEP-NCAR reanalysis. The spatial resolution of the data is 2.5 x 2.5 latitude longitude grid.

## 2.2 Methods of analysis

Figure 2.1 provides the broad area under the present study. The basic data set used being INSAT Infrared Brightness Temperature, this study employs different threshold temperatures (TT) to define types of clouds. For

various analyses in this thesis simple statistical techniques have been utilised. The details of each method are explained within the body of the thesis at the point of first use in the respective sections.

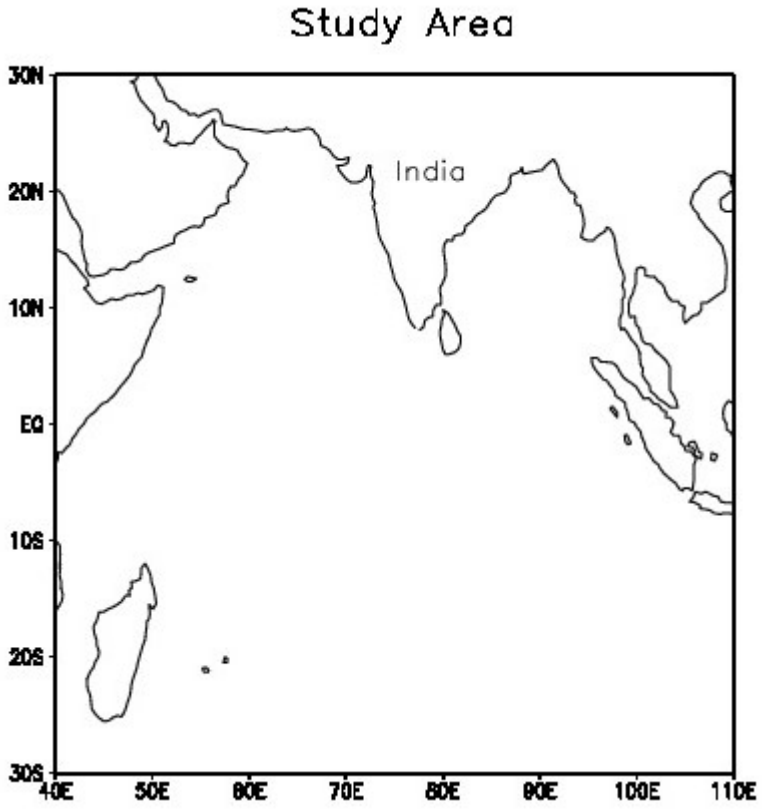


**Figure 2.1 Area of present study.**

# Chapter-3

# Distribution of Cloudiness and Categorization of Rainfall Types

## 3.1. Introduction

Over the Indian sub-continent and surrounding oceanic region, clouds are present in abundance during the south west monsoon season. The peak-monsoon months (June-September) witness mean cloud amounts increasing to 50–80% in north eastern India and the Arabian Sea, and up to 90% over a large portion of the northern Bay of Bengal (Wonsick *et al.,* 2009). The INSAT series of geostationary satellites observe the region continuously from the space ever since the first Indian geostationary satellite was launched in 1982. Cloud top temperatures derived from thermal infra-red channel are available throughout day and night and can be thus used as an effective proxy to rainfall occurring underneath. In oceanic regions where continuous observation of rainfall from ground is not available, geostationary satellite observations have proven to provide a huge wealth of data over these data sparse region. Even though plenty of satellite data is available with India Meteorological Department (IMD), the entire pixel level INSAT data is not freely available. For this reason, the number of studies utilising INSAT data are limited.

While IR sensors measure upwelling radiation that originates primarily near the tops of clouds which gives only indirect measurement of underlying precipitation (Arkin et. al., 1994)microwave-based imagers are better suited to quantitative measurement of precipitation due to the physical connection between upwelling microwave radiation and the underlying cloud precipitation

structure. Rain estimates prepared by utilising both the microwave and IR channels from multiple satellites are available at very high spatio-temporal resolutions (Huffman *et al.,* 2007). However, for most of the global rainfall estimations, data from INSAT is not incorporated. Data from Japanese geostationary meteorological satellite (GSM) and European Meteosat-5 geostationary satellite are being used widely as alternatives to INSAT data over the region.

There have been various attempts to understand the cloudiness in the Indian and surrounding oceanic regions. Srinivasan (1968) proposed that southwest monsoon region is not uniformly clouded but has zones of maximum or minimum cloudiness. Using weekly averages, a study on the Large scale precipitation and Outgoing Long Wave radiation (OLR) from INSAT-1B carried out by Arkin *et al.,* (1989) for the monsoon season (June to September) of 1986 showed that there existed high correlation between quantitative precipitation estimates (QPE) from OLR and rainfall observations for most of places under study. Rao and Rao (1992) studied diurnal variation of fractional cloudiness over the Indian region using INSAT-1 IR data for 3 monsoon seasons 1987-1989. They employed two Infrared brightness temperature (IRBT) thresholds viz. 265$^{o}$K and 235$^{o}$K to classify the clouds to total convective and deep convective clouds with an average cloud top height of 6 Km and 9-10 Km respectively. They have noticed that clouds associated with convection are more abundant in Head Bay of Bengal, while there is practically no convection over western Arabian Sea, south east Peninsular India and adjoining Sri Lankan region. Further, they have concluded that deep convection is much less frequent over the west coast. The presence of heavy rains on the west coast despite the absence of deep clouds is attributed to shallow orographic clouds. Gambeer and Bhat (2000) have studied the life

cycle characteristics of deep cloud systems over the Indian region using INSAT-1B pixel data, using threshold temperatures ranging between 201°K and 261°K to classify clouds with approximate heights of 15 and 8 Km respectively. The same authors have studied the diurnal variation of deep cloud systems using INSAT 1B pixel data for the period April 1988 to February 1989 (Gambeer and Bhat 2001). The threshold temperatures used for that study are 201°K, 221°K, 241°K and 261°K.

In the present study, an independent analysis of concurrent observations of INSAT IR data and TRMM PR 3B42 rainfall estimates is carried out. The main objective of the analysis is to quantify the association of different threshold values of BT to the rainfalls of varying intensity classes. Further we explored the relationship between CTT rainfall rate over four regions which exhibits distinct characteristics of rainfall and cloud distribution. The regions are selected based on the cloudiness resulting from varying physical mechanisms which leads to occurrence of deep convection, moderate convection and orographic clouds.

## 3.2. Data and Methodology

### *3.2.1 INSAT IR Brightness Temperature*

The present study utilises Indian geostationary satellite Kalpana-1 very high resolution radiometer (VHRR) Infrared (IR) pixel level radiance data having a temporal resolution of 3 hours for the period from 00:00 hr of 01$^{st}$ June to 21:00 hr of 30$^{th}$ September for the years 2007 and 2008. The original INSAT VHRR IR radiance values are converted into equivalent Brightness Temperatures (BT) and regrided to 0.25X0.25 degree resolution. The years for the analysis were chosen arbitrarily based on the availability of the INSAT data sets. Further, part of the period for which the data is available coincides

with Year of Tropical Convection (YOTC) (May 2008 to April 2010).

### *3.2.2 TRMM PR 3B42 V7 Rainfall*

Tropical Rainfall Monitoring Mission (TRMM) Precipitation Radar (PR) 3B42 V7 hourly Rain Rate (RR) having a temporal resolution of 3 hours and spatial resolution of 0.25 º x 0.25 º for the period of the available INSAT data is used for the present study. This product depends on input from both microwave and IR channels (Huffman *et al.,* 2007).

### *3.2.3 Methodology*

The data were prepared in such a way that the geographical grid cells of TRMM PR and INSAT BT co locate. Frequency of occurrence of BT in ranges of 10 degree interval between 180 K and 270 K is compared with the rain amounts estimated in the same grid point for all available pairs of BT and RR during the study period. Primarily three rain intensity categories are defined. Light (less than 4.5 mm), Moderate (between 4.5 and 9 mm) and Heavy (above 9mm) cumulative rainfall in three hours. The rain type classification was arbitrarily, but objectively chosen. Several studies have used similar rain intensity classification with slightly different range of values (for eg: Hamzaetal., 2010; Kumar etal., 2014). We have arrived at the optimum rain classification ranges for the present analysis after trying out different rain rate – BT combinations over the Indian Summer Monsoon region for the available period.

The frequency of occurrence of cloud tops with different temperature threshold (TT) values is calculated. Considering the differences in the features of clouds prevalent in different regions, four sub regions are identified for analysis. They are (a) Head Bay of Bengal (16-21ºN, 89-94ºE), (b) Central Indian land region (18–25ºN, 75–82ºE) , (c) Eastern Arabian Sea and West

coast of India (9-18$^{o}$N, 72–76$^{o}$E), and (d) South west Indian Ocean (7-2$^{o}$S, 60-70$^{o}$E). The selection of the boxes were so made as to include regions where maximum rainfall occur during the season with differences in the rainfall formation mechanism. The boxes are of varying sizes and the total number of data points within the boxes varies. Normalisation is carried out while calculating all parameters within the boxes so as to make the results comparable. The Head Bay of Bengal box is a region where normally a series of monsoon depressions occur during the season (Zuidema, 2003). Rainfall is comparatively less over the western side of the central Indian land box. Rainfall over the region is mainly contributed from westward moving monsoon depressions which usually form over Bay of Bengal (Lau and Lau, 1992). The eastern Arabian Sea and west coast covers both the immediate windward and leeward sides of the Western Ghats. The rainfall in this region mostly occurs during the season due to orographic ascent of wind blowing from the south west direction from the Arabian Sea. The south west Indian Ocean box considered is located over the ocean in the southern hemisphere where considerable amount of precipitation is found to occur during the monsoon season. Hence each the four regions considered has distinct characteristic cloudiness and rain intensity patterns.

Different authors have used slightly different cloud top temperature thresholds for classifying cloud types (Rao and Rao 1992, Gambeer and Bhat 2000, Zuidema 2002, Roca *et al.,* 2005, Wonsick *et al.,* 2009). It is understood that colder cloud tops correspond more closely to heavier rainfall events (Chen and Houze 1997; Rickenbach and Rutledge 1998). In the present study, CTT BT values ranging between 235 and 265$^{o}$K are considered as shallow clouds, between 220 and 235$^{o}$K as middle to high level clouds and below 220$^{o}$K as very deep clouds. Since precipitating clouds may be assumed to have high

infrared opacity, the cloud-top heights corresponding to 201 and 261°K threshold temperatures are approximately 15 and 8 km, respectively (Gambeer and Bhat, 2000); as the climatological 500 mb temperature in the region 0-20° N latitude is 267 K (Crutcher and Meserve, 1970) the present classification of clouds as shallow, moderate to high and deep are realistic.

## 3.3. Results and discussion

One of the known limitations in deriving cloud information from Brightness Temperature is that it gives the temperature of the topmost layer of the clouds present in a region. However, as BT is available throughout day and night, it provides very useful information regarding the average rainfall activity occurring at a place.

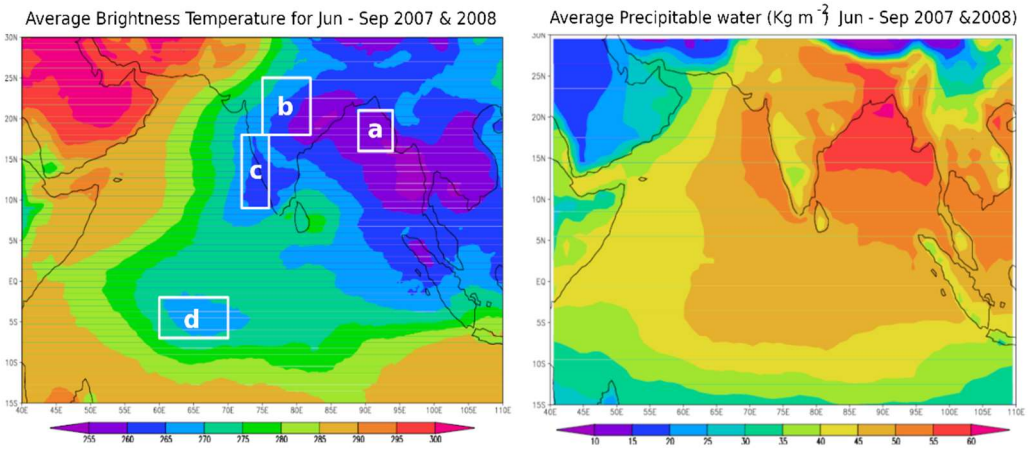


A B

Figure 3.1: (a) Average Brightness Temperature for the monsoon period (June-Sep) for the years 2007 and 2008 combined. (b) Precipitable water for the same period.

Figure 3.1(a) provides the average Brightness Temperature for the monsoon seasons of 2007 and 2008 combined. There are low BT value present over the Head Bay of Bengal (marked 'a') and the adjoining areas along the Gangetic plains. The central Indian land region (b) and west cost of India (c)

have temperature of cloud top on an average ranging between 255 and 265°K. Another location where the BT is low is at the south West Indian Ocean region marked 'd' in the figure. The spatial pattern BT is comparable to the high cloud distribution provided by Kang *et al.,* (1999) and matches the observed rainfall climatology shown by Lau *et al.,* (1988). Seasonal (1st June to 30th September) rainfall over India for the year 2007 and 2008 was 106 and 98% respectively of its long period average (LPA). We have compared the seasonal average of total precipitable water (TPW) during 2007 and 2008 monsoon season obtained from Atmospheric Infrared Sounder (AIRS) level 3 version 6 data sets with the brightness temperature and is presented in Fig.3.1 (b). It is found that high values of TPW well corresponds with the low values of Brightness Temperature especially over the four boxes identified for further analysis.

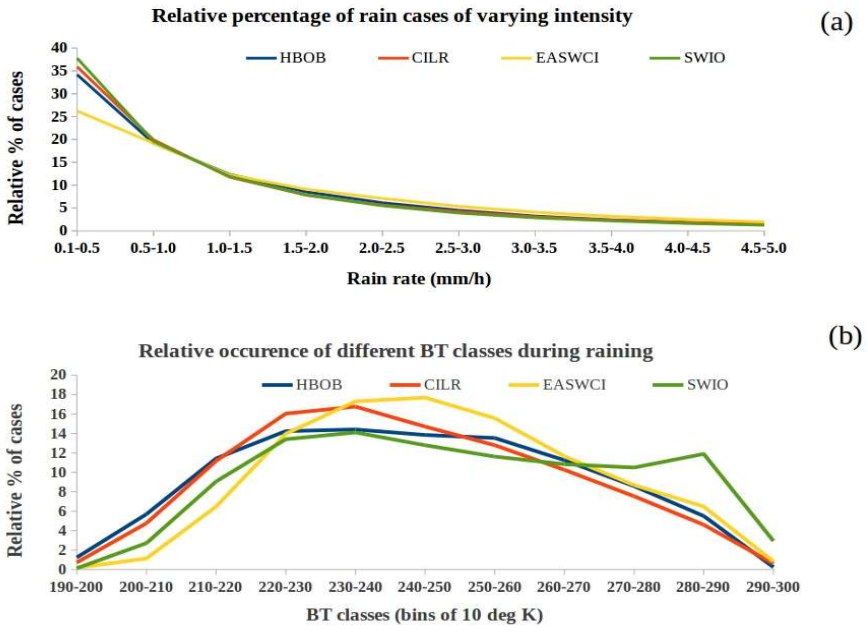


Figure 3.2: (a) Relative occurrence of rain cases of different intensities of 0.5 mm/h width bins from 0.1 mm/h to 5 mm/h. (b) Relative occurrence of different BT classes of raining pixels.

Figure 3.2 (a) shows the frequency distribution of rain intensity over the 4 selected regions marked as rectangles in Fig. 3.1 (a).Distributions of rain rate over all four regions are similar. However, Light rain rate is most favoured over South West Indian Ocean (SWIO) and least favoured over Eastern Arabian Sea and West Coast of India (EASWCI). High rain rate is most favoured over EASWCI. Relative occurrence of 0.5 to 1.5 mm/h rain is found to be same over all regions. It is found that the high intensity rates greater than 3 mm/hr is more pronounced over EASWCI followed by head Bay of Bengal (HBOB) and central Indian land region (CILR). However, occurrence of heavy rain rate is minimum over SWIO region. In Fig.3.2 (b), we have compared the BT distribution corresponding to all rainy pixels. Regional variations in the 200-210$^{o}$K range are drastic, ranging over a factor of 4 or so, most frequent in HBOB and almost absent in EASWCI.

It is noted that a bimodal distribution of BT values are found over SWIO region with a primary peak at BT values of 230-240$^{o}$Kand a secondary peak around 280-290$^{o}$K. Such existences of bimodal storm heights have been observed by Short and Nakamura (2000) over tropical Oceans. As evident from figure 3.2, the low intensity rainfall over this region is mainly contributed from low and middle to high level clouds. The very light rainy pixels with BT values less than 210$^{o}$K suggests that, this lower BT values can be cirrus contamination and there is possibility of presence of lower or middle to high level clouds beneath the cirrus clouds. More interestingly, BT values of 240-250$^{o}$K is most favoured over EASWCI regions and BT values lower than 210$^{o}$K is mostly absent. Along with the distribution of rain rate this also suggests that, over EASWCI all classes of rain is chiefly produced from middle level clouds. Though, distribution of rain rate is similar over HBOB and CILR regions, clear distinction can be found in the distribution of BT

values over these two regions. Over CILR, rain is mainly produced from vertically developing very deep clouds whereas over HBOB, middle to high level clouds are major contributors of rainfall. The proportion of very high clouds is greater in HBOB as compared to CILR.

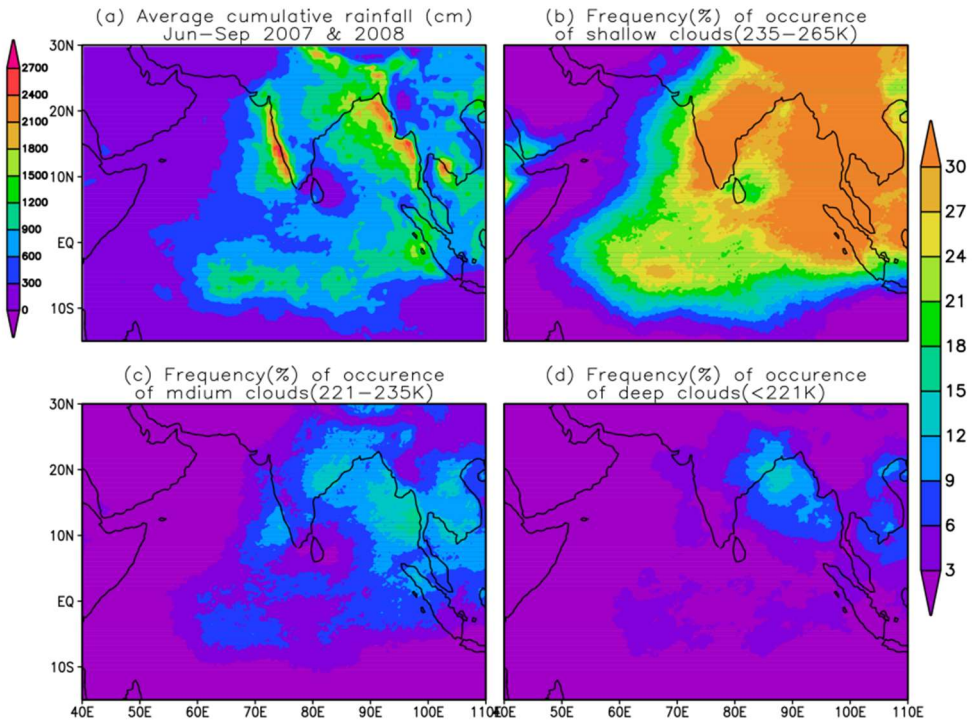


Figure 3.3: (a).Average cumulative Rainfall for 2007& 2008 from TRMM PR, (b) frequency of occurrence of clouds with top temperature ranging exclusively between 235 and 265°K, (c) between 221 and 235°K and (d) below 221°K**.**

Figure 3.3 (a) provides the cumulative rainfall averaged for the monsoon season for the two years selected for the study. It can be seen that the highest amounts of rainfall over the region occurs on the western sides of prominent land masses. The major reason for such high amounts of rainfall is that rain over the region mainly comes from orographic clouds (Xie Ping *et al.,* 2006) as the land blocks the wind from the Ocean during the season. The wind blows for a considerable time over the ocean having high sea surface

temperatures (SST) and the air becomes laden with enough moisture to produce high amounts of rainfall. Figure 3.3 (b, c, d) gives the frequency of occurrence of shallow, medium to high and deep clouds over the region. It can be seen that clouds with top temperature lower than 265°K do occur almost everywhere of the sub regions considered. However, the rainfall is not being produced in most of the places. Medium to high level clouds are present in most of the places where rainfall has occurred. Very deep clouds are present only along the east coast of Orissa where though rainfall occurs, is not as much as that occurs at other prominent rainfall regions. Hence the cloud top temperature alone cannot be considered as the sole indicator of the amount of rain produced from overgrowing clouds. For different regions, BT values indicate different amounts of rainfall.

Deep clouds with CTT colder than 221°Kare found to occur in the Head Bay region as well as in an area along the normal axis of the monsoon trough during the active monsoon period. However, the frequency of occurrence of deep clouds decreases with distance from the coast and becomes negligible a few hundred kilometres inward to land from the shore. Two major maxima of frequency of occurrence of CTT ranging between 221 and 235°K can be identified. They are (1) West of the west coast of India, on the windward side of the Ghats confined between latitudes 16 and 22°N and (2) On the land region over the State of Orissa, Jharkhand and West Bengal along the east coast of India. Of these, while the former maximum is present over the ocean and is almost absent in the land region, the latter is found to be lying in a southwest-northeast direction parallel to the coast, limiting its presence completely in the land region. Irrespective of the differences in the presence of deep clouds or medium clouds, the clouds with low top height (temperature higher than 235°K but lower than 265°K) are found to occur at maximum

frequency in all the sub regions under study. However, such types of clouds are present less frequently over "the pool of inhibited cloudiness" which Anish Kumar *et. al* (2011) have observed to exist in the region between 3–13$^{O}$N and 77–90$^{O}$E over the Bay of Bengal (BoB) throughout the Asian summer monsoon season.

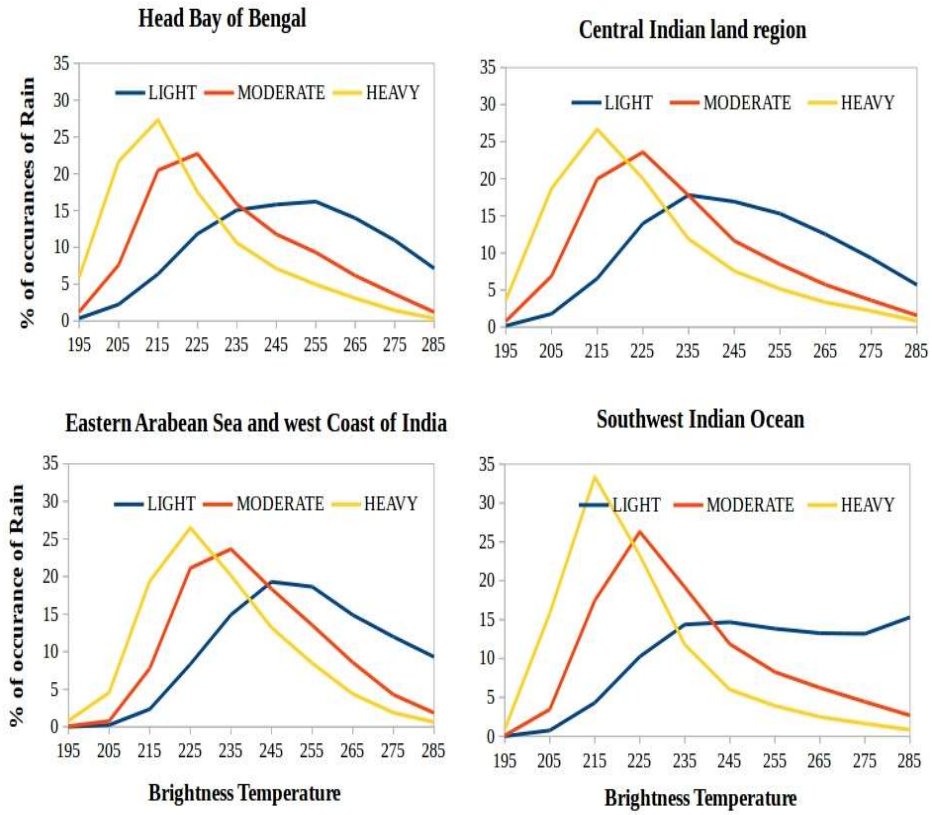


Figure 3.4: Average Percentage of occurrence of three categories of rain versus Brightness temperature for the four sub regions.

Figure3.4 presents the Percentage of occurrence of rain versus Brightness temperature for the four regions under study. Heavy rainfall events defined on the basis of magnitude of 3 mm per hour and above is found to occur in the Head Bay region mostly when cloud top temperature reaches in the range 205-220$^{o}$K. Moderate rainfall (rain rate 1.5-3 mm/h) in the region is

attributable mostly to the CTT range 215-230°K. Light rainfall (less than 1.5 mm/h) occurs in a wide range of BT, 255-285°K.

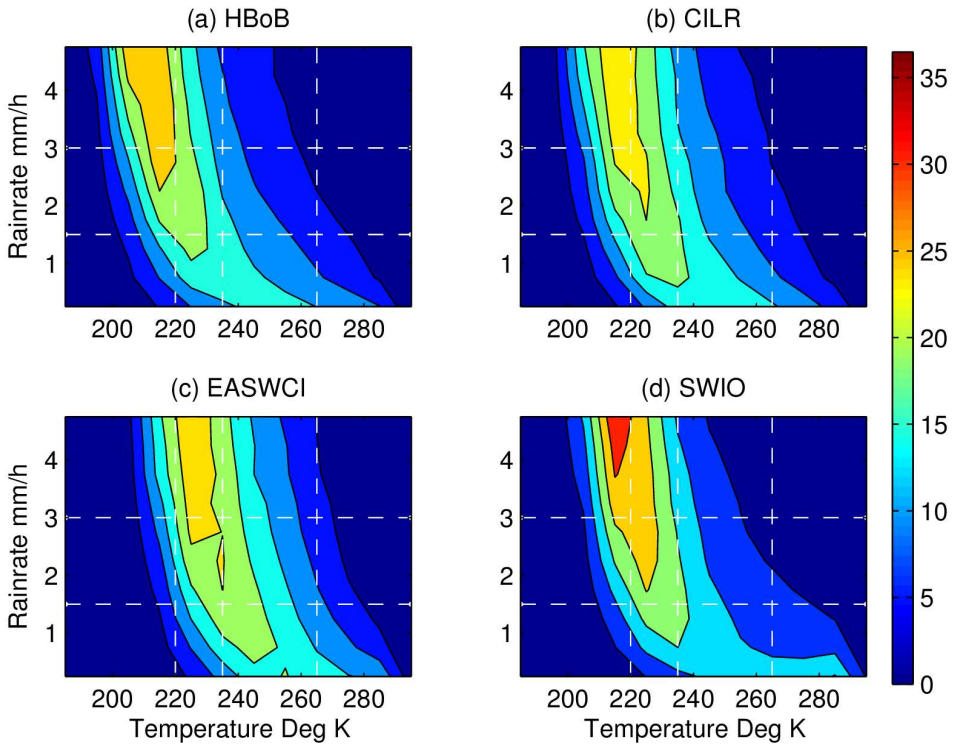


Figure 3.5: Percentage of occurrence of cases out of total in different BT-RR classes in 10-K bins between 180 and 290°K is plotted for the four sub regions.

Similarly, as in the case of Head Bay, in central Indian land region heavy rainfall peaks when BT values are in the range 205-225°K, maximum cases of moderate rain occur when BT ranges between 215 and 235°K and light rain is contributed by a wide range of clouds viz. 225 -265°K. In EASWC region, heavy rainfall mostly comes from CTT ranging between 215 and 235°K. Moderate rains results the most when 225-245°K is the CTT and most of the light rain in the region comes from clouds with top height in the range 240-260°K. SWIO region has heavy rainfall peak when BT is in the range 210-220°K, moderate rain in 220-240°K and light rain in a wide range of BT

values. Interestingly, a secondary peak of light rain is present in the 275-290$^{o}$K temperature range indicating the presence rainfall associated with shallow clouds in the region. Light rainfall may be occurring in this region produced by clouds which do not grow up very high.

The percentage of occurrence of rainfall in different brightness temperature varied in 10-K bins starting from 180 to 290$^{o}$K and the corresponding rain in intervals of 0.5 mm/h rain rate is shown is figure 3.5**.** It is seen that *'banana'* shape pattern is more evident in all figures and the shape has regional dependency. In Head Bay of Bengal, for instance, most of the high intensity (3-5 mm/h) and moderate intensity (1.5-3 mm/h) rainfall is found to occur in concurrence with very low cloud top temperatures < 220$^{o}$K, implying that the clods in the region do grow very deep and produce very heavy to moderate rainfall. A considerable amount of moderate and light (<1.5 mm/h) rainfall is obtained in temperature range 240-260$^{o}$K. In the central Indian land region, major share of high intensity rainfall is contributed by very deep clouds but most of the moderate rainfall is being produced by middle to high level clouds. At the same time, major share of light rain in the region is also being produced mostly by cloud top ranging between 230-240$^{o}$K. Further, light rainfall is also obtained from cloud top temperature range 240-260$^{o}$K. In the EASWCI region high intensity rain is contributed mainly by clouds at middle to high levels. Moderate rain is contributed by middle to high level clouds as well as shallow clouds. Major share of light rain comes from clouds with CTT 240-250$^{o}$K. Very light rain is contributed by relatively warm clouds as well. SWIO region is having a unique pattern with a secondary peak of light rainfall at relatively higher CTT values. In fact, the occurrence of high intensity rainfall is very rare in the region. The high magnitude of high intensity rain and low CTT is insignificant as the number of data points are

negligibly less as compared to the other classes of rainfall in the region.

### 3.4. Conclusions

Characteristics of Brightness temperature and associated rainfall distribution in four sub regions are documented. While monsoon circulation remains the common factor determining the weather in the Indian subcontinent and surrounding ocean during the season (June to September) both the BT and rainfall distribution are highly spatially varying. The four sub regions have distinct features of cloudiness. The association of BT and rainfall is also found to dependent greatly on location. While the top of precipitating clouds in the head Bay of Bengal region is very deep, the clouds in the Southwest Indian Ocean rarely grow high. While the clouds in the EASWC is mostly rain producing, clouds occurring at the same height in central Indian land region produce less amounts of rain. Characteristic BT values in correspondence to three classes of rainfall intensities are suggested. In the HBOB region and CILR, the maximum frequency of BT values associated with very heavy rainfall is <220$^{o}$K whereas the same for EASWCI and SWIO is 220-240$^{o}$K. In general, moderate rainfall is favoured by clouds with top temperature 220-240$^{o}$K in all the four sub regions. Clouds associated with Light rainfall are found to occur at a wide range of levels, suggesting that cirrus contamination could be a prominent reason for low BT values in concurrence with light rain. The bimodal rain – BT association observed in the SWIO region is particularly interesting. A major share of light rain in the region is occurring from warm (260-290$^{o}$K) clouds with very low top height.

# Chapter-4

# Seasonal and Intraseasonal Variability of Cloudiness and Rainfall

## 4.1. Introduction

The seasonal reversal of the meridional temperatures, pressure gradients and the wind circulations is the most remarkable feature of the climate over the Indian region and allows the happening of the summer and winter monsoons. A major portion of the annual rainfall over most parts of the country is received during a short span of four months from June to September. This period is commonly being referred to as the summer monsoon season and the rainfall during the period, Indian Summer Monsoon Rainfall (ISMR). The prevailing wind during this season is south-westerly. From October to December, the wind blows from reverses direction viz northeast to southwest (North-easterly) constituting the winter or Post monsoon season. The conditions for the onset of the summer monsoon are getting established during the months from March to May and are known as Pre monsoon season. During the three characteristic seasons, distinct synoptic scale features and patterns of weather parameters exist over the Indian subcontinent and the surrounding Oceanic region.

Although the Asian monsoon is a complex phenomenon involving many timescales of variations, the seasonal and intraseasonal variability are more distinctive. They are characterised by wet and dry phases of seasonal mean and it’s inter annual variability. Intra seasonal variability is commonly realised as Active-Break phases within the season.

It is known that most of the summer monsoon rainfall over India occurs owing to the synoptic and large scale convection associated with the continental Inter tropical Convergence Zone (ITCZ) (Gadgil *et al.,* 1984, Sikka and Gadgil., 1980, Yasunari., 1979, Krishnamurthi and Subramanyam., 1982). Sadler (1975) reported that the Indian longitudes (70-90°E) are characterised by a large excursion of maximum cloud zone (MCZ). Sikka and Gadgil (1980) using visible cloud imagery from National Oceanic and Atmospheric Administration (NOAA) satellite data demonstrated that the MCZ had two preferred regions during the Indian summer monsoon. The primary location of MCZ observed around 20°N over the monsoon trough and a secondary location over the equatorial region. They showed that cloud bands from the equatorial region move to the monsoon trough at the rate of around 1° latitude per day. Further they showed that during some occasions, clouds emanating from the equatorial region move northward and southward simultaneously.

In this chapter, we attempt to analyse the prominent cloud features during the three rainfall seasons of India using Kalpana-1 IR BT data for the 5 years period, 2013-17. Further, we attempt to do a detailed study on the intra seasonal characteristics of cloudiness and rainfall during the summer monsoon season for the reason that nearly 80% (Wang and Linho, 2002) of the annual rainfall occurs and significant intraseasonal variability is reported during this season (Krishnamurti and Bhalme., 1976, Yasunari 1979, Krishnamurti and Ardanuy., 1980, Chen and Chen., 1993, Wang and Xie., 1997, Annamalai and Slingo., 2001, Waliser *et al.,* 2003, Sengupta *et al.,* 2001, Goswami, 2005, Hoyos and Webster., 2007, Rajeevan *et al.,* 2010 etc ).

## 4.2. D**ata and Methodology**

The data sets used for the present analysis are hourly Kalpana-1 IR BT, TRMM3B42RT three hourly rain rates and daily gridded IMD4 rainfall (Pai *et al.,* 2014) originally obtained from the network of rain gauges located over the land. All the three data sets have similar spatial resolution viz. 0.25 x 0.25 degree latitude longitude.

Three categories of clouds are defined based on the cloud top temperature thresholds. Brightness Temperature (BT) colder than $220^{O}$K is considered as very deep or deep clouds. BT between 220 and $240^{O}$K are defined as moderate to high clouds and the BT values between 240 and $260^{O}$K are taken as shallow clouds. Spatial variation of these three types of clouds during the three seasons is studied using frequency of occurrence of the clouds.

Most of the earlier studies on extreme rainfall considered only rainfall data sets. Here, for the first time we demonstrate the synergic use of combination of hourly BT and 3 hourly TRMM rainfalls for better characterisation of heavy rainfall events and associated cloud types.

We have studied the extreme rainfall events and the associated cloud and rain patterns. For this analysis, we used TRMM3B42RT rain data and considered a threshold rainfall of 10 mm/hr and above to define extreme rain events. This nearly corresponds to the India Meteorological Department's definition of category 3 extreme rainfall (244.4 mm per day and above - Exceptionally heavy). However, we have not considered the daily cumulative, but rather picked up all events during the season where the hourly rainfall exceeded 10 mm/hr. Frequency of occurrence of such extreme rainfall events

(Rfrq) and Fraction of rain contributed (FRC) by the extreme rain events to the seasonal total is calculated and presented.

Intra seasonal characteristics of rainfall and associated clouds during monsoon season is studied by following the analysis methods of Rajeevan *et al.,* (2010) for active and break spells for the period 2013-17 using IR BT data and IMD gridded rain data. We defined active and break spells based on the criteria mostly similar to Rajeevan *et al.,* (2010). The average daily rainfall in the region 69-87 E and 18-27 N known as the core monsoon zone is the standard used for finding the active and break spells. Time series of average daily rainfall in this core monsoon zone for the two months namely July and August for the period 1981-2017 is prepared first. The time series of daily anomaly is found by subtracting the long term daily normal (1981-2017) from the daily time series. This anomaly time series was then divided by the daily standard deviation to obtain the normalised anomaly. For preparing the climatology, we have used data for the period 1981-2017. The break and active spells for the period 2013-2017 only is considered for the present study as the BT data for the same period is also available and so a comparison is possible.

The active spells has been identified as the period during which standardised rainfall anomaly is more than +1.0 consecutively for three days or more. Similarly the break spells are identified as periods during which the standardised rainfall anomaly is less than -1.0 consecutively for three days or more. The composites of all active days and break days were prepared separately and the TRMM3B42 daily average rainfall is compared with the frequency of occurrence of two ranges of cloud top BT viz less than 220°K and exclusively between 220 and 255°K. These thresholds were arbitrarily

chosen so as to get insight into two categories of clouds namely deep to very deep convection and high to moderate and shallow level convection.

The evolution of active and break phases for the period 2013-17 is examined by using lagged composites of daily rainfall anomalies for lags ranging from -12 to +12 days. Lag-0 refers to the midpoint of the active/break spell. Frequency of occurrence of two ranges of cloud top BT viz less than $220^{O}K$ and exclusively between 220 and $255^{O}K$ are compared with the corresponding IMD gridded daily rainfall anomaly conditions for the lagged composites for the range of lags.

## 4.3. Results and discussions

### *4.3. (a) Seasonal variations in spatial patterns of rainfall and cloudiness*

Top panel of Fig.4.1 provides the average Brightness temperature (BT) overhead rainy pixels and the bottom panel corresponding cumulative rainfall (RF) during the three, pre (MAM), summer (JJAS) and post (OND) monsoon seasons. For this analysis, BT pixels in correspondence with rainy pixels of TRMM3B42RT only are considered for averaging so as to minimise contamination by non-rain producing clouds. During pre-monsoon season, the hotspot of rain is located over the Sumatra island and off west of the island. Further off west of Sumatra, confined nearly between 10-5 S, and 85-95 E has a region where rain is interestingly higher as compared to the surrounding oceanic waters. This unique region over the south equatorial latitudes is further termed as “Enhanced Cloud Zone (ECZ)” during pre and summer monsoon seasons. Although this is part of an elongated westward extension of rainy region from the west coast of Sumatra which extends westward up to 70 E consistent existence of ECZ during pre and summer monsoon season is enthralling.

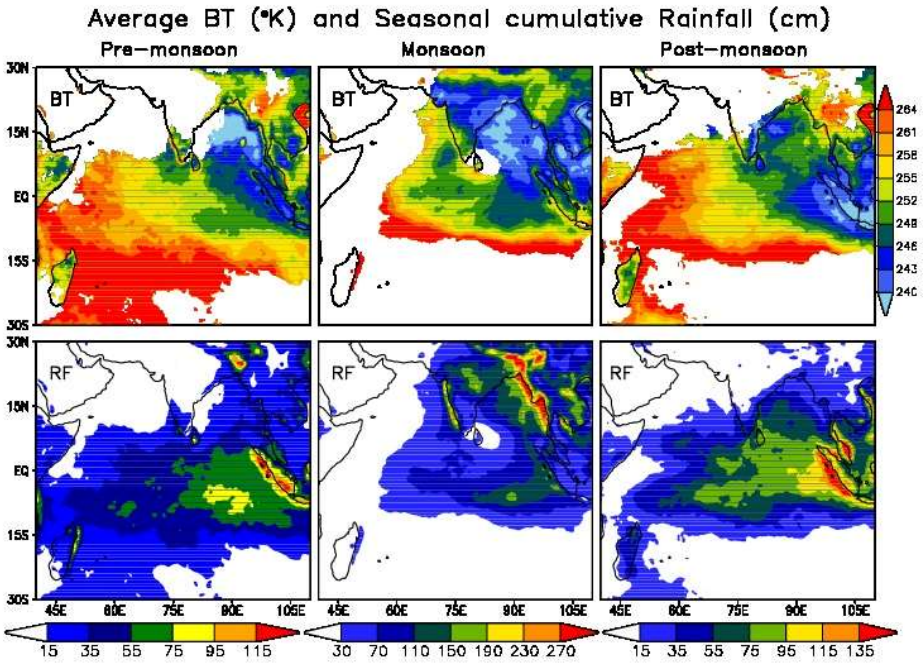


Figure 4.1. Average Brightness temperature overhead rainy pixels and the cumulative rainfall for pre monsoon (left top and left bottom respectively), monsoon (middle top and middle bottom respectively), and post monsoon (right top and right bottom respectively) seasons. BT values are obtained from Kalpana-1 and the rainfall shown is TRMM3B42RT for the period Oct 2012 – Sep 2017. Separate colour bar is provided for rainfall as the value ranges vary considerably from season to season.

During the pre-monsoon, two main rainfall regions are identified over Indian mainland. They are (1) the southwest tip of the peninsula and (2) the north eastern states. Large amount of rainfall is received during the season over the Bangladesh and Meghalaya region. As we have observed in the Chapter-1, the colder values of BT correlate well with the largest rainfall amounts over many regions but not essentially everywhere. Even though the amount of rainfall received in the Bay of Bengal during the pre-monsoon is relatively low, the average BT values over the bay are also very low. This shows that whatever little rainfall over the BoB during pre-monsoon season, is mainly contributed by high clouds. It is interesting to note that the BT values

overhead rainy pixels is becoming higher going from the east to the west and to the southwest through the equatorial region indicating the increasing fractional contribution of rain by more warm shallow clouds. Average BT values overhead and the west coast of Sumatra Island where the rain maximum occurs during the season lie in the range 240-246°K. Further off west of Sumatra, in the open ocean, the rain maximum is collocated with BT values above 250°K.

In the monsoon season, the hotspots of rain are shifted to the northern hemisphere, with the maximum located across the northeaster and central states of India and the west coasts of India, Myanmar and Thailand. The highest of clouds over the land region during the summer monsoon are present in the latitude belt 15-25$^{O}$N over Indian mainland and over Thailand, Vietnam and Laos. Clouds over the Myanmar land region and foothills of Himalayas are of lower height compared to that over the Bay of Bengal. The BT values are the lowest in the Bay of Bengal and the north central India (less than 245$^{O}$K). Clouds in the Arabian Sea are shallower as compared to the clouds in the Bay of Bengal. Off west coast of India, BT is comparatively warmer than in the off west coast of Myanmar and Thailand.

The location of maximum rain is in the southern hemisphere during the post monsoon season, with the focus of maximum rainfall located over and off west coast of Sumatra. Southeast coastal states of India receive rain during this season. Rainfall over the northeast states of India and Bangladesh is considerably law during this season. The average BT values over most parts of the Bay of Bengal is a little higher in magnitude (>250$^{O}$K) during this season as compared to the other two seasons. The only region in the Indian mainland where good amounts of rainfall is being received during all the three seasons is

the southwest tip of India. The clouds in this region are the deepest during the pre-monsoon season.

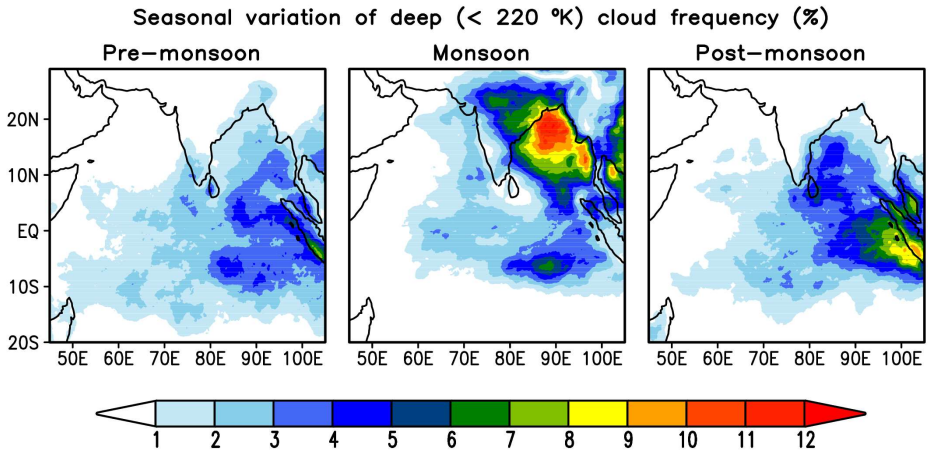


Figure 4.2. Seasonal variation of deep (<220°K) cloud frequency over the Indian monsoon region

To study the seasonal variation in the cloud types, we have presented the frequency of occurrence of three classes of BT values in which BT<220$^{O}$K represents deep to very deep clouds, BT value between 220 and 240$^{O}$K medium to high clouds and shallow clouds are represented by BT in the range 240-260$^{O}$K. Figure 4.2 provides the seasonal variation of cloud tops colder than 220$^{O}$K during different seasons.

In general, the deep cloud frequency is the maximum during the monsoon season followed by the post monsoon season. During the monsoon season, the maximum frequency of deep clouds is present in the head Bay of Bengal. Overhead the elongated monsoon trough, through which the depressions which usually originate in the Head Bay during the season would travel westward have considerable deep cloud presence. Deep clouds are almost absent in the south west regions of the peninsular India. Deep clouds occur in east central bay and east equatorial Indian Ocean.

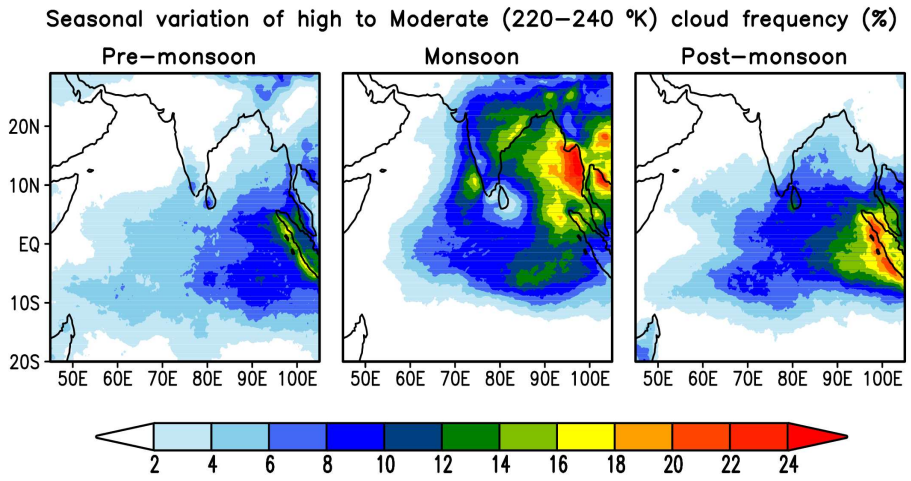


Figure 4.3 Seasonal variation of moderate to high (220-240 K) cloud frequency over the Indian monsoon region

During pre and post monsoon season, the maximum presence of deep to very deep clouds is witnessed over and off west of Sumatra. Noticeably such category of clouds are concentrated over and off west of south than the north Sumatra. Increased presence of deep to very deep clouds during pre and summer monsoon and their reduction during post monsoon season in the ECZ is noticeable.

Fig 4.3 provides the frequency of moderate to high clouds with top temperature ranging between 220 and 240 K. Over the Indian mainland and most parts of the northern Indian Ocean, the presence of clouds in this range is limited mostly to the summer monsoon season. During the season, the maximum concentration of medium to moderate clouds is in the east central Bay of Bengal, off west coast of Myanmar and Thailand. Off southwest coast of India, there is a region nearly between 10-15 N latitude where the concentration of moderate to high clouds is high. These clouds may be associated to the dynamically explained offshore troughs which is a significant feature of summer monsoon climatology as suggested by Grossman and

Durran (1984). It is interesting to note that despite the similarities in the orography and wind patterns off west of Western Ghats and the ArakanMountains of Myanmar, the cloud heights in these two regions significantly differ. While the clouds off west of Western Ghats largely remain shallow, that off west of Arakan prefer to grow deeper. It may therefore be assumed that this difference is brought about by the difference in the relative roles that the dynamics play in the two regions.

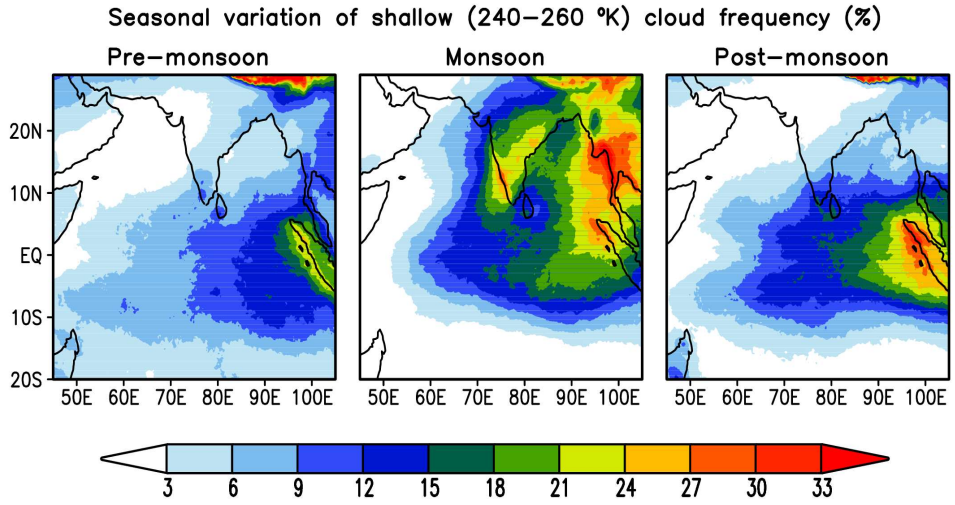


Figure 4.4 Seasonal variation of shallow (240-260 K) cloud frequency over the Indian monsoon region

During pre and post monsoon, distribution of clouds belonging in moderate to high category in the Sumatran region is sharing almost same spatial pattern but its magnitudes differ considerably. While clouds are present more frequently westward and northward from this region during post monsoon, their presence is comparatively confined to only the immediate proximity of this region during pre-monsoon season. It may be noted that compared to the deep to very deep clouds, the presence of moderate to high clouds play a lead role in the precipitation over and off west north Sumatra

during both these seasons. While concentration of moderate to high level clouds are high in the ECZ in south equatorial Indian Ocean (explained earlier) during pre and summer monsoon seasons, that of this category of clouds are less in the region during post monsoon season.

Figure.4.4 provides the frequency of occurrence of clouds in the BT range 240-260 K defined to favour our discussion as shallow. The concentration of clouds in this category along the west coast of India, during the summer monsoon season is noticeable. In most areas east of the Ghats where deep and moderate to high clouds are absent, shallow clouds is present in abundance. Prominent presence of this class of clouds in the eastern Bay of Bengal, over the land regions of Myanmar, Thailand and North Sumatra is evident. This category of clouds is prominently present over the Bangladesh, Meghalaya and other foothill regions of the Himalayas. However, the red patch in the Himalaya region that is present in all the three seasons is unlikely to be clouds. The normal surface temperature in the region may belong within in the range of threshold temperature used to define shallow clouds.

The pattern of shallow cloudiness during pre-monsoon and post monsoon is broadly similar to that of moderate to high cloudiness during pre-monsoon and monsoon season.

### *4.3. (b) Seasonal difference in extreme rainfall events*

In the present climate change scenario, incidents of heavy down pour over a short period of time is becoming more frequent over Indian region (Gadgil *et al.,* 2004, Francis and Gadgil 2004, Goswami *et al.,* 2006, Joshi and Rajeevan 2006, Rajeevan *et al.,* 2008, Krishnamurthy *et al.,* 2009 etc). Earlier studies of extreme rainfall events have used gridded daily rainfall from IMD or 3 hourly TRMM data sets. Here we introduce synergic use of 3 hourly

TRMM rainfall and hourly BT data to quantify the contribution of different categories of clouds associated with observed heavy rainfall events.

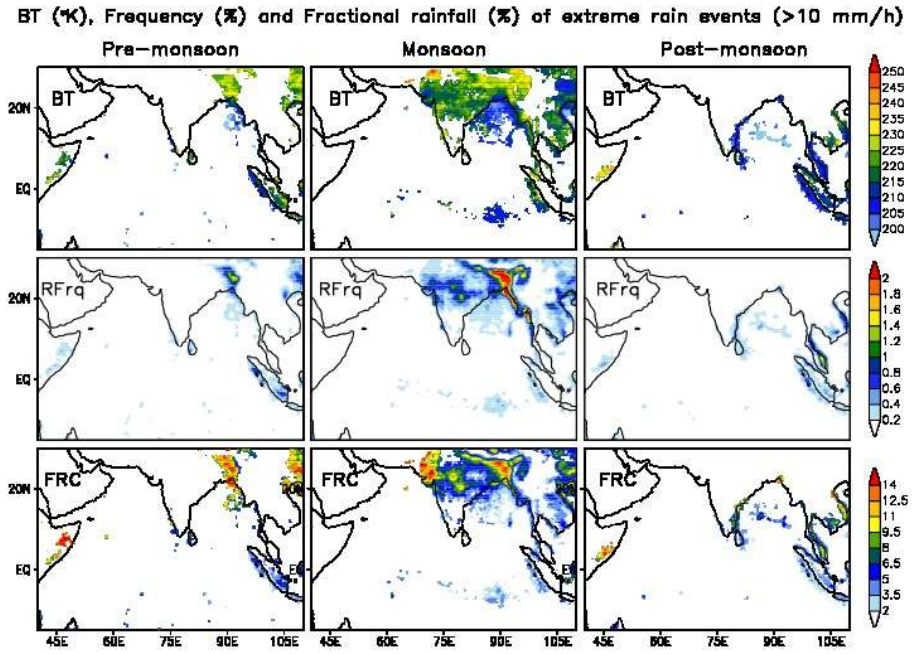


Figure 4.5.Brightness Temperature (BT from Kalpana-1 IR), Frequency of occurrence of events (RFrq from TRMM3B42RT) and fraction of rain contributed to the total (FRC TRMM3B42RT) associated of extreme rain events (hourly rain rate 10 mm and above) for pre, summer and post monsoon seasons for the period Oct 2012 to Sep 2017.

Figure.4.5 provides the spatial distribution of features corresponding to the cases where rainfall has exceeded 10 mm/hr during different seasons of the five years under the study. Top panel gives average BT, middle panel the frequency of rain events in percentage and the bottom panel the fractional contribution by the extreme rain events to the total seasonal rainfall. In general, it is over the land region that extreme rain events are more common as compared to the ocean. Northeast and central India is the two regions where rain events of this magnitude are more frequent. While the former witness

such events in the pre and summer monsoon period, the later experience such extreme events during the monsoon period alone.

Another region where extreme rain events are witnessed are southwest tip of India during pre-monsoon, west coast of India during summer monsoon and east coast of India during the post monsoon season. Over Ocean, while the Arabian Sea remain devoid of any such extreme rain events, northern and south central Bay of Bengal experience limited number of such heavy rain events during pre and post monsoon seasons respectively and almost entire of north and central bay experience extreme rain events during the summer monsoon season.

It may be noticed that the average BT values associated with extreme rain events over the land is a little higher than that over the Ocean. This signifies the presence of medium to high clouds contribution of extremes over land region during monsoon season  The west central region is the normal region where mid tropospheric cyclones (MTC) normally occur during the monsoon season. For producing extreme rainfall events of this category, the clouds need not grow deep. Instead, the continuous supply of moisture feeds the clouds to produce continuous rainfall of greater than 10 mm/hr during the monsoon season. However, the average BT values associated with to post monsoon extreme rains events in the east coast of India is the lowest and comparable to the same in the adjacent ocean.

Even though the frequency of extreme rain events are relatively less during any given season, the contribution of rain by such events to the total of the season is significant in many regions. For instance in the foothills of Himalaya, especially over the Bangladesh and Meghalaya, 15 % of seasonal rainfall is being contributed by extreme rainfall events during both the summer

and pre monsoon seasons. The North West states of India receive a considerable amount (more than 15 % of the seasonal total) in the form of extreme rain during the monsoon season.

Apart from India, the noticeable regions where extreme rains occur are west coast of Myanmar and Thailand (during pre and summer monsoon), over and off west of Sumatra (during all three seasons), and the east Somalia coast (during pre and post monsoon). During the monsoon season, further off west of Sumatra nearly coinciding the 90 E longitude and 8 S latitude is a confined region (we earlier identified an ECZ) where instances of heavy rain events and corresponding low BT values are concentrated.

### *4.3. (c) Active and Break Spells of monsoon and associated cloud features*

Intra seasonal variation in rainfall in the monsoon trough zone had been identified far long ago. Blandford in 1886 first used the term 'during the heights of rain' to indicate periods of large-scale rainfall over the Indian monsoon zone and 'intervals of drought' to indicate interruption of rainfall for several days in the peak monsoon months of July and August. These two terms have been later identified as 'Active' and 'break' in the monsoon by Indian meteorologists for over a hundred years and numerous studies have helped to explore different aspects of Active and Break spells (eg. Ramamurthy 1969; Raghavan 1973; Krishnamurti and Bhalme 1976; Alexander *et al.,* 1978; Sikka 1980; Rodwell 1997; Webster *et al.,* 1998; Krishnan *et al.,* 2000; Krishnamurti and Shukla 2000, 2007, 2008; Annamalai and Slingo 2001; Goswami and Ajayamohan 2001; Lawrence and Webster 2001; De and Mukhopadhyay 2002; Gadgil and Joseph 2003; Goswami *et al.,* 2003; Waliser *et al.,* 2003; Kripalani *et al.,* 2004; Wang *et al.,* 2005; Mandke *et al.,* 2007; Suhas *et al.,* 2013 etc).

Table. 4.1. Active and Break days during the five year (2013-17) period selected for the analysis.

| Year | Active Days | Break Days |
|---|---|---|
| 2013 | 11-13 July<br>20-22 July | 25-27 August |
| 2014 | 19-23 July<br>29-31 July,<br>4-6 August | 8-10 July<br>15-21 August |
| 2015 | 25-29 July | 13-15 July<br>6-10 Aug<br>21-25 August |
| 2016 | 2-6 July<br>9-12 July<br>2-6 August | - |
| 2017 | 23-25 July | 31July-7 August<br>15-17 August |

After providing a detailed review of various definitions and methods of classifications adopted in previous studies, Rajeevan *et al.,* (2010) have provided a reasonable objective method for identifying the Active and break events based on gridded IMD4 rainfall data. We have adopted a similar method, but with a slight difference in the area of core monsoon zone. Detailed analysis of the rainfall patterns in the core monsoon zone during the active and break phases of monsoon and have suggested that the revival from breaks occurs primarily from the northward propagations of the convective cloud zones (Rajeevan *et al.,* 2010). Earlier works on Intra Seasonal Oscillations' (ISO's) utilises either rainfall, OLR or wind data in

characterising the time evolution of the Active and Break phases. In this study, we have extensively used the BT values in conjunction with rainfall to understand the role of different types of clouds during each phases and their transition periods. The study analyse the BT data to understand more on the cloud characteristic during the AB spells occurred during the recent five years. For the analysis, clouds are grouped into two, based on threshold temperatures (TT). Group-1 clouds are deep to very deep with TT<220$^{O}$K and group-2 clouds include shallow to medium and high clouds with in TT ranging between 220 and 255$^{O}$K.

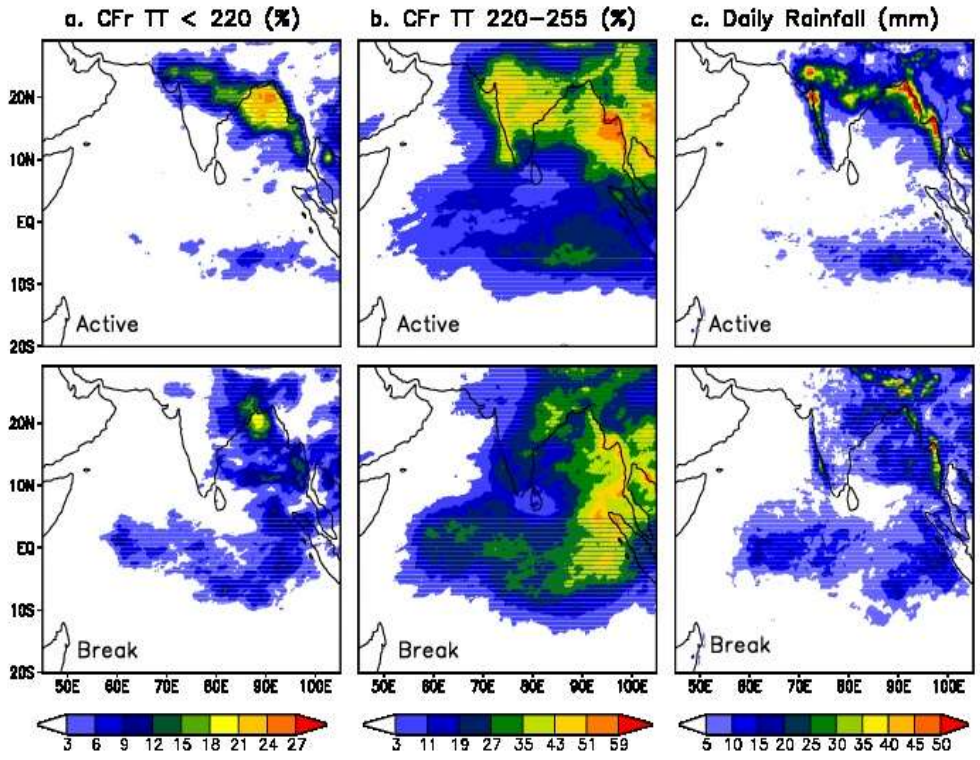


Figure 4.6. Composites of (a) Frequency of cloud top colder than 220$^{O}$K (b) Frequency of cloud top between 240 and 255$^{O}$K during and (c) Daily averaged TRMM3B42RT rainfall during active (top) and break (bottom) periods.

Fig.4.6 provides the cloud frequency (CFr) of group-1 clouds (left), group-2 clouds (centre) and the average daily TRMM3B42RT rainfall (right) during active (top panel) and break (bottom panel) situations. It may be noticed that the active period is characterised by abundant presence of group-1 and group-2 clouds and heavy rainfall in core monsoon zone. Group-1 clouds become almost absent in central and southern Bay of Bengal. This indicates that rainfall during Active phase is mostly contributed from both group-1 and group-2 categories. The rainfall is maximum over the Indian land region along the monsoon trough, central western states and the west coast. Rainfall is found to peak along and off west coast of Myanmar and Thailand during the active periods. While the major type of clouds present in the Head Bay is group-1 during the period that along the eastern boundary of central Bay of Bengal is group-2 clouds. Group-1 clouds are almost absent in the peninsular India south of nearly 15$^{O}$N but group-2 clouds dominates in these areas and west coast of India.

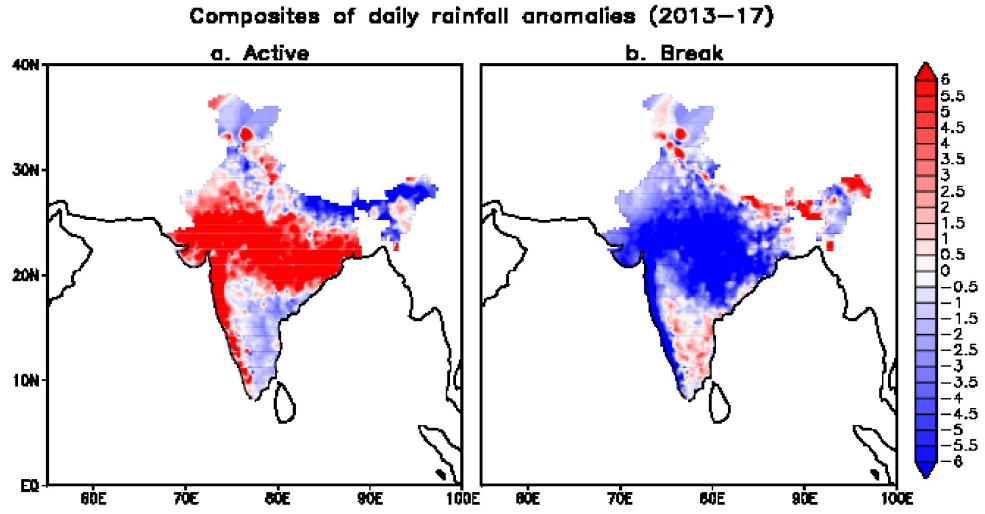


Figure.4.7. Composites of daily rainfall anomalies for the period 2013-17 during (a) Active and (b) Break spells.

During the break situation, maximum rainfall appears near to the foothills of Himalaya. There is substantial reduction in group-1 and group-2 cloud amounts nearly west of 80°E during the break period. The presence of group-1 clouds is limited to the northern most regions of Bay of Bengal and spreads to the foothills and a little eastward over the land regions of Bangladesh, Meghalaya and Assam. There is considerable increase in group-1 and 2 clouds in the longitude belt $10^{O}$S to $5^{O}$N. The eastern portion of maximum cloud zone has spread more to the south and become prominent. In general, during active (break) period, there is a general reduction (enhancement) in group-1 and 2 cloud amounts in all comparable latitudes and longitudes of the south equatorial ECZ, but there is not much of change in such cloud amounts overhead the ECZ as such during either of these periods.

Anomaly composites of IMD gridded daily rainfall (available only over the land) during the active and break periods are provided in Fig.4.7. Evidently, anomalies during Active and Break periods are mirror images. Positive (negative) anomalies are precisely present over the core monsoon zone and west coast of India during active (break) situations. The negative anomalies present during Active near to the foothills of Himalayas become positive during Break. Over the rain shadow regions in the southern peninsula also, there is change of sign of rainfall anomalies from negative to positive switching from Active to Break. However, rainfall amounts over rain shadow regions is only little during summer monsoon season.

Composite spatial and temporal structure of the Active and Break phases with respect to core monsoon zone and its transitions before and after the peak A-B days are studied using methods similar to that by Rajeevan *et al.,* (2010).

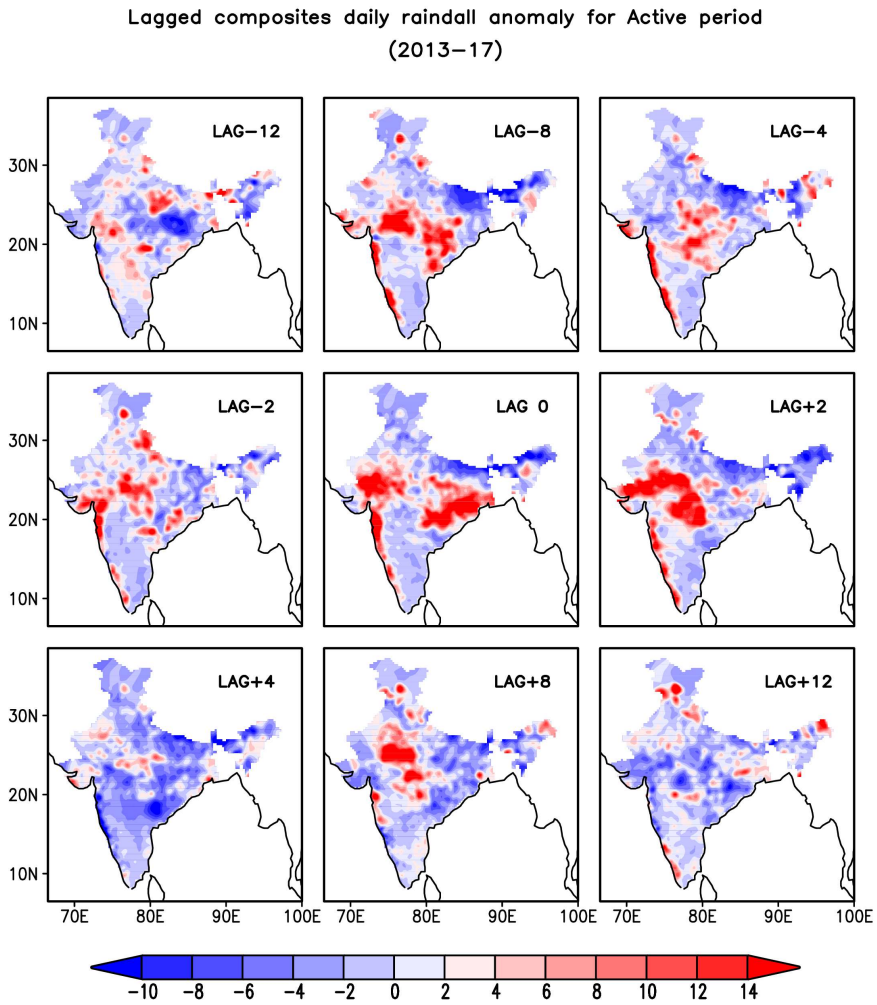


Figure4.8. Lagged composites of daily rainfall anomalies during the active spells (2013-17)

Composite evolution of rainfall anomaly starting from 12 days before and 12 days after the Active and Break days are presented in Fig.4.8& 4.9. Commencement of active phase typically starts from the break condition as evident from the rainfall anomaly composite 12 days prior to peak active days (Fig.4.8). Then the arrival of active phase first visible as positive rainfall anomaly over the southwest peninsular Indian and south central Indian region about 8 days prior to the peak active days over the central India. Afterwards, it

slowly spread to central Indian region during 4 to 2 days prior to the peak active days. At lag-0 (exactly the central day of the peak active spell), positive rainfall anomaly is mostly established over the central Indian region. This is followed by the migration of positive rainfall anomaly towards the northern region and a transition from Active to Break phase starts at about 12 days after the peak active days. The reverse is true for the break phase (Fig 4.9).

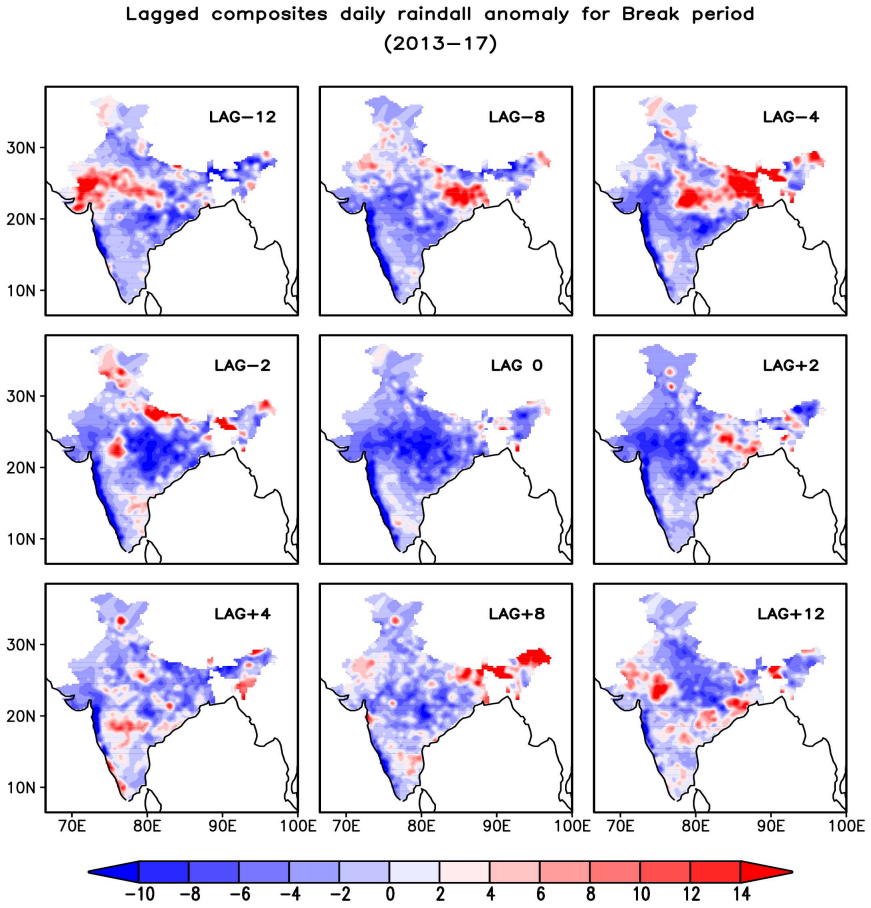


Figure 4.9. Lagged composites of daily rainfall anomalies during the Break spells (2013-17)

The spatiotemporal evolution of two dominant class of clouds prior to and after the peak Active and Break phases are presented in the following

sections. Fig 4.10 &4.11 presents the composite spatio-temporal evolution of group-1 & 2 clouds (described in previous section) respectively, centred on the peak Active and Break days. This analysis will provide more insight into the contribution of different types of organised clouds on the spatial and temporal evolution of the monsoon intraseasonal oscillations, particularly in modulating the Active and Break phases. The monsoon ISO's are mostly convectively couple process and a need exists to understand its link to the different types of organised convection (Chatopadyay *et al.,* 2009). Role of deep and stratiform convection in monsoon ISO's is largely discussed in many studies (Tian *et al.,* 2004, Stano *et al.,* 2002, Houze *et al.,* 2007, Chattopadyay *et al.,* 2009). Apart from deep and stratiform fraction, we explored the role of shallow to high clouds in the time-space evolution of different phases of ISO's namely, Active and Break spells.

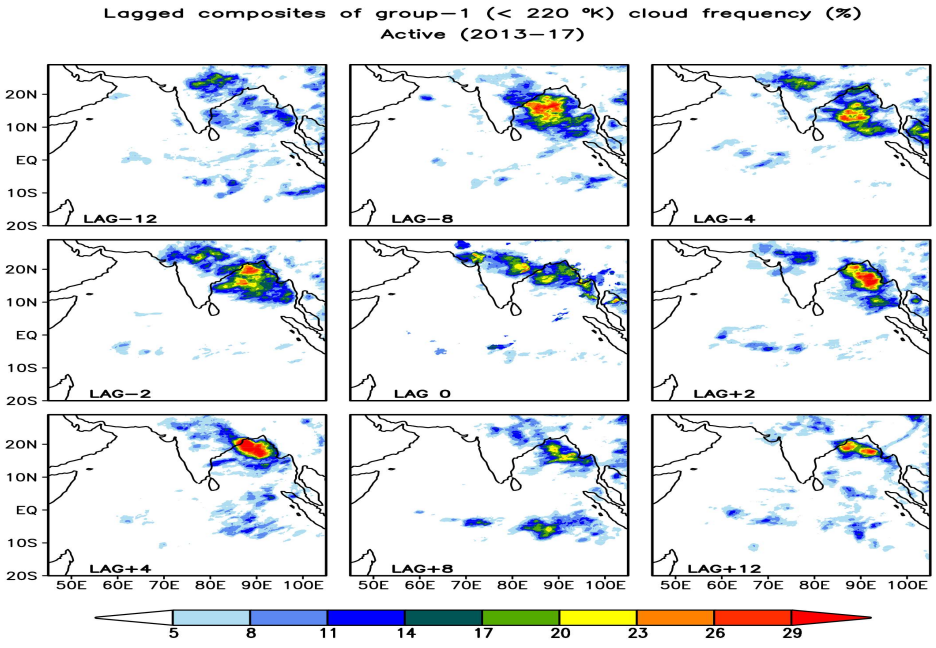


Figure 4.10. Lagged composites of group-1 (TBT <220$^{O}$K) cloud frequency during Active spells (2013-17)

It is seen from Fig.4.10 that, deep clouds start to form over the head Bay region almost 8 days prior to the peak active days. This region of maximum deep clouds moves north-westward towards the east coastal regions during 4-2 days prior to the establishment of active phase over the central Indian region. During the established phase of active spell over the central Indian region, there exist three prominent sub regions of deep clouds, one over the western central India over Gujarat, another over the eastern central India and another maximum zone over the north central Bay of Bengal. Subsequently, deep clouds dissipate over the central Indian region and maximum occurrence is more shifted towards head Bay and along eastern portions of the foothills, where monsoon trough shift during the transition to Break condition.

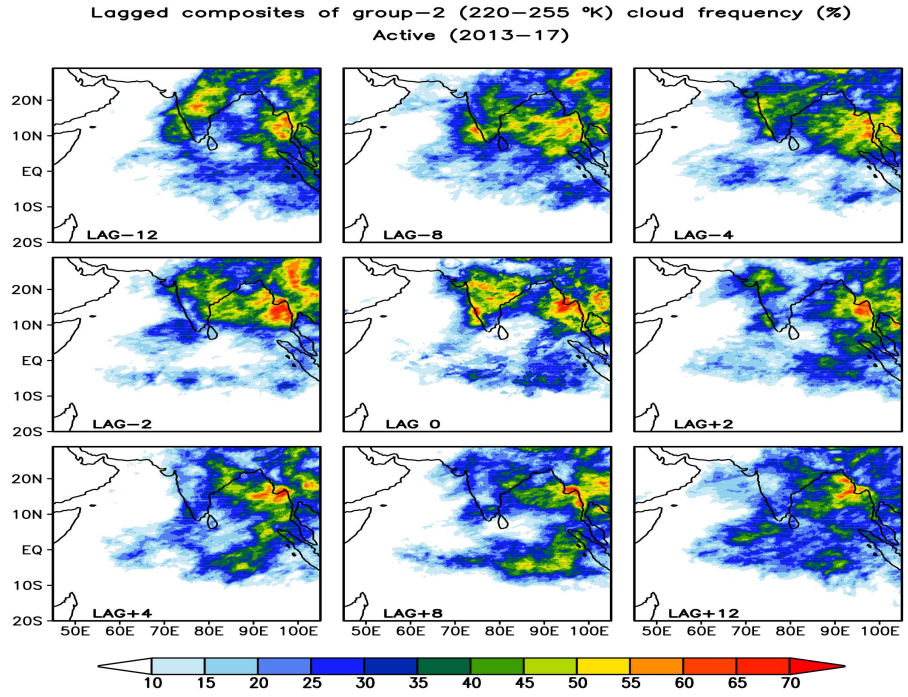


Figure 4.11. Lagged composites of group-2 (TBT 220-255$^{O}$K) cloud frequency during Active Spells (2013-17)

As seen in Fig.4.11, shallow to high clouds begin to grow over the south Bay of Bengal and over southwest peninsular Indian region around 8 days prior to the establishment of Active phase. Then, this shallow to high convection band shifts towards north to the northern peninsular India and to southern central Indian regions during 4-2 days prior to the peak active days. During Active phase, though presence of deep clouds is confined mostly over the monsoon trough region, shallow to high clouds are present almost everywhere over the southern peninsula and central and northern peninsular India. This clearly shows that, deep convective clouds mostly move west to north-westward prior to the establishment of Active phase. However, shallow to high clouds mostly propagates northward. These two cloud types and their distinct propagation characteristics are together contributing to the established phase of Active spells over Indian region.

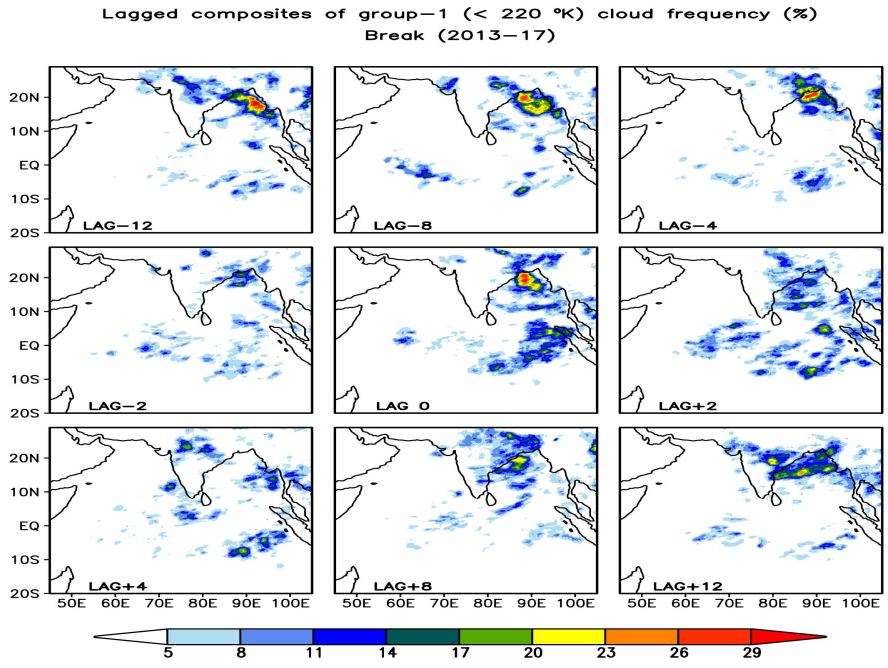


Figure 4.12 Lagged composites of group-1 (TBT< 220$^{O}$K) cloud frequency during Break spells (2013-17)

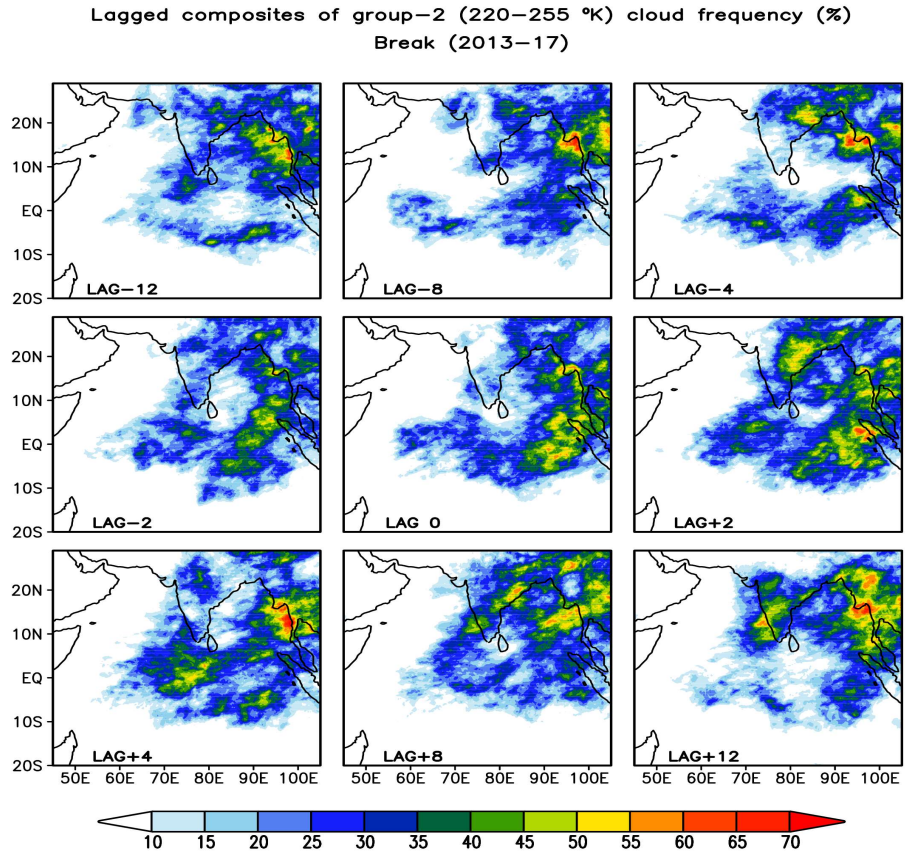


Figure4.13. Lagged Composites of group-2 (TBT 220-255$^{O}$K) cloud frequency during Break Spells (2013-17)

Spatio-temporal evolution of the break spells provided in Fig.4.12& 4.13 reveals the distinct type of clouds that dominates in the two major limbs of cloud bands that appear during the break condition (lag-0). Deep clouds are located in the North Bay of Bengal and foothills of Himalaya whereas shallow to high type clouds dominate the east equatorial limb. Eight days prior to the lag-0 day of break, most of the deep clouds from the central Indian region have disappeared and the concentrations of deep clouds are witnessed in the Head Bay. From lag-2 to lag+2, deep clouds tend to spread further to the north and east along the foothills of Himalaya. From lag+4, deep clouds starts to re

appear in isolated placed over the central India. By lag+12, a transition condition from break to active starts in the form of fresh development of deep convective clouds over Bay of Bengal that may eventually lead to the beginning of active phase as similar to lag -12 of active composite. From the spatio-temporal evolution of shallow to high (group-2) clouds, as the cloud band shift towards foothills, simultaneous re-emergence of fresh shallow to high clouds over South Equatorial Indian Ocean (SEIO) is also seen from lag-8 onwards. By about lag-4 day, shallow to high clouds begin to spread over a large region of SEIO and by lag 0, the maximum of shallow to high clouds appear over this region. By lag+4 day, the location of the maximum of group-2 clouds move further north and at about lag +12, a condition similar to lag -12 day of active condition establishes over Southern Peninsula India and south east bay of Bengal. This explains the role of shallow to high clouds in the time-space evolution and observed temporal and spatial scales of Active to Break and Break to Active transition observed over Indian subcontinent and adjoining oceanic region.

## 4.4. Conclusions

Prominent cloud features over the Asian monsoon regions during different seasons was explored using INSAT brightness temperature data. In general during the pre and summer monsoon seasons, deepest of clouds occur over the north and central Bay of Bengal. During the post monsoon season, deepest clouds are present in the east equatorial Indian Ocean and over Sumatra Island. The height of clouds in the Bay of Bengal during the post monsoon season is a little lower compared to the other two seasons. The Indian mainland is largely covered by clouds during the summer monsoon season. The highest of clouds over the Indian mainland during the summer

monsoon season are present in the latitude belt 15-25$^{O}$N. Over the Arabian Sea and off west of west coast of India, prominent rain producing clouds are shallow to high rather than deep. Rain producing clouds in the western equatorial Indian Ocean are mostly shallow during all seasons.

Analysis of seasonal variation of extreme rainfall events revealed that such events are more frequent over the land as compared to ocean. West central and central states of India experience frequent extreme rain incidents during the summer monsoon season. Northeast states of India receive extreme rainfall during both the pre and summer monsoon seasons. During all three seasons, extreme rain events occur over the southwest tip of India. Southeast coastal states of the country are prone to extreme rain events during the post monsoon season. Extreme rainfall significantly contributes to the total rain obtained in a season over the northeast and northwest states of India and some regions of central India.

Spatio-temporal evolution of active and break events are studied for the first time using brightness temperature data. The most significant inference from the analysis is the differential behaviour of very deep and shallow to high clouds during the Active phase of Indian summer monsoon. Deep convective clouds move west to north-westward whereas shallow to high clouds mostly propagates northward. These two cloud types and their distinct propagation characteristics are together contributing to the Active spell over Indian region.

# Chapter-5

# Diurnal Variation of Convection over the Indian Monsoon Region

## 5.1. Introduction

Satellite observations are the primary source of large scale information on clouds. Diurnal variation of cloudiness can be efficiently studied using geostationary satellites as they provide continuous observational coverage over the same geographical area. The infrared (IR) radiances give brightness temperature (BT) of the top of the clouds day-and-night. Lower values of temperature are a measure of enhanced convective activity. Indian region has continuously been monitored by INSAT series of geostationary satellites since 1982. The Indian Meteorological Department (IMD) had shared INSAT IR imageries for a short period (1988-89) with the National Centre for Atmospheric Research (NCAR) and this data set has been extensively used for many studies (eg. Gambeer and Bhat, 2000 and 2001; Roca and Ramanathan, 2000; Zuidema, 2003; Roca *et al.,* 2005 etc). Limited public availability of INSAT data had necessitated many studies to depend on alternate sources for observational data such as the European Meteosat-5 (eg. Krishnamurthi and Kishtawal, 2000; Wonsick *et al.,* 2009), the Japanese Geostationary Satellite (GSM) (eg. Murakami, 1983; Sui *et al.,* 1997) or the multiple satellite projects such as European Union Cloud Archive User Service (CLAUS) (eg. Yang and Slingo, 2001). Data from polar orbiting satellites like Tropical Rainfall Monitoring Mission (TRMM) (eg.Sorooshian *et al.,* 2002; Sahany *et al.,* 2010), Defence Meteorological Satellite Program (DMSP) Special Sensor

Microwave Image (SSM/I) (eg. Janowiak *et al.,* 1994) etc. have also been utilised for various studies. However, thanks to its suitable overhead position (74ºE longitude), INSAT remains as the ideal source of data for the analysis of cloud features in the Asian summer monsoon region.

INSAT IR BT data from 2009 have been made available by Meteorological and Oceanographic Satellite Data Archival Centre (MOSDAC) of Indian Space Research Organisation (ISRO). In this chapter, we attempt to carry out an analysis of the rarely utilized hourly Brightness Temperature (BT) data sets from the Kalpana-1 satellite over a period of 5 years to derive features of the diurnal variation of convective activity over the Indian subcontinent and surrounding oceanic region during pre (March-May), summer (June-September) and post (October-December) monsoon seasons. Further, the results are compared with TRMM 3B42RT three hourly rainfall to get a clear image of the prominent spatio-temporal features of cloud-rain associations with special emphasis on diurnal evolutions.

Convection and associated cloudiness and precipitation exhibit variation on diurnal to seasonal and inter-annual time scales. Among the various time scales of tropical clouds, Diurnal Variation (DV) is highly prominent and perhaps the most fundamental of all (Nitta and Sekine, 1994; Hall and Von der Haar, 1999). Diurnal variability in convection and rainfall may be associated with one or a combination of varying reasons such as intense surface heating, topography, the advance of a sea breeze front, the convergence of sea–land breezes, mountain and valley winds, interactions of local circulations with synoptic flows, and perhaps night-time cooling of cloud tops. The diurnal variations of tropical deep convection and precipitation play an important role in modulating energy budget of climate systems (Bergman,

1997). Several authors (e.g., Imaoka and Spencer, 2000; Sorooshian *et al.,* 2002; Nesbitt and Zipser, 2003; Yang and Smith, 2006; Basu, 2007) have used a single year or few years of satellite or station based rainfall data for their studies so that generalisations of the results to a reasonable extent is difficult.

In a pioneering study using ground based observation Grey and Jacobson (1977) have demonstrated that diurnal variation in convective activity is highly prominent in the tropical regions. They have found that a diurnal cycle is more evident when the deep convection is intense and associated with organised weather systems. Among the various studies, some (e.g., Hendon and Woodberry, 1993; Janowiak *et al.,* 1994; Chen and Houze, 1997) conclude that the convective maximum preferentially occurred during late afternoon/early evening over land and in the early morning over the open oceans while some others (e.g., McGarry and Reed, 1978; Shin *et al.,* 1990) showed an afternoon maximum in precipitation over the oceans.

Many authors have studied the diurnal variation of precipitation over India (eg. Prasad 1970, 1974; Bhattacharya and Bhattacharyya 1980; Halder *et al.,* 1991; Puri *et al.,* 1994; Basu 2007 etc.). Ohsawa *et al.,* (2001) using station and remotely sensed observations of rainfall in tropical Asia reported that the maximum convective activity occurs during the early evening over land and late night/early morning over coastal regions and windward sides of mountains. Roca and Ramanathan (2000) have provided diurnal statistics of convective systems with respect to the cloud size for January 1989 and conclude that diurnal cycle depends significantly on scales and exhibits complex patterns.

Using Meteosat-5 IR data, Wonsick *et al.,* (2009) showed that coldest convection occurs in the earlier hours over the ocean and in the later hours over the land. Mahakur *et al.,*(2013) using three hourly outgoing longwave radiation (OLR) estimated from Kalpana-1 VHRR for the period 2004-2012 showed that the amplitude of the diurnal variations over the continents is more pronounced compared to that over the oceanic areas. Gambeer and Bhat (2001) observed that the largest DV of convective systems are evident at coldest temperature thresholds (201K) while the DV is weaker but broadly similar at warmer thresholds used (221, 241 & 261 K). Zuidema (2003) showed a distinct spatial grouping of convective systems by size over the Bay of Bengal. Size of convective systems over the east side of the Bay was found relatively small, short lived, and frequent. She further reported that offshore nocturnal convection begins near shore and that later convection occurs farther out over the Bay and attains a larger size. Using TRMM precipitation estimates, Mao and Wu (2012) have explored further features of the diurnal variations in the Bay of Bengal and observed a distinct zonal propagation of the diurnal phase. The maximum precipitation zone originates from the land-sea boundary of the eastern coast of the Indian peninsula at around 0300 LST, and then propagates eastward with increasing time to reach the eastern coast of the BOB on 1800 LST, finally migrates into the Indochina continent on about 2100 LST.

Hirose and Nakamura (2005) investigated the diurnal variation of precipitating systems by examining the fine spatial distribution of rainfall amount and scale-based systems using TRMM PR data. They found that, over India, small systems prevail in the early afternoon, and large systems become relatively dominant in the evening. They have observed that large systems

disappear off the western shore (the windward side of the Western Ghats) in the late afternoon.

Cloud cover, cloud radiative temperature, and clear sky radiative temperature have an impact on the earth's radiative balance (Harrison *et al.,* 1990). Brightness temperature of clouds is one direct parameter to study the properties of clouds. In most of the diurnal variation studies, precipitation or outgoing long wave radiation is used as the prime parameter for the analysis and the temporal resolution of data is usually 3 hourly or less. The objective the present analysis is to understand more of the diurnal variation of cloudiness and rainfall over Indian region during different seasons using high spatio-temporal resolution BT datasets.

## 5.2. Data and Methodology

The INSAT Kalpana-1 hourly infrared brightness Temperature (IRBT) and TRMM 3B42RT data with a spatial resolution of 0.25x 0.25$^{O}$ for the period October 2013 to September 2017 is used for the present study. A subset of data is prepared for the Indian region such that the grid points of 3B42RT coincide exactly with that of INSAT so as to use for pixel to pixel comparison between rain rate and corresponding cloud types.

### *5.2.1 Threshold Temperatures*

A range of temperature thresholds can be seen in the IR satellite literature like the ones summarized in Mapes and Houze (1993) and Machado *et al.,* (1998). In general, temperatures close to 255$^{O}$K are considered as upper threshold limit of convective type of cloudiness in most of the previous studies (Kulkarni *et al.,* 1993, 1997; Roca and Ramanathan, 2000; Machado *et al.,*

1992). For the present analysis, three temperature thresholds are employed. BT values less than 220$^{O}$K represents very deep, 220-240$^{O}$K for moderate to high and 240-260$^{O}$K for shallow convective clouds. For preparing seasonal averages of brightness temperature, values less than 255$^{O}$K only are considered to obtain reasonably high cloud fraction matching the pattern of rain in all seasons and to exclude cloud free conditions. This does not implicate the absence of rain bearing clouds above these threshold values. There are regions in the Indian monsoon field such as the south west Indian Ocean where considerable amounts of light precipitation is resulted by very shallow clouds with cloud top temperature (CTT) as warm as 280$^{O}$K and above (Vijaykumar *et al.,*2017). For providing hour of maximum frequency of clouds with top temperature less than 240 $^{O}$K, a 'cut off' minimum frequency (10%) is used to obtain realistic spatial pattern of peak convection.

All types of clouds present in the sky have been considered for certain analyses in this study. A cloudy pixel is identified using the method similar as to the one described by Shah *et al.,* (2010). The assumption is that any pixel in the image will not be covered by cloud for several days. So, the maximum BT value of each pixel (BT max) in a given season is discovered first. It will represent the cloud free condition over its location, preferably when the temperature at the surface is the maximum. Further, it is assumed that the maximum surface temperature does not vary much during a season. For the Indian land region, where the sub regions are considered for detailed analysis, a variation of 15 $^{O}$K is attributable to normal diurnal change in surface temperature but a drop in observed temperature greater than 15 $^{O}$K from the cloud free condition (BT max) is considered as clouds. Over ocean, since the temperature variations on diurnal scale is comparatively less as compared to

the land, 6 $^{O}$K drop in temperature from the cloud free condition (BT max) is considered as cloud.

### *5.2.2 Sub-regions for studying rain intensity classes and cloud types*

Eight 1 x 1$^{O}$ latitude-longitude boxes comprising of 25 pixels each are considered over (a) Close to and Off west of Southwest India over the Arabian Sea (b) Southwest of India over land, (c) Central India, (d) East of central India, (e) west Head Bay of Bengal, (f) Central Bay of Bengal, (g) Off west of Thailand over the east central Bay of Bengal and (h) Over the Thailand land regions. Three rain intensity classes are defined based on the TRMM 3B42RT rain rate. The classes are (i) Light (< 2 mm/hr) (ii) Moderate (2-4 mm/hr) and (iii) High (>4 mm/hr). Three classes of clouds are defined based on IR BT Thresholds namely, (i) deep clouds (<220$^{O}$K), (ii) Medium to high clouds (220-240$^{O}$K), (iii) Shallow clouds (240-260$^{O}$K) and (iv) Warm clouds (260$^{O}$K to maximum threshold defined for a cloud). The contribution to the total rain by the different intensity classes of rain and the classes of clouds co-existing with the rainy pixels at each of the boxes during different hours of the day is studied. Since the TRMM 3B42RT is three hourly and the Kalpana-1 BT hourly, the Kalpana-1 data for three consecutive hours centred on the rainfall data hour is used to calculate the fractional contribution by each cloud type.

## 5.3. Results and Discussions

The Brightness temperature (BT) values obtained from IR channel are physical equivalents of temperature of the emitting surface. When the sky is cloud free, the emission will be from the surface of the earth and when the clouds are present, the emission will be from the top of the topmost clouds.

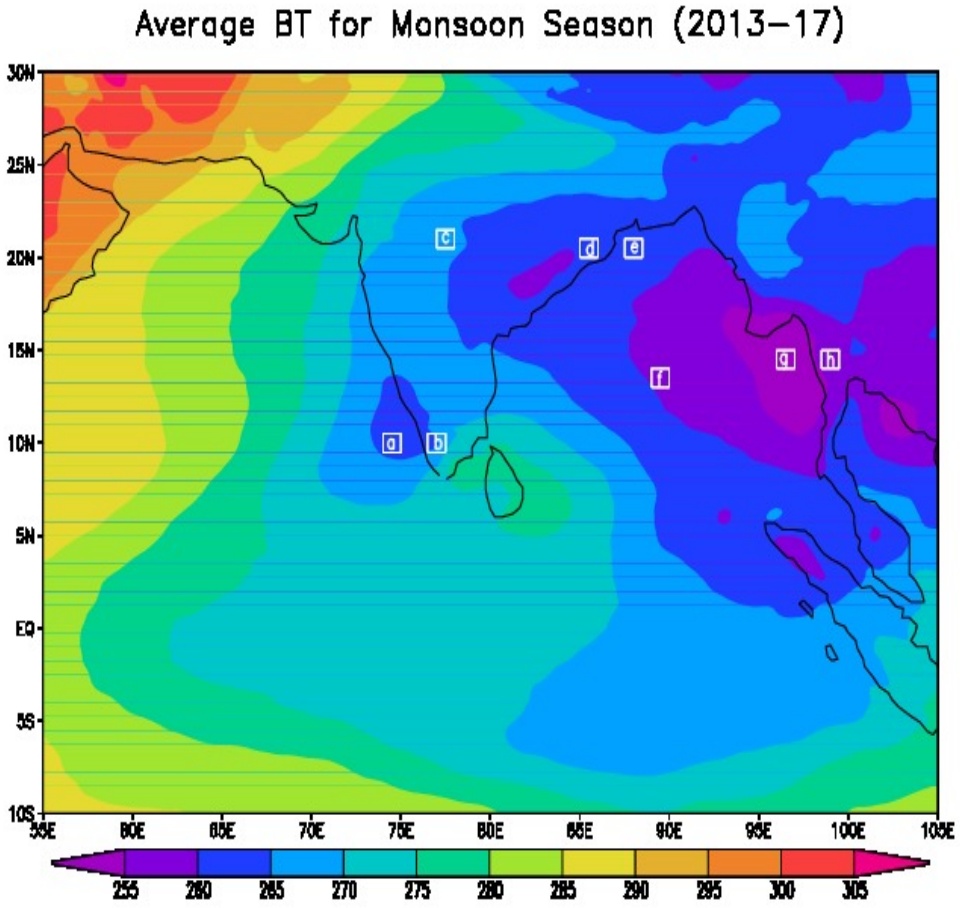


Figure 5.1 Average Brightness Temperature (BT) for the monsoon seasons (JJAS) for the period 2013-17. The boxes marked from (a)-(h) are the sub regions used for studying diurnal variation in rain intensity classes and cloud types in detail during the monsoon season**.**

Since clouds over a location may appear, disappear and exhibit large horizontal and vertical fluctuations from scene to scene of satellite observations, averaging of BT values will make it difficult to explain cloud feature physically. However, large scale features of cloudiness can be derived directly from the average BT values. Figure 5.1 provides the average BT for the monsoon seasons of 2013-17. The lowest of average BT is observed over the north east Bay of Bengal and the land area east of it. The BT is low over

most parts of the bay, north east and east central India and off south west of the Western Ghats. To distinguish between cloudy and non-cloudy condition and to define frequency of occurrence of various type of clouds, we employed different BT thresholds values as briefly explained in the methodology section. Sub regions marked as (a)-(h) in the figure 5.1 are used for studying diurnal variation of vertical extensions of cloud tops in detail.

### *5.3.1 Seasonal Variation of average IR Brightness Temperature (colder than 255$^{O}$K)*

Figure 5.2 provides seasonal variation of average Brightness temperature in the Indian subcontinent and the tropical Indian Ocean overlaid with the frequency of cloud occurrence. In order to exclude low level clouds and cloud free conditions, only BT values colder than a threshold temperature of 255$^{O}$K is considered for averaging. Further, it is assumed that all clouds with top temperature <255$^{O}$K are convective in nature for convenience of the discussions in this chapter. Such assumptions are in tune with the results of some previous works (Roca *et al.,* 2005). During the peak monsoon months the Indian region is widely cloudy whereas less amounts of clouds appear over the Indian mainland and the Arabian Sea during the pre and post monsoon seasons.

One prominent feature revealed regarding the cloudiness from the average BT is that, over the Bay of Bengal, the position of cloud tops are the deepest irrespective of the seasonal variations in the frequency of occurrence. Along the west coast of India and Myanmar, the two hotspots of rainfall during the peak monsoon months, the average BT is a little higher than that over the head Bay of Bengal. This confirms that the vertical extension of

clouds is not in proportion to the enormous amounts of rainfall obtained in these regions. The rainfall in these regions is more of the result of orography, where the mountain walls serve as impediment to the humid air that blows from the warm Arabian Sea and the Bay of Bengal. Over the southwest tip of India, where considerable rainfall is received during all three seasons, pre monsoon has the coldest of temperatures, indicating higher depth of the towering cumulonimbus which contributes the rainfall in this region during the season. Among the three seasons, it is during the post monsoon that the BT values over the Southeast coastal India appear the minimum. This is the main rainy season over the region.

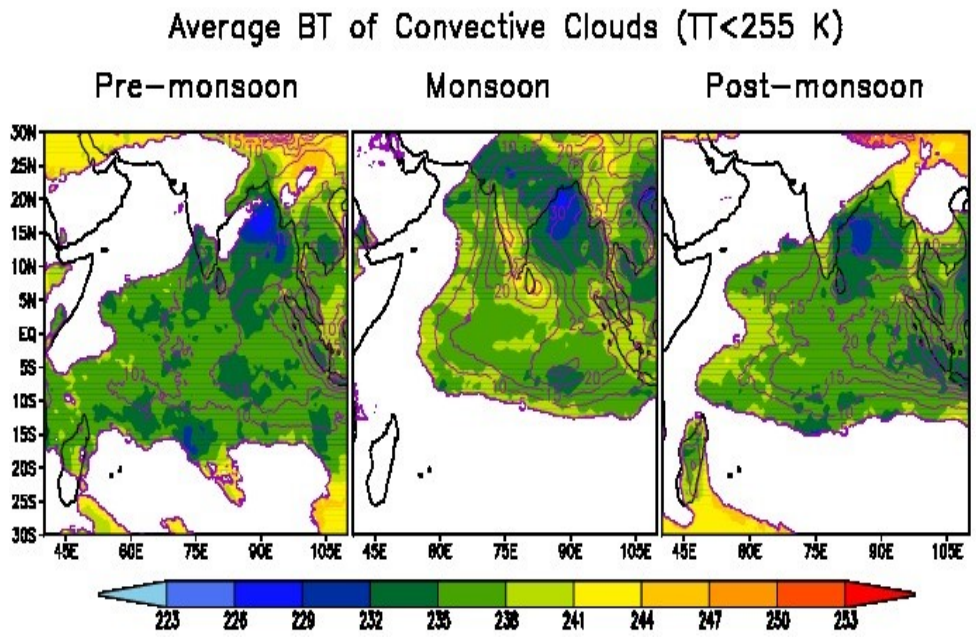


Figure 5.2. Five year average brightness temperature (BT) of convective clouds during pre-monsoon (MAM), monsoon (JJAS) and post monsoon (OND) seasons overlaid with the frequency (%) of occurrence. BT values >255$^{O}$K are ignored to eliminate low laying clouds. Less frequent (<5%) cases are considered as noise and is masked.

Low BT values in the enhanced cloud zone (ECZ, described in previous chapters) of equatorial Indian Ocean is prominent during pre and summer monsoon seasons.

### *5.3.2. Frequency of occurrence of deep convective clouds*

The frequency of occurrence of different types of clouds is presented. The deepest of clouds are considered of having BT values < $220^{O}$K. Moderate to high clouds have BT values exclusively ranging in between 220 and $240^{O}$K. Clouds with top temperature between 240 and $260^{O}$K are considered as shallow convection but the results are not presented since the pattern is weaker and broadly similar to the case of moderate to high clouds.

#### *5.3.2 (a) Pre monsoon Season (MAM)*

In discussions to follow, the time of satellite observation is expressed in Greenwich Mean Time (GMT). As we have considered a larger area, there will be regional differences in local standard times (LST). The local time corresponding to 00:00 GMT over India is 05:30 LST.

The spatial pattern of diurnal variation of deep convection during pre-monsoon period is provided in Figure 5.3. During the season, the frequency of occurrence of very deep convection is low as compared to the monsoon season (discussed in following sub-section), but the diurnal variation in deep convection is largely evident. Throughout the season, deep convective clouds are mostly absent over the Indian mainland excepting a small area at the southwest tip of the peninsula and some regions over the north-eastern states. Large diurnal variability is present in deep convection in these regions. Up to 09:00 GMT, deep convection is limited to the oceanic regions and is found

widely over the equatorial Indian Ocean and east central Bay of Bengal. By 11:00 GMT, convection appears to begin at the southwest tip and over the northeast coastal regions of India and Bangladesh coinciding with considerable decrease in oceanic convection.

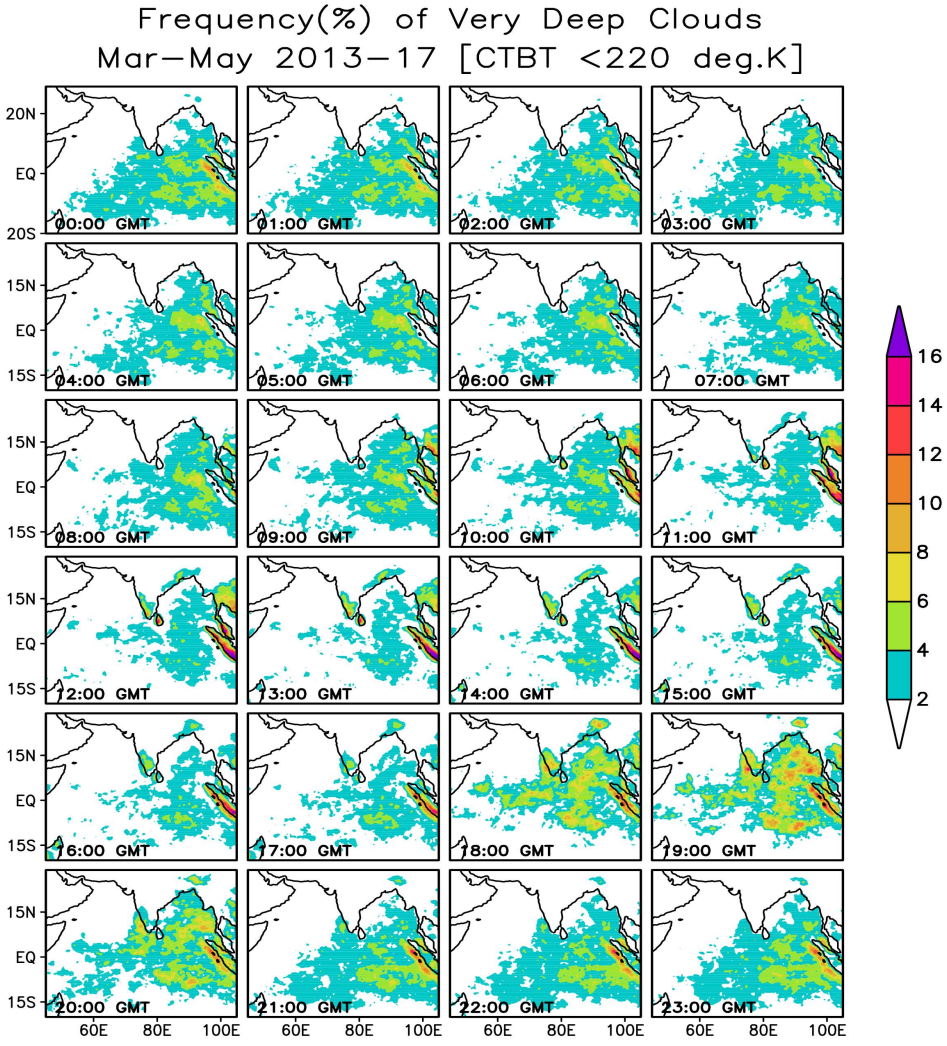


Figure 5.3. Frequency of occurrence of very deep (< 220$^{O}$K) clouds as observed in hourly images from 00:00 GMT to 23:00 GMT during pre-monsoon season (MAM).

Deep convection over the land continues up to 20:00 GMT with the peak frequency observed during 18:00-19:00 GMT. Oceanic convection remains weak up to 17:00 GMT and suddenly peaks through 18:00-20:00 GMT extending to the entire Bay of Bengal and to westward to the south of the Arabian Sea along the equator. After 20:00 GMT, the convection over the land region is almost absent and that over the Bay of Bengal weakens. Excepting 18:00-20:00 GMT hours, convection along a narrow belt over the western Bay of Bengal lying parallel to the east coast of India remain free of deep clouds throughout the day.

Along the eastern boundary of equatorial Indian Ocean, behaviour of deep convective activity is a little different. By 07:00 GMT, convection is appeared over the land regions of Thailand and Sumatra islands and they become more prominent during 9:00-14:00 GMT. During these hours, deep convection spreads northward to Southwest China and subsequently weakens after 15:00 GMT. Nature of convection off west of Sumatra along a narrow belt lying parallel to its west coast is interesting. When deep convection peaks inland Sumatra Island, convection in this belt weakens. Afterwards, by 17:00 GMT, this region becomes very active and continues to remain so, up to 00:00 GMT (7:00 LST). Another noticeable feature of the region is the differential diurnal behaviour of deep clouds over the land area of Sumatra and Thailand. By 20:00 GMT, the deep clouds disappear from the land region of Thailand whereas; the adjacent south-westward located Sumatra land continues to remain cloudy up to 23:00 GMT.

Deep convection in the ECZ of equatorial Indian Ocean is visible throughout day but intensifies from 17:00 GMT and sustains strong up to 03:00 GMT during the season.

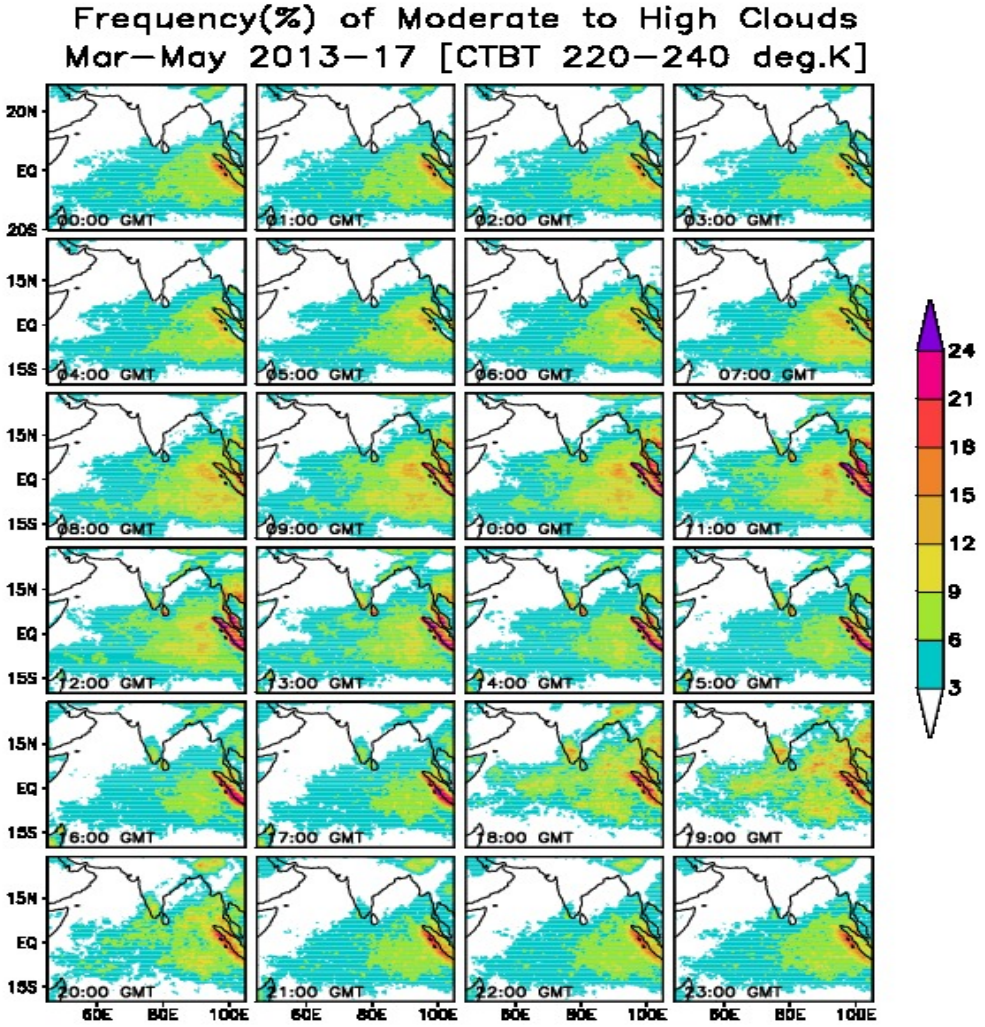


Figure 5.4. Frequency of occurrence of moderate to high (BT ranging exclusively between 220 and 240$^{O}$K) clouds as observed in hourly images from 00:00 GMT to 23:00 GMT during pre-monsoon season (MAM). Compared to very deep convection, deep convection is more frequent and has similar pattern of diurnal variation.

Broadly similar but less pronounced diurnal variation can be observed in the moderate to high cloudiness (BT exclusively ranging between 220 and 240$^{O}$K) provided in Figure 5.4. The development and peaking of convection

inland parallel to the east coast of India, during 09:00 – 19:00 GMT hours is observed. But the adjacent ocean remains devoid of clouds.

### *5.3.2 (b) Monsoon Season (JJAS)*

During the summer monsoon season, frequency of occurrence of very deep convection over northern latitudes covering India and Bay of Bengal is the highest. Figure 5.5 provides the spatial pattern of diurnal variation during the season. The major deep convective regions are identified as the Bay of Bengal and the monsoon trough area where large amplitude of diurnal variation exists. There are different preferred timings for peaking of deep convection over the land and ocean. Convection over the Bay of Bengal is the minimum during 15:00-17:00 GMT. After 17 GMT, convection deepens especially over the eastern parts of north and central Bay. Deep convection spreads westward and northward and intensifies further by 23:00 GMT. Very gradual deepening of organised convection concentrated over a location close to the east coast of India in the Northern Bay of Bengal is observed to reach its peak by 08:00 GMT. On the other hand, the Indian mainland remains largely free of deep convective clouds from 03:00 GMT up to this 07:00 GMT. From 08:00 GMT onwards, the location of convection starts to shifts from the ocean to the land across the east coast of India. Then, convection is observed to develop and spread westward in concurrence with a marked subsidence of deep convection over the Bay. During 10:00-11:00 GMT hours, two distinct patches of apparently independent organised convection co-exists, one over the ocean and the other over inland close to the coast. These two patches of convection is seemingly separated by the coastline along which, convective clouds tend to form less frequent. By 12:00 GMT, deep convection over the

land reaches its peak and is present extended westward while the convection over the Bay of Bengal is on a subsiding phase.

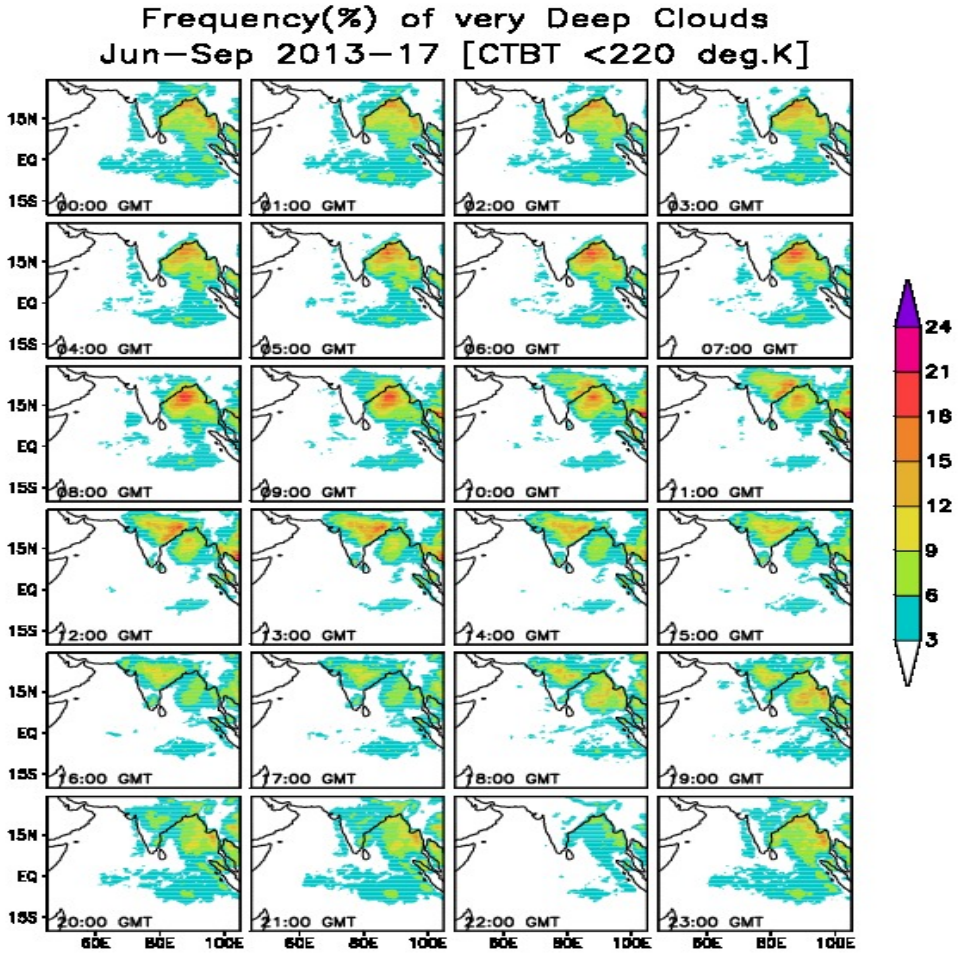


Figure 5.5. Frequency of occurrence of very deep (<220$^{O}$K) clouds as observed in hourly images from 00:00 GMT to 23:00 GMT during monsoon season (JJAS).

Convection over the land recedes very gradually and the Indian mainland becomes bare of deep clouds by 21:00 GMT meanwhile the convection over the east and central Bay of Bengal is building up again. Thus a general migration of convection from east to west is evident both over the ocean and the land. While oceanic convection takes considerable time for the

intensification and peaking, that over the land region is relatively faster. Convection spreads almost all of central India and takes longer time to subside.

Over the Arabian Sea, deep clouds are almost absent during the season. However, close to the Western Ghats on the west is a narrow parallel strip of prominent rainy region where the clouds are formed chiefly due to the orography of the Ghats. Humid air approaching from south west direction is blocked by the Ghats leading to heavy precipitation. But it is found that such clouds are moderate to high rather than very deep. Even though the frequency of very deep clouds is relatively low, a diurnal variation is evident. Off west coast of India, preferred timing of appearance of very deep clouds is during 20:00-04:00 GMT.

Considerable deep convection and diurnal variation is observed in the east equatorial region as well. Over Thailand, deep clouds are identified from 08:00 GMT up to 22:00 GMT, whereas over north Sumatra, onset of deep convection is a little delayed. Deep convection over north Sumatra begins by 10:00 GMT and lasts up to around 00:00 GMT. During the monsoon season as well, deep convection in the ECZ of equatorial Indian Ocean is visible throughout day.

Figure 5.6 provides hourly frequency of occurrence of moderate to high convection during the summer monsoon season. Weak but similar diurnal variation is present as compared to very deep convection. Most of the clouds appearing west of Western Ghats is highly rain producing. Vijaykumar *et al.,*(2017) have demonstrated that the heavy to moderate rain is mostly favoured by clouds with top temperature >220$^{O}$K in this region. The diurnal

variation in precipitable clouds is found less pronounced in the region, implying that occurrence of moderate to heavy precipitation throughout day and night is equally likely. Although clouds are present widely over the Indian land mass, the rainfall is not following a similar spatial pattern. East of the Western Ghats, rainfall is comparatively low and over north east India and central Gangetic plains, rainfall is more intense.

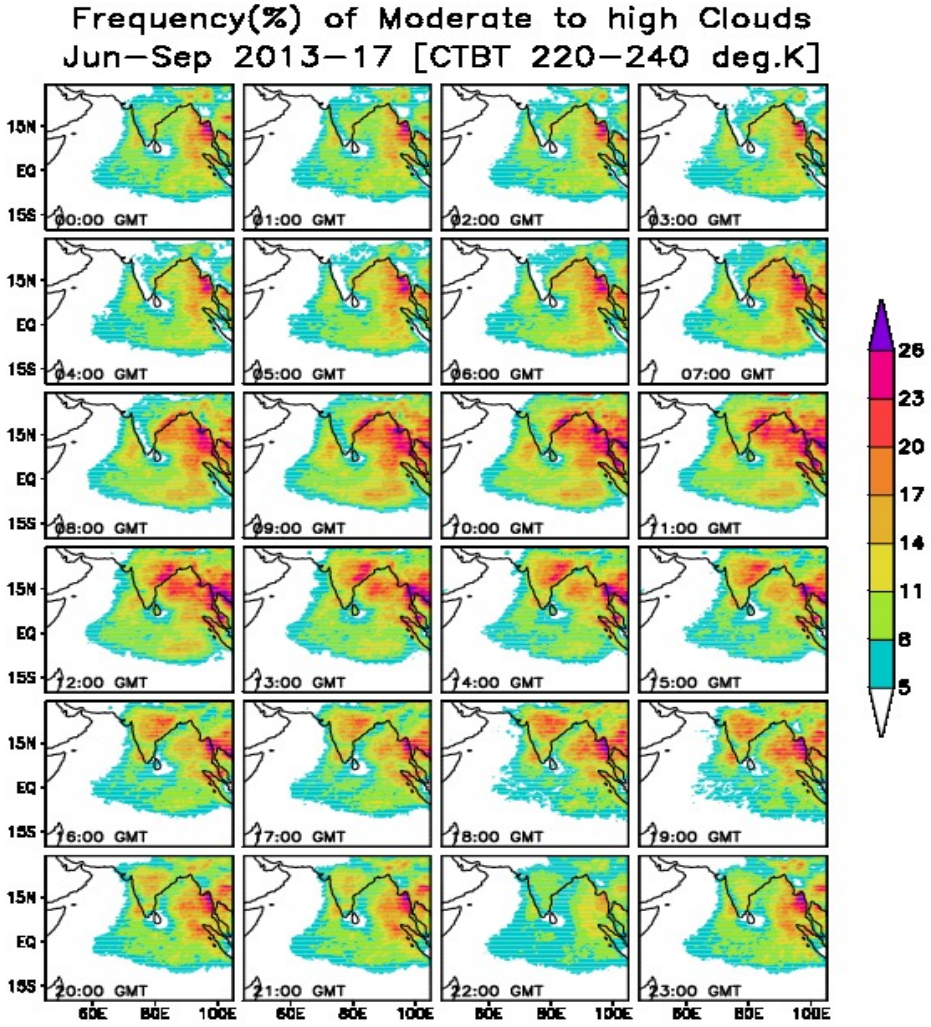


Figure 5.6. Frequency of occurrence of moderate to high clouds (BT ranging exclusively between 220 and 240K) during monsoon (JJAS) season.

### *5.3.2 (c) Post Monsoon Season (OND)*

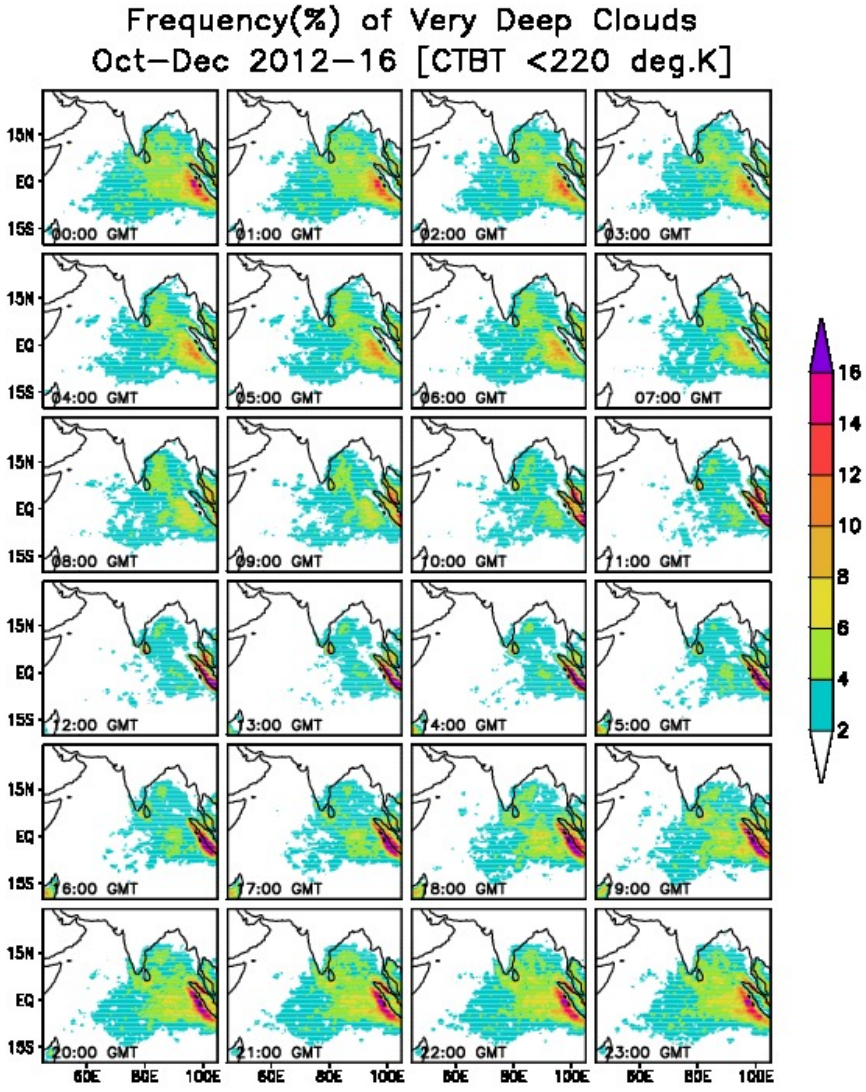


Figure 5.7. Frequency of occurrence of very deep (<22 0K) clouds as observed in hourly images from 00:00 GMT to 23:00 GMT during post monsoon (OND) season.

Figure 5.7 provides spatial pattern of diurnal variation during post monsoon season. The magnitude and spatial pattern of very deep convection over oceanic region is mostly similar to that of pre monsoon season. Excepting

east coastal regions and a small area near the southeast tip, most of the land area over the Indian mainland is short of any significant deep convection during the season.

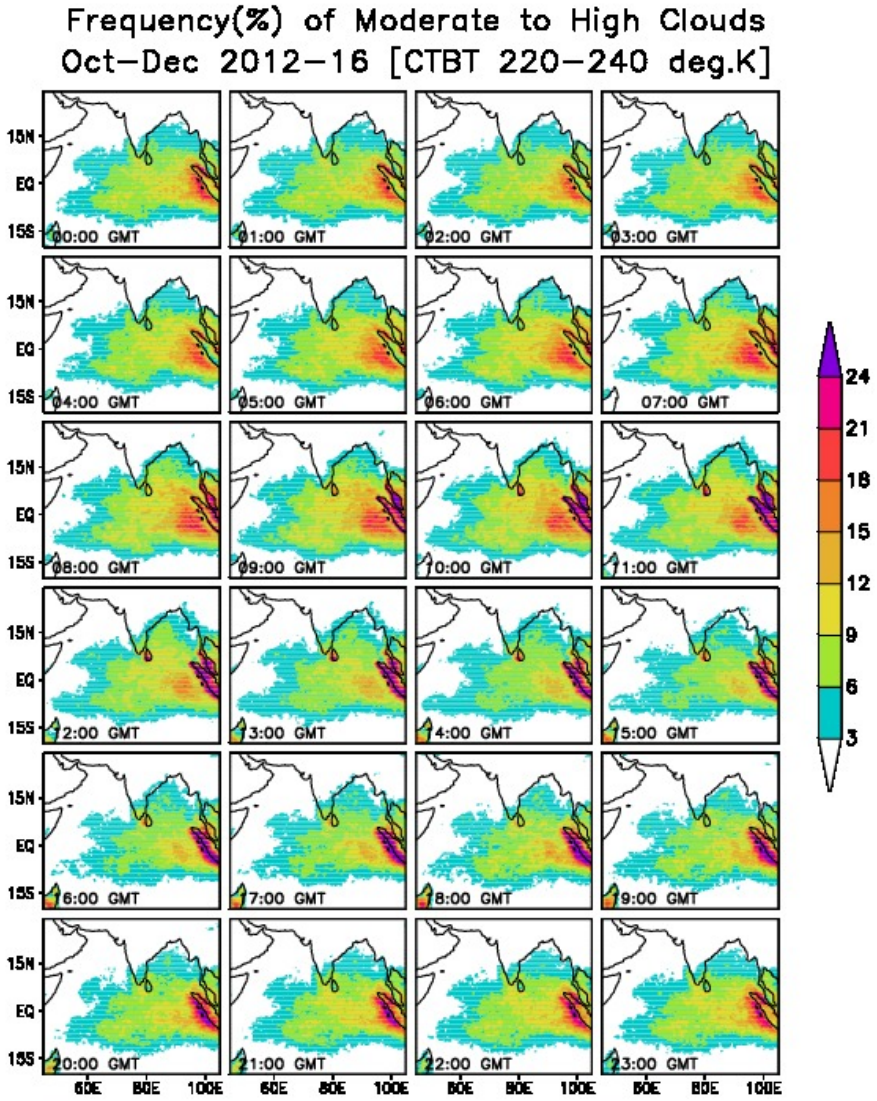


Figure 5.8. Frequency of occurrence of moderate to high clouds (BT ranging exclusively between 220-240ºK) as observed in hourly images from 00:00 GMT to 23:00 GMT during post monsoon season (OND).

The hotspot of very deep convection is located over Sumatra Island and parallel off west over the ocean. Very deep convection is considerably frequent in the east equatorial Indian Ocean and southwest Bay of Bengal with noticeable diurnal variation. By and large, deep convection over the oceanic region is the minimum during 11:00-16:00 GMT whereas that over the Sumatra land region peaks during these same hours. Towards 17:00 GMT, oceanic convection begins to increase and the most intense convective region shifts to off west of Sumatra. Major deep convective area over the equatorial Indian Ocean is confined mainly between 80-100 $^{O}$E and 10 $^{O}$S - 15 $^{O}$N. Sustained oceanic convection is present through 18:00-02:00 GMT hours in this area.

Over the southeast coastal India, very deep convection is present almost throughout the day whereas during the hours 11-17 GMT, in concurrence with the reduction of deep convective activity in the south Bay of Bengal, land regions over the south west tip of Indian mainland become convectively active.

### *5.3.3 Hour of maximum frequency of deep clouds (colder than 240 K)*

Figure 5.9 provides the hour of maximum frequency of occurrence of cloud tops colder than 240 $^{O}$K for the pre-monsoon, monsoon and post monsoon seasons. It is evident that there is large seasonal variability in the most preferred hour of convection. During the pre-monsoon months, convection over the Bay of Bengal mostly occurs during time centred on 17:00-19:00 GMT which corresponds to midnight local time. The regions at the southwest tip of the peninsular India where considerable amount of pre monsoon rain is received also show peaking of convective activity towards

midnight local time. Over the land area of Sumatra, Malaysia, Thailand, Cambodia, Vietnam and Laos, time of occurrence of maximum convection is a little earlier than in the adjacent oceanic regions. The hour of maximum frequency in these regions is centred on 12:00 GMT.

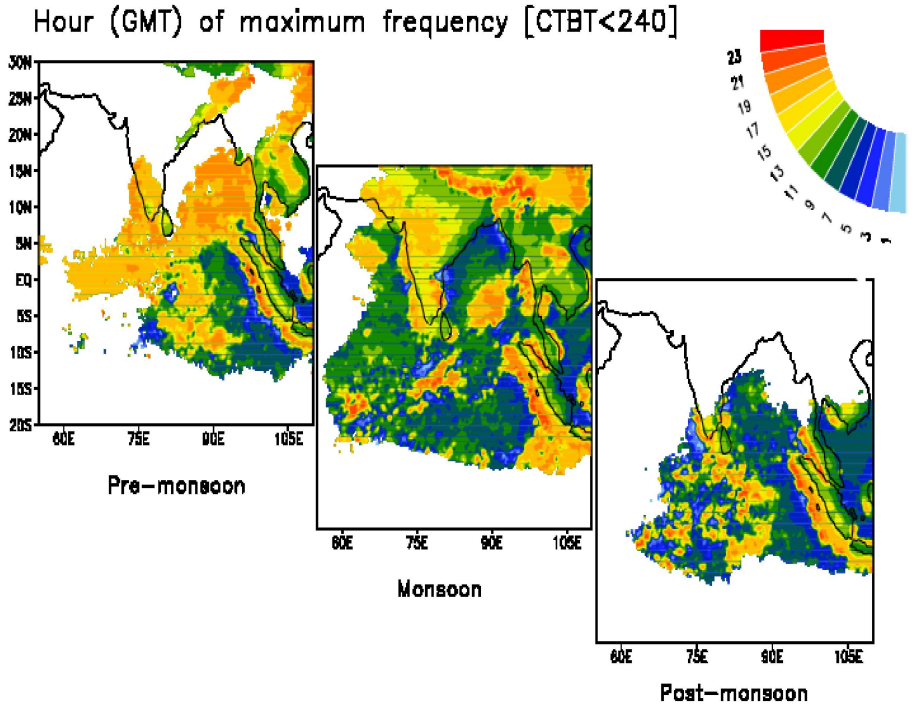


Figure 5.9. Spatial pattern of hour of maximum frequency (GMT) of occurrence of cloud tops colder than 240 K.

Parallel to west coast of Sumatra, there is a narrow strip where maximum frequency of convection occur around 16-17 GMT during all seasons. Further off west of this strip, maximum convection occurs preferably during 03:00-09:00 GMT. Convection over the Bay of Bengal preferably occurs during 03:00-07:00 GMT hours both during the monsoon and post monsoon season. However, over a large area in central and east central Bay of Bengal, convection peaks by nearly 17:00-19:00 GMT hours. The interval

between maximum convection over the ocean off east coast of India and that over the mainland and west coast is roughly 10 hours. During the post monsoon season, the maximum convection occurs in the afternoon hours (after 11:00 GMT) over the southwest tip of India, but a distinct diurnal signal is absent along the southeast coastal region.

### *5.3.4 Diurnal variation in TRMM 3B42RT data*

The diurnal variation in rainfall is examined using 3 hourly TRMM 3B42RT rainfall data. Figure 5.10 provides the diurnal variation in average cumulative rainfall for every 3 hour interval for the five years of pre monsoon days. Comparable to the observations in the spatial pattern of deep cloud distribution, most of the raining events during the season occur south of roughly 5$^{o}$S latitude. There are two main regions where significant amounts of rainfall are received north of this latitude line. These regions are located exclusively over the land area and are identified as (a) Over the Sri Lanka Island and south west tip of India and (b) Over the foothills of Himalaya covering the Bangladesh and Bhutan regions. The diurnal variability in rainfall during the season is highly prominent. Rainfall is present over the southwest tip of India and over the Sri Lanka regions from 09:00-12:00 GMT hours, but the rainfall over the foothills of Himalaya is observed to increase by 12:00 GMT and peak a little later, at 18:00 GMT. By 18:00 GMT, the rainfall over the Sri Lankan and Southwest Indian land region is found to shift westward to the adjacent oceanic regions though with reduced magnitude. A strikingly comparable preference in timing of oceanic and land rain occurrence is evident over the Malaysia and Sumatran Island. There is no significant rainfall over these regions at 06:00 GMT, but by 09:00 GMT, the rainfall significantly increases. By 12:00 GMT, the rainfall is at its peak but after 15:00 GMT,

rainfall over the land starts to shift westward to the adjacent ocean. In a strip parallel to the Bukit Barcia mountains, rainfall persists strongly off westward of Sumatra during 18:00 to 09:00 GMT hours.

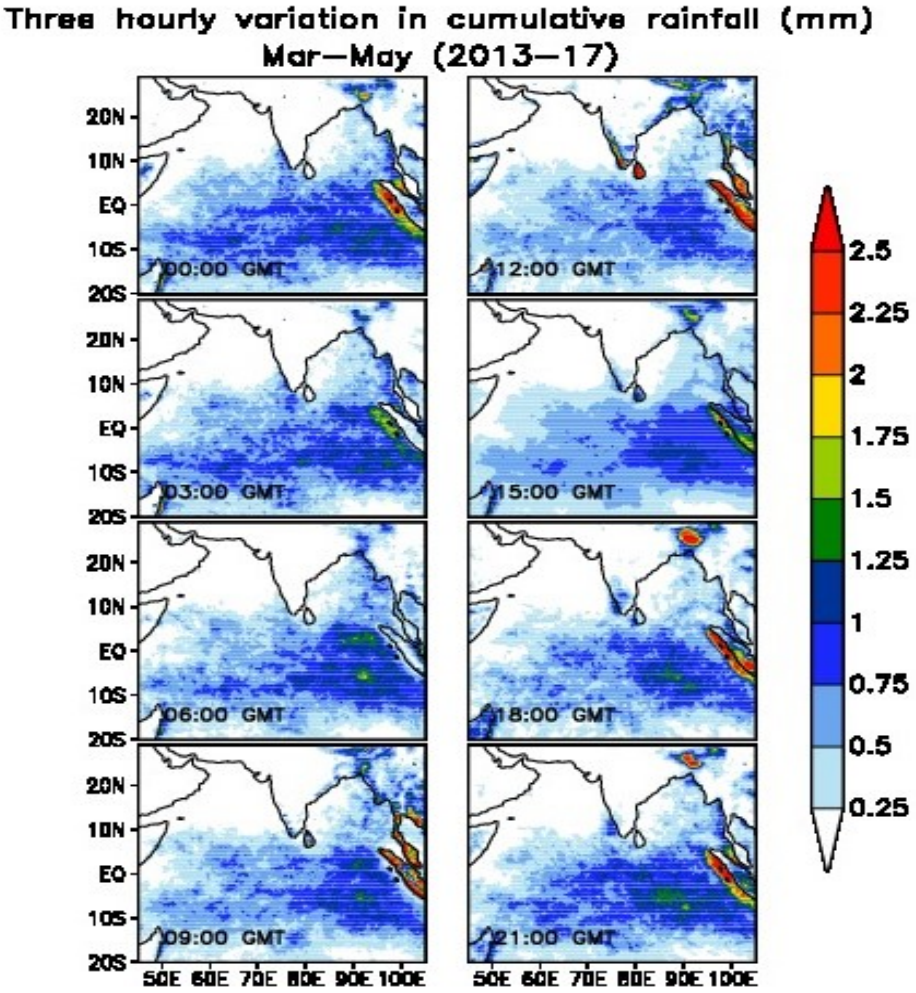


Figure 5.10. Diurnal variation in rainfall during the pre-monsoon season from TRMM 3B42RT three hourly data

Comparing to the monsoon and post monsoon seasons, less amounts of rainfall is received over the Bay of Bengal during the pre-monsoon period.

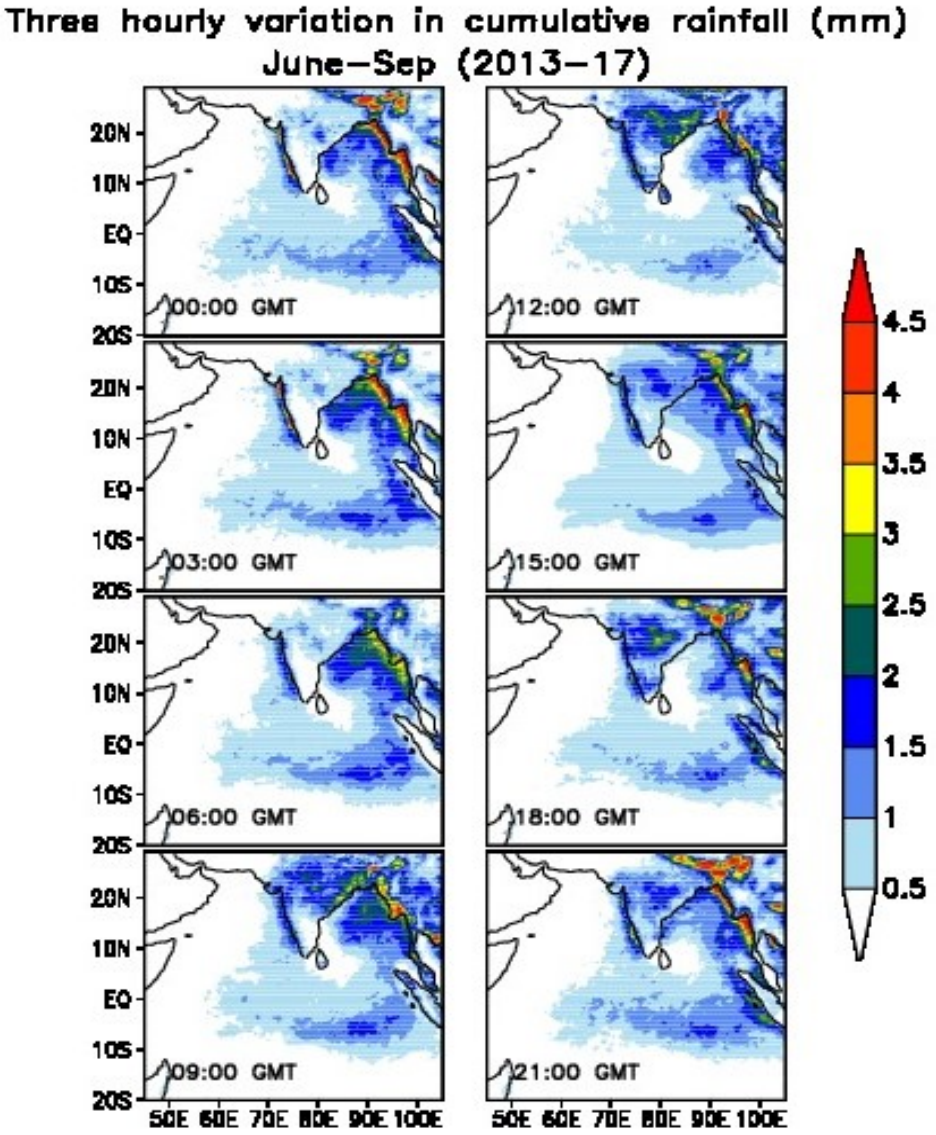


Figure 5.11. Diurnal variation in rainfall during the monsoon season from TRMM 3B42RT three hourly data

Figure 5.11 provides the spatial variation in average three hourly rain for the monsoon season obtained from TRMM 3B42RT data sets. Following the patterns revealed through the deep cloud distribution, the rainfall exhibits significant diurnal variations. It can be seen that the intrusion of rain over to

the Indian mainland chiefly occur after 09:00 GMT, before which the of rainfall over the Bay of Bengal have already established.

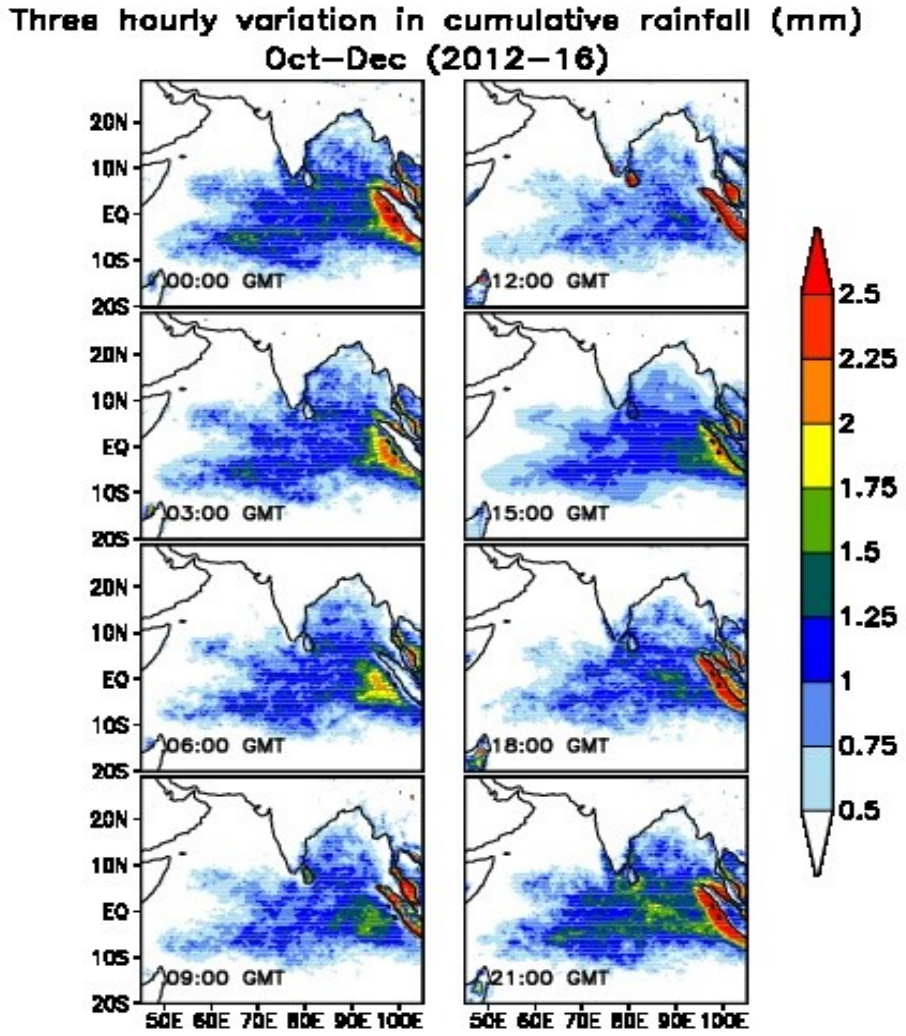


Figure 5.12. Diurnal variation in rainfall during the post monsoon season from TRMM 3B42RT three hourly data

The regions where the largest amounts of rainfall received during the season are the immediate off and over the west coast of India, Myanmar and Thailand, over the land regions covering the Bangladesh, Bhutan and North-

eastern India. Off west coast of India, rain is present almost throughout the day but with significant peeking through 21:00 to 03:00 GMT hours.

During the post monsoon season, the rainfall is mostly concentrated in the southern latitudes. The major centre of intense rain is the east equatorial regions covering the Malaysia, Sumatra and the westward laying adjacent oceanic region. The phase change in land and oceanic convection is clearly noticeable. Up to 06:00 GMT, the convection is more confined to oceanic region where as by 09:00 GMT; the Sumatran and Malaysian land regions become centres of convection and associated rainfall. By 15:00 GMT, the rainfall over the land area recedes and the peaking of rain is witnessed in the adjacent oceans laying westward to these land regions. The convection over the oceanic region continues to remain intense until 00:00 GMT and thereafter slowly weakens.

Concerning the Indian mainland, the rain pattern during post monsoon season is almost similar to that in the pre-monsoon season. However, the significant rainfall received over the Bay of Bengal and southeast India during post monsoon is a major difference. During the season, rain is the absent over the Bangladesh and Bhutan region.

### 5.3.5 Diurnal features of rainfall and cloudiness in sub regions

The diurnal variation of average rainfall, contribution to the total rain by different rain classes and fractional contribution of different types of clouds overhead rainy pixels in the sub regions chosen are presented in figures 5.13 - 5.16. Though the results are arranged in groups based on the alphabetical order in which the boxes were named, this grouping is convenient to compare the

major differences in diurnal patterns between land and ocean, two land regions and two oceanic regions.

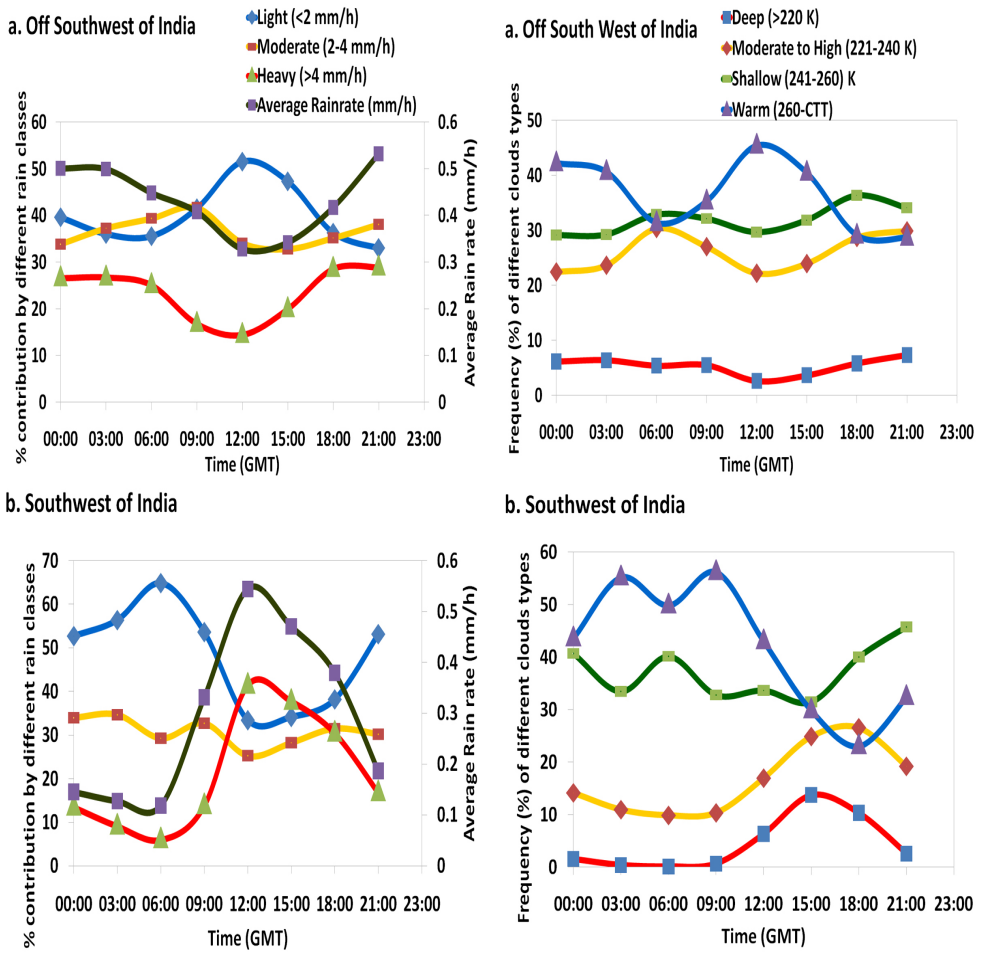


Figure 5.13. Diurnal variation of average rain rate and contribution to the total rain by different rain classes in Off Southwest of India box (a) (Top Left), Southwest of India box (b) (Bottom Left), and the fractional contribution of different classes of cloud types present overhead rainy pixels in the respective boxes (Top Right and Bottom Right).

In Figure 5.13 the results from the boxes marked as (a) and (b) in Figure 5.1 are provided. The average rainfall off west of Southwest India is almost consistent throughout the day avoiding a small decrease during 9:00-

18:00 GMT hours. The heavy rain contribution to the total rain is always less than the moderate and light rain classes. The presence of very deep clouds overhead rainy pixels are less than 10 % and are not showing much of diurnal variation despite a small drop at 12:00 GMT hours. Moderate and shallow clouds contribute mostly to the rainfall where a considerable amount of light rain is appeared to be obtained from warm clouds in the region. This may be attributed to the modulation of rainfall in the region by the orography of the Western Ghats.

In the land box-b which lies adjacent and in the same latitudes as box-a, the results are strikingly different. Part of the box is over and on the windward side of the Western Ghats. A prominent peak in the average rainfall and heavy rain class contribution is observed to occur centred around 12:00 GMT. Moderate rainfall is found to exhibit weak diurnal variation. Light rain contributes mostly during the early local morning hours. The cloud types are found to exhibit a similar pattern as that of rain. Very deep clouds are mostly absent during the early morning hours. From 09:00 GMT onwards, there is significant increase in very deep and medium to high clouds that co-exist with rain. Shallow convective and warm clouds are present throughout the day co-existing with rainy pixels.

Figure 5.14 provides the opportunity to examine difference between two land regions in comparable latitudes over the Indian mainland. Box (c) is located in the central India and box (d) is located far east of box (c). The average rainfall in both the regions is mostly been contributed by heavy rains. Over the Central India box (c), the average rainfall increases from 06:00 GMT and peaks by 12:00 GMT. A secondary peak is observed by nearly 18:00 GMT. Even during the hours of low average rainfall during a day, the heavy

rain type is the major contributor. Amounts of deep, medium to high and shallow clouds is found to increase from 09:00 GMT onwards, but the presence of warm clouds co-existing with the rainfall occurring during 06:00-09:00 GMT suggests that some of the rain during this time is obtained from warm clouds as well in the region.

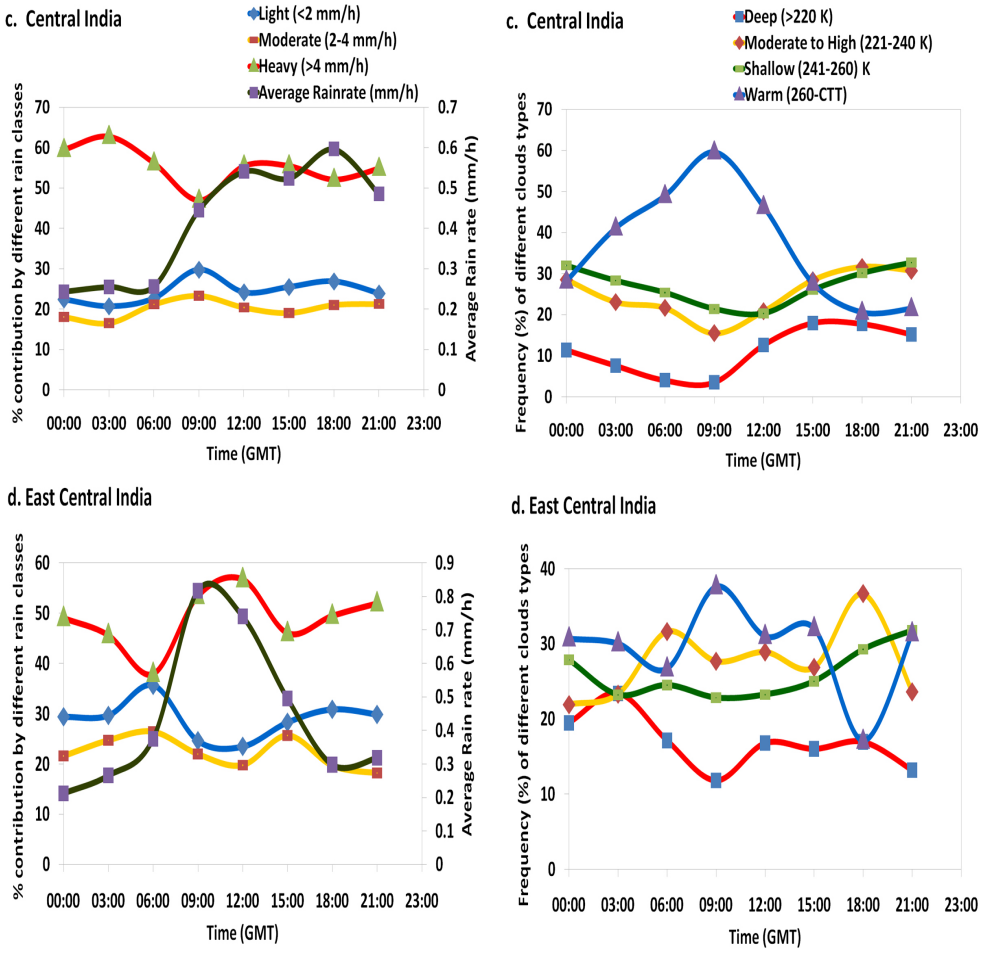


Figure 5.14. Diurnal variation of average rain rate and contribution to the total rain by different rain classes in Central India box (c) (Top Left), East Central India box (d) (Bottom Left), and the fractional contribution of different classes of cloud types present overhead rainy pixels in the respective boxes (Top Right and Bottom Right).

Unlike in the central India box, a secondary peak is not observed in the east central India box (d). the peaking of average rainfall is centred roughly on 09:00 GMT. In this box as well, the main contributor to the total rainfall is heavy rain class. All types of clouds are found to co exist with cloudy pixels in comparable proportions. Presence of very deep clouds in the less raining hours suggests that they are either/both convective debris or/and cirrus contamination.

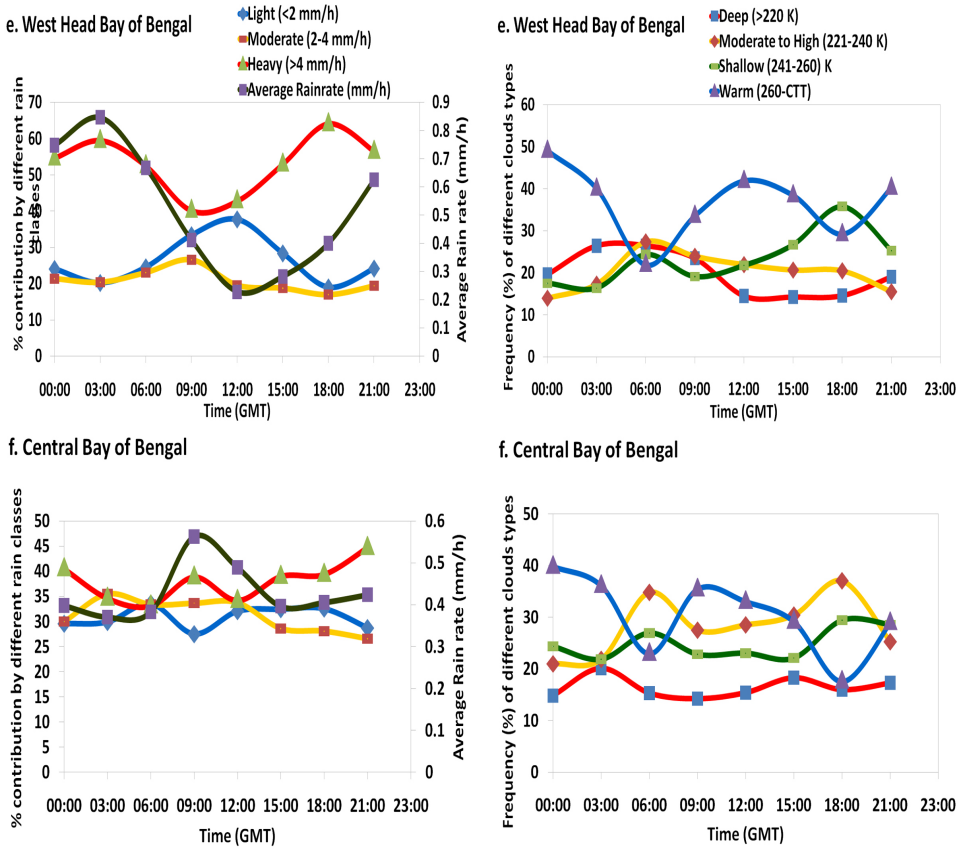


Figure 5.15: Diurnal variation of average rain rate and contribution to the total rain by different rain classes in west Head Bay of Bengal box (Top Left), Central Bay of Bengal box (Bottom Left), and the fractional contribution of different classes of cloud types present overhead rainy pixels in the respective boxes (Top Right and Bottom Right).

Strikingly different from the adjacent and longitudinally parallel land box (d), the rain peaks in the east head Bay of Bengal box (e) in early local morning hours (fig 5.15). By the time the rainfall reaches maximum over the land west to this box; the rainfall here becomes the minimum. However, throughout the day, the contribution by heavy rain class is consistently higher than other two rain classes same as in box (d). Very deep clouds are present in plenty and the curve lies almost parallel to the average rainfall curve. Compared to the east Head Bay, the diurnal variation of rainfall over the central Bay box is weak. There is a light peak in average rainfall by 12:00 GMT and almost all classes of rain types contribute more or less equally to the total rainfall. Dominance of moderate to high clouds is observed in the region, along with presence of other classes of clouds throughout the day.

Similar to the observations in the west coast of India box (a), the peaking of average rainfall over the ocean box (g) occurs roughly 9 hours before that over the land box (h) (fig. 5.16). However, the average rainfall over the oceanic region is almost double that over the land. The contribution of heavy class rain is high during the peak rain hours but light and moderate rain contributes significantly to the total rain during weak rainy hours. Proportion of Very deep cloud increase during peak raining hours but moderate and shallow clouds are present throughout in almost equal proportion suggesting orographic modulation. In the adjacent eastward land box, rain peaks by 12:00 GMT with significant increase in high rain class contribution. Heavy and moderate clouds increase during the peak raining hours in the region.

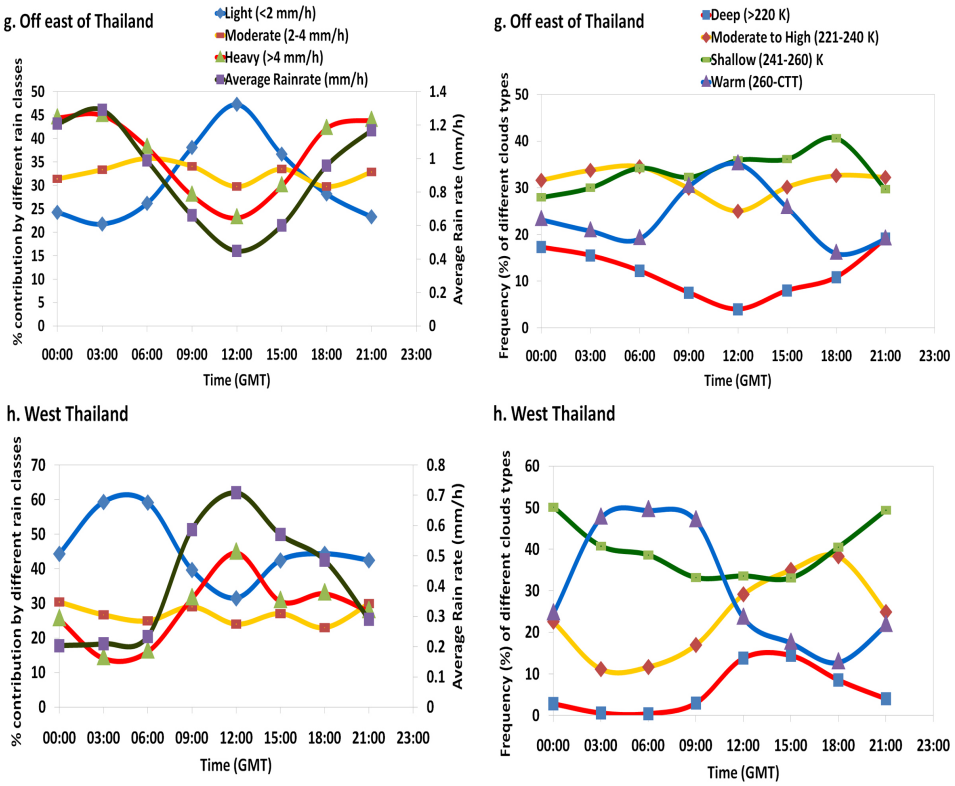


Figure 5.16. Diurnal variation of average rain rate and contribution to the total rain by different rain classes in Off east of Thailand box (Top Left), West Thailand box (Bottom Left), and the fractional contribution of different classes of cloud types present overhead rainy pixels in the respective boxes (Top Right and Bottom Right).

## 5.4. Conclusions

Over Indian mainland and surrounding Oceanic regions significant diurnal variation of convective activity is observed during all three seasons under study. In general, the amplitude of DV is high over land as compared to ocean. Among the different classes of convection studied, deep ($<220^{O}K$) convection exhibits the most distinct spatial patterns of DV. During the pre-monsoon season, the preferable time of occurrence of deep convection in a day over regions like the north-eastern States and southwest tip of India and

Bangladesh is roughly between 11:00 and 20:00 GMT, with the peaking between 18:00-19:00 GMT hours. Oceanic convection remains weak during 11:00 to 17:00 GMT and suddenly peaks afterwards and continues to sustain longer.

During the summer monsoon season, deep convection over the Bay of Bengal and Indian mainland are in opposite phases. A northwest march of deep convection over ocean and land is evident. From 17:00 GMT onwards, intensification of convection over the east central Bay of Bengal is observed. Deep convection spreads westward and north-westward and intensify further by 23:00 GMT. Organised deep convection in an area close to the east coast of India in the head Bay is prominent by 08:00 GMT. From 08:00 GMT onwards, location of convection starts to shift from the ocean to the land across the east coast of India. During 10:00-11:00 GMT hours, two distinct patches of apparently independent organised convection co-exists, one over the north west Bay of Bengal and the other over the inland close to the east central coast of India. The Oceanic convective region then starts to subside whereas the land convection spreads further west north-westward. Off west coast of India, very deep clouds preferably appear during 20:00-04:00 GMT hours during the summer monsoon season.

The spatial pattern of post monsoon season is largely similar to that of the pre monsoon but the oceanic convection is present more prevalent and prolonged. Along the Southeast coastal regions of India, deep convection is present day long whereas over the southwest tip of India, convection peaks during 12:00-17:00 GMT hours.

There are considerable diurnal variations in the average rainfall, contribution to the total rain by different rain intensity classes and the fractional contribution of different category of clouds associated with the rain in the sub regions chosen for the study. In regions where the rainfall is modulated largely by the orography, light to moderate type rain has a major role to play. In north central India, East coast of India and northwest Bay of Bengal, intense rain class contributes the most to the total rainfall. Over the central Bay of Bengal, all three intensity classes of rain have more or less equal share into the total rainfall.

# Chapter-6

# Latent Heating and Hydrometeor structure during Indian summer monsoon season with respect to different ENSO phases

## 6.1. Introduction

Every year nearly 80% of the annual rainfall over Indian subcontinent and surrounding ocean is received during the four months from June to September (South West monsoon season). Variability is an inherent feature of Indian Summer Monsoon Rainfall (ISMR) which leads to uncertainties in agriculture activities, resulting in huge social and economic impacts. Monsoon rainfall is known to fluctuate on the diurnal, synoptic, intra-seasonal and inter-annual time scales. Among the many factors which are believed to contribute to the interannual variability of ISMR, El Niño and La Niña conditions over the Pacific Ocean are prominent, and potentially predictable. El Niño (La Niña) refers to warm (cool) anomalies in sea surface temperatures across the central and east-central Equatorial Pacific. Several studies have examined the role of El Niño-Southern Oscillation (ENSO) in producing the interannual and intraseasonal variability of rainfall. (Sikka 1980; Rasmusson and Carpenter 1983, Pant and Parthasarathy, 1981; Ropelewski and Halpert, 1987; Krishnamurthy and Kirtman, 2003). In general, a cool or La Niña condition in Pacific Ocean favours an above normal monsoon rainfall and a warm or El Niño condition is associated with below normal monsoon rainfall over the Indian region. However, years of moderate to extreme El Niño's have

not been reliably dry as shown by Kumar *et al.,* (2006). They have also shown that India is more prone to drought when the ocean warming signature of El Niño extends westward to the central basin rather than being confined in the eastern equatorial Pacific Ocean. Kumar *et al.,* (1999) suggest that a recent decadal shift in Walker circulation anomalies and enhanced land-sea gradient are muting the historical monsoon-ENSO inverse relationship, keeping the monsoon at a normal level despite increased ENSO activity in the recent decades. Further, they propose that global warming has broken the link between ENSO and the monsoon, preventing monsoon failure.

Long-distance dynamics in the atmosphere may depend on the vertical structure of anomalies. Based on this generality, but without any presumptions, we carried out an analysis of the TRMM PR profiles for a decade and half to find out whether there exist prominent differences in the structure and types of rainfall in sub regions of importance over the Indian subcontinent and the surrounding ocean, during episodes of El Niño, La Niña and normal conditions defined based on the Oceanic Niño Index (ONI).

The vertical structure of the mean heat source depends on the proportion of different cloud types (depths) present in the atmosphere (Tao *et al.,* 2001). Latent heating is the dominant component in the total diabatic heating in the atmosphere followed by radiative heating and vertical eddy heat transports. Houze (1982, 1989) demonstrated that higher fractions of stratiform rainfall are associated with an upward shift in the level of maximum heating and an increase in the vertical heating gradient in the upper troposphere. Zuluaga *et al.,* (2010) used the TRMM-PR and TMI rainfall products on monthly basis at the resolution of 0.5° x 0.5° to derive vertical profiles of latent heating over different areas and for different years. The vertical distribution of latent heating was found to have major maxima at

about 7 km height and minor maxima at 3 km height along several areas of South Asia. According to them the major maxima at 7 km represented the contribution by stratiform precipitation and the minor one resulting from convective precipitation.

Vertical heating profiles of precipitating cloud systems have been observed to vary over space and time across the Tropics (e.g., Thompson *et al.,* 1979; Frank and McBride 1989). Schumacher *et al.,* (2003) utilised the TRMM PR 2.5x2.5$^{o}$ annually averaged rain accumulation from 1998–2000 to observe that the stratiform rain fraction is generally lower over land and higher over the oceans with some noted exceptions at a few regions. Regarding the cloud structure over the Indian region, Stano *et al.,* (2002) used TRMM-PR data to map rainfall structure around composited monsoon depressions over the Indian mainland. They showed that the stratiform rain contributes significantly to rainfall amounts, with fewer deep convective elements, under active monsoon spells associated with monsoon depressions.

While many studies, as discussed above, have utilised the TRMM PR data sets for varying purposes, the present analysis is the first of its kind in attempting to understand the convective and stratiform cloud fractions distribution, latent heating and hydrometeor profiles and dynamical aspects focussing on sub regions having varying rainfall characteristics. The analysis is carried out by classifying the years into El Niño, La Niña and normal years. One limitation of the study is the absence of representative cases for strong to very strong El Niño or La Niña events during the study period. The El Niño and La Niña cases available for the analysis are moderate to weak.

## 6.2. Data and Methodology

The data sets used for the analysis are taken from TRMM derived

multi-level products referred to as 3H31 and 3B31. Monthly 2.5x2.5$^{o}$ resolution Vertical pressure velocity ($\omega$) data obtained from NCEP-NCAR reanalysis (Kalnay *et al.,* 1996) is used for the analysis.

The years for which data is available are classified into El Niño, La Niña and Normal based on the Oceanic Nino Index (ONI). The ONI is the de-facto standard that NOAA uses for identifying El Niño (warm) and La Niña (cool) events in the tropical Pacific. It is the running 3 month mean SST anomaly for the Niño 3.4 region (i.e.,5$^{O}$N-5$^{O}$S, 120$^{O}$-170$^{O}$W). Events are defined as 5 consecutive overlapping 3 month periods at or above the + 0.5$^{O}$ anomaly for warm (El Niño) events and at or below the - 0.5$^{O}$ anomaly for cold (La Niña) events. The threshold is further broken down into Weak (with a 0.5 to 0.9 SST anomaly), Moderate (1.0 to 1.4), Strong (1.5 to 1.9) and Very Strong ($\geq$ 2.0) events.

There are 4 years with El Niño, 6 years with La Niña and 7 years with Normal conditions during the period from 1998 to 2014 as detailed in Table 1. The analysis is carried out by preparing composites of all data sets for Jun-Sep months which represent Indian Summer Monsoon. Climatological Latent Heating, Rainwater, Snow and Graupel profiles and anomalies during El Niño, La Niña and Normal years are prepared. Lower level total heating is calculated by summing Latent Heating from 1 to 4 Km and Upper level by summing the same from 5 to 10 Km. Stratiform rain fractions are multiplied by total surface precipitation to calculate stratiform rain contribution. The remaining quantity of rain in total surface precipitation is considered as convective rain contribution. Anomalies of stratiform and convective rain amounts are calculated for the El Niño, La Niña and Normal years. For analysing major meridional differences in heating and pressure velocities in the Arabian Sea,

Indian mainland and the Bay of Bengal, strips of equal with (5 degree) were considered between 67-72$^{O}$E, 77-82$^{O}$E and 90-95$^{O}$E longitudes respectively between 15$^{O}$S and 30$^{O}$N longitudes. To understand zonal difference in heating, latent heating in 3 latitude belts, namely 10-0 $^{O}$ S, 5-15$^{O}$N and 15-25$^{O}$ N were averaged.

### *6.2.1 Sub regions*

The present study focuses on 6 sub regions over Indian main land and surrounding Ocean, shown in the map of Figure 6.1. They are (a) Eastern Bay of Bengal (EBB, 9-18$^{o}$ N, 95-99$^{o}$E), (b) Head Bay of Bengal (HBB, 14–22$^{o}$N, 85–95$^{o}$E), (c) Central Indian land region (CILR, 18–24$^{o}$N, 73–85$^{o}$E), (d) Eastern Arabian Sea and West coast of India (EASWCI, 9–18$^{o}$N, 72–76$^{o}$E), (e) South west Indian Ocean (SWIO, -8- 0$^{o}$N, 60–70$^{o}$E) and (f) South east Indian Ocean (SEIO, 8-0$^{o}$ S, 85-95$^{o}$E). These sub regions receive maximum quantity of rainfall during the monsoon season and exhibits high interannual variability (Krishnamurthy and Shukla, 2000; Goswami and Mohan, 2000). The boxes marked ‘a’ and ‘d’ and the boxes marked ‘e’ and ‘f’ share same latitudes. Similarly, the boxes marked 'b' and 'f' share same longitudes. This enables normalised comparison in between the boxes.

The boxes were selected based on the differences in the nature of rain types. Western Ghats and west Myanmar coasts are known for the orographic rains (Xie *et al.,* 2006). The magnitude of rain produced in these two locations is the highest and comparable. The Head Bay of Bengal is a region where normally a series of monsoon depressions occur during the season (Zuidema, 2003). Central Indian box is completely located over land region and the rainfall in the region is being contributed mostly by the westward moving monsoon depressions which usually form over Bay of Bengal (Lau and Lau, 1992). Low

amounts of Rainfall occur at the western half of the box compared to the eastern half. The south west Indian Ocean box and south east Indian Ocean boxes considered are located over the ocean in the southern hemisphere where considerable amount of precipitation is found to occur during the monsoon season.

## 6.3. Results and discussion

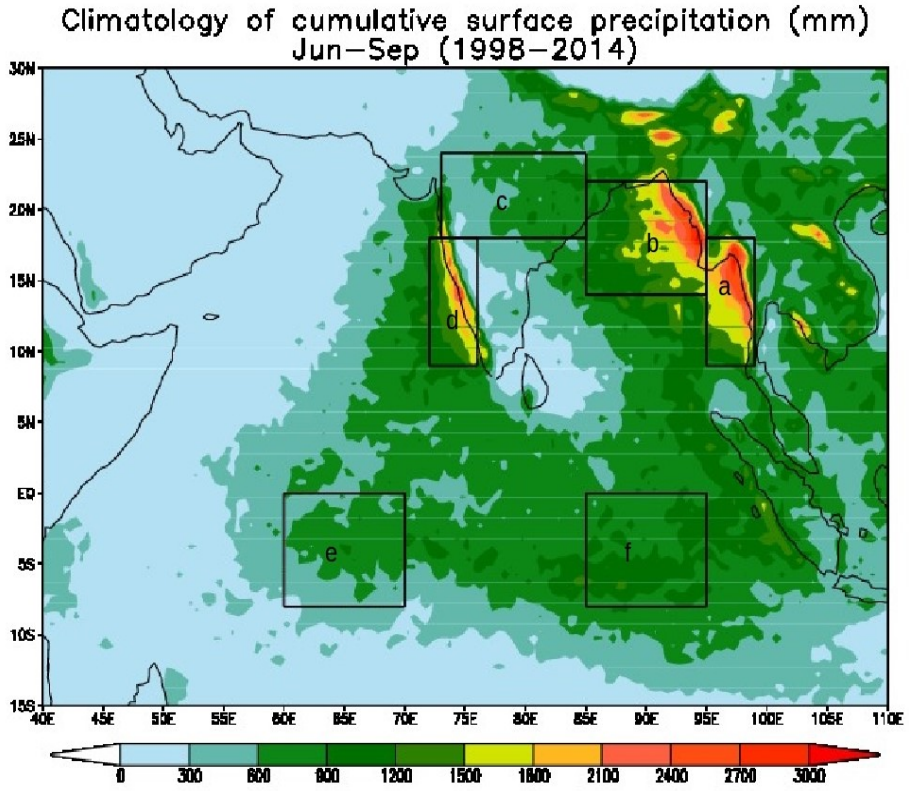


Figure 6.1 Climatology of cumulative surface precipitation for the period from 1998 to 2014. The boxes marked are sub regions considered for detailed analysis of latent heating and hydrometeor profiles.

Figure 6.1 provides climatology of cumulative rainfall during Jun-Sep for the period from 1998 to 2014. The regions where prominent rainfall occurs are the west coast of India, the Bay of Bengal and the west cost of Myanmar

and Thailand. Comparing to the Bay of Bengal, the rainfall occurring over most parts of the Arabian Sea is in low amounts.

Table 6.1. List of years with El Niño, La Niña and normal conditions during the study period. M-moderate, W–weak years are indicated in parenthesis. No strong El Niño or La Niña cases were present during the study period.

| | **El Niño** | **La Niña** | **Normal** |
|---|---|---|---|
| **Years** | 2002 (M) | 1998 (M) | 2001 |
| | 2004 (W), | 1999 (M) | 2003 |
| | 2006 (W) | 2000 (W) | 2005 |
| | 2009 (M) | 2007 (M) | 2008 |
| | | 2010 (M) | 2012 |
| | | 2011 (W) | 2013 |
| | | | 2014 |

The interannual variability of convective and stratiform type rainfall over the Indian subcontinent and adjoining oceanic region has been documented by Pokrel and Sikka (2013). They have observed that the stratiform and convective fractions contribute almost equally to the total rainfall (45–55 %) over Indian mainland as well as for all the seven major sub-regions they considered. Chttopadhyay *et al.,* (2009) and Zuluaga *et al.,* (2010) observed dominance of stratiform fraction over equatorial Indian Ocean and Bay of Bengal respectively. According to Chattopadhyay over the Indian subcontinent and Indian Ocean, the stratiform fraction shows large scale organization during both the break and active phases of monsoon with larger amplitude of anomalies over certain regions than the convective counterpart.

The present analysis confirms predominance (>50%) of stratiform rain fraction over the Indian mainland, except in the monsoon trough region and a narrow inland strip parallel to the west coast of India. Over the Oceanic region, there are some locations where convective and others where stratiform type rains dominate. Offshore of the east coast of India, a parallel strip of western Bay of Bengal has dominance of stratiform type rain, along with the west coast of Myanmar and Thailand and Sumatra Island. In the central Bay of Bengal and the Head Bay regions, convective type rain predominates. Along the equatorial region, in longitudes confined between 90 and 100$^{o}$ E, there is dominance of stratiform type rain. Over the South West Indian Ocean region, the contribution of convective rain is larger than the stratiform type rain.

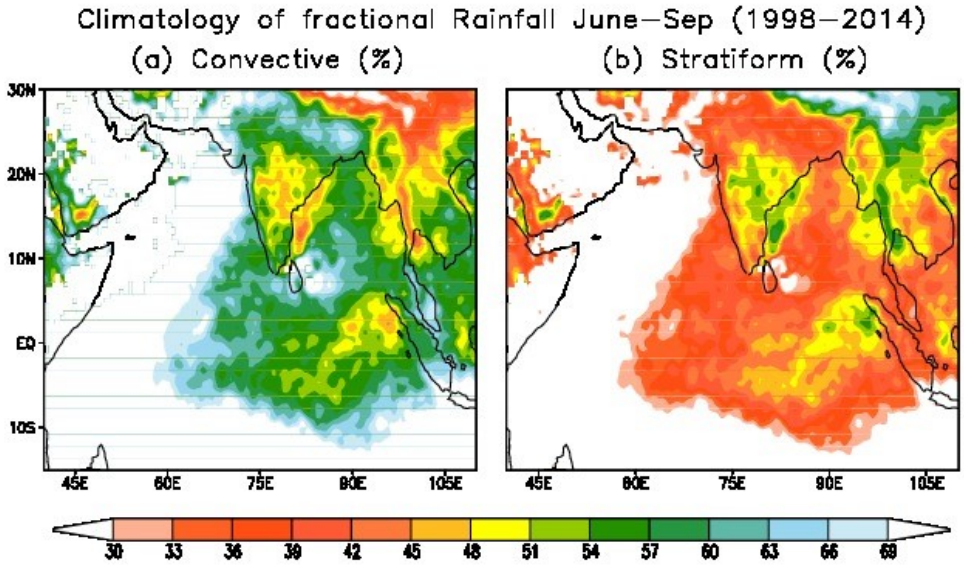


F

Figure 6.2. Convective and Stratiform rain climatology during the period 1998 to 2014. The regions with <30% and >70% proportion of convective and stratiform type rain is shown in white colour for realistic rain pattern.

The relative importance of convective and stratiform precipitation varies across the Tropics (Schumacher and Houze 2013). Stratiform rain

production is not very dependent on the strength of convection. This relationship is especially evident over the ocean, where there are weaker convective rain rates than over the land but relatively larger stratiform rain amounts.

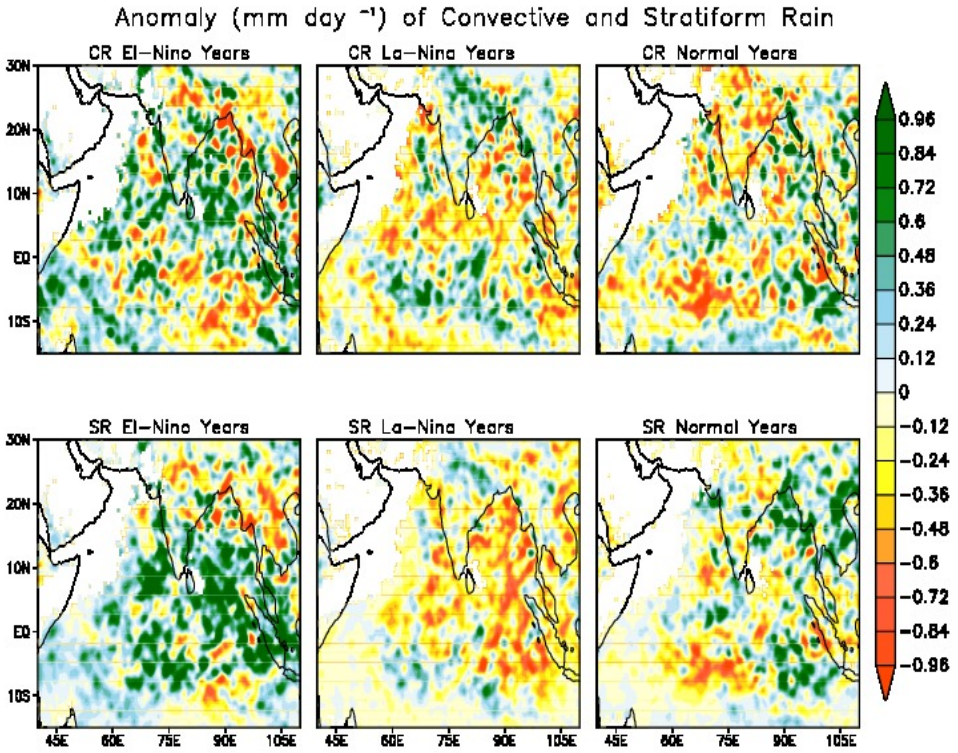


Figure 6.3. Anomaly of Convective and Stratiform rain during El Niño, La Niña and normal years. Top panel figures provide convective rain (CR) anomalies and the bottom panel figures stratiform rain (SR) anomalies.

Interannual anomalies in Figure 6.3 show that convective as well as stratiform rain amount over oceanic regions are anomalously high during years of El Niño condition, especially over the Bay of Bengal region. Off the west coast of India convective rain activity is suppressed during El Niño years. Equatorial Indian Ocean convective rain anomaly is negative whereas the stratiform rain anomaly is positive. Over land regions, both the convective

and stratiform rain fraction shows reduction during the El Niño years. Rainfall in the Monsoon trough of northeast India exhibits reduction in both convective and stratiform type rain. During La Niña years, the reverse pattern occurs in both stratiform and convective type rain in general over the ocean and the land, a result following in part from the definition of anomalies. The enhancement of convective type rain over the Indian mainland in general and along the monsoon trough region in particular is observed. The stratiform contribution of rain remains less variant over most parts of the Indian mainland with the exception of enhancement along the monsoon trough region.

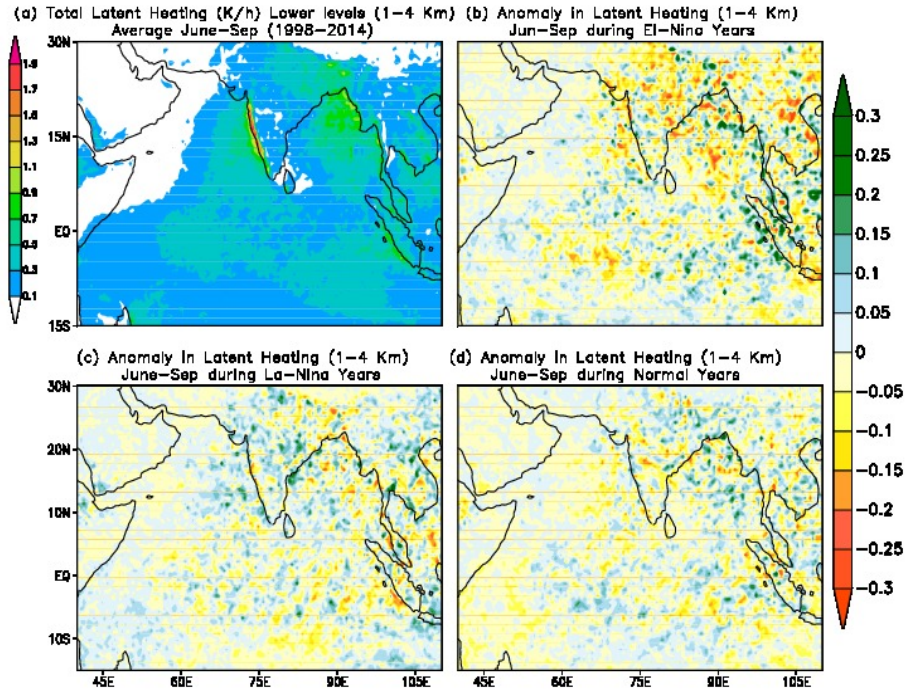


Figure 6.4. Integrated latent heating in lower levels (1-4 Km from the surface) attributable to chiefly convective type of precipitation (a) and the anomalies during El Niño (b), La Niña(c) and Normal (d) years.

The stratiform rain is less during La Niña years almost everywhere over the oceanic region. The convective rain is found to have an upper hand

off the west coast of India and along the equator and slightly south of it. During the normal years, negative anomaly of convective type rain and positive anomaly in stratiform fraction is witnessed over the Bay of Bengal and over the Indian mainland.

From figure 6.4 (a), it could be observed that lower level heating is predominant along the west coast of India. This is largely attributable to the orographic convection. There is predominant negative anomaly in lower level latent heating over the Indian mainland during El Niño (Figure 6.4.b) where the positive anomaly during La Niña (Figure 6.4.c) is also evident. A mixed pattern is visible during normal years with moderate convection present in magnitude over the Indian land region.

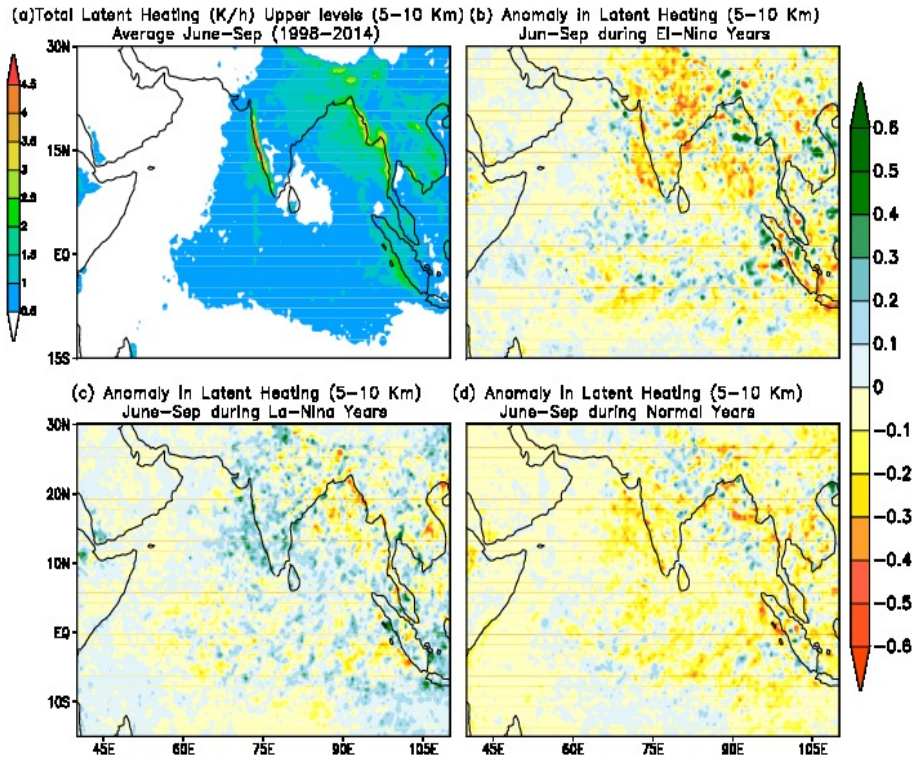


Figure 6.5. Integrated latent heating in upper levels (5-10 Km from the surface) attributable to chiefly stratiform type of precipitation (a) and the anomalies during El

Niño (b), La Niña(c) and Normal (d) years.

Figure 6.5 (a) shows upper level heating integrated from level 5 to 10 Km. The magnitude of integrated latent heating in the upper levels is of the order of roughly three times the latent heating at lower levels. During El Niño Years, strong negative anomaly is observed over the land region, off the west coast of India and in the Bay of Bengal region between latitudes 5$^{o}$N and 15$^{o}$N. However, over the Head Bay of Bengal region north of the 15$^{o}$N latitudes, there is positive anomaly in upper level latent heating. On the contrary, the La Niña years are marked by presence of strong positive anomaly in upper level heating almost entirely over the Indian land region and off the west coast of India. However, over the Head Bay region, on the other hand, anomalous negative upper level heating is present during the La Niña years. During normal years, positive anomaly in upper level heating is present along the monsoon trough region and central Bay of Bengal, while the rest of the region often has slight negative anomalies.

From Figure 6.6 (a), it may be seen that there is a basic heating with varying magnitudes centred on nearly 7 Km at all the sub regions under the analysis. While the two highly raining hot spots (the eastern Bay of Bengal and the West coast of India) rank as 1 and 2 in the highest values, the Head bay and central Indian land regions rank 3 and 4 respectively in the amounts of latent heating. Heating over the South East Indian Ocean and the South West Indian Ocean are less, ranking 5 and 6 respectively. A very interesting feature noticed is that all boxes containing land exhibits a pronounced secondary maxima at around 3 Km. This is less evident over the Oceanic region, and almost absent in the Head bay region. Over the Head Bay region, however, large heating is present for a wide range of vertical levels. The heating is almost uniform from 3 to 9 Km with the peaking of values roughly around 7

Km.

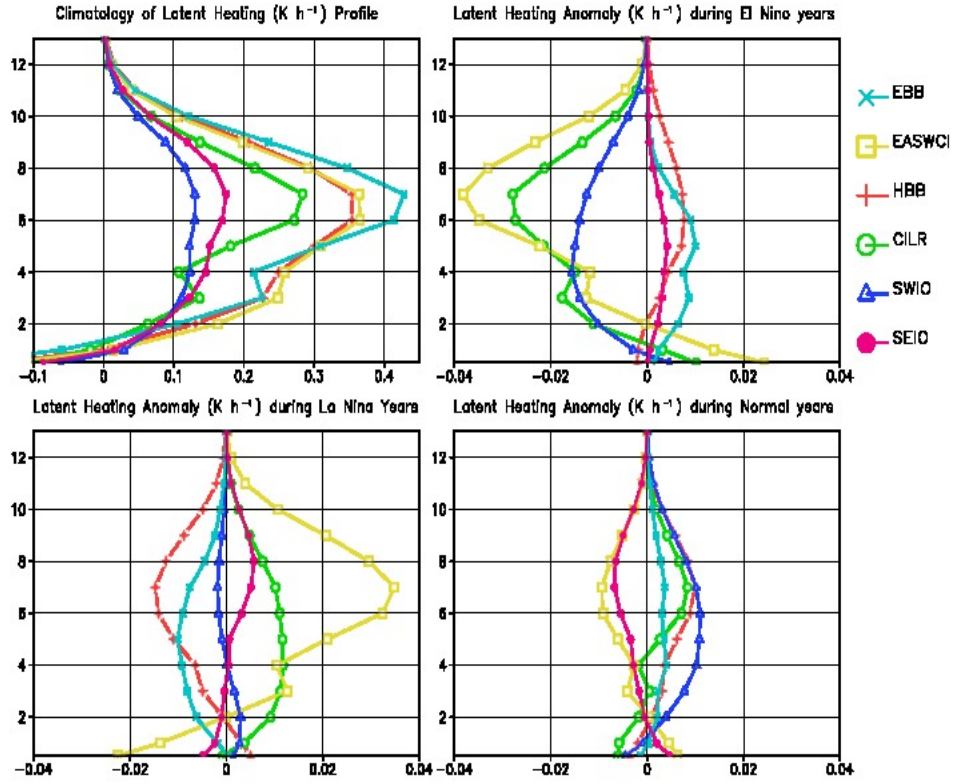


Figure 6.6. Profiles of (a) climatological latent heating (for the period 1998 to 2014), anomaly in latent heating during (b) ElNino years, (c) LaNiña years and (d) Normal years.

It is evident that there are regions with marked differences in latent heating with respect to the El Niño and La Niña conditions. The boxes considered in the Head bay, Eastern Bay of Bengal and the Southeast Indian Ocean region have positive (negative) heating anomaly over all levels during El Niño (La Nina) years whereas the other three boxes namely the Central Indian Land region, the West coast of India and the South West Indian Ocean have negative (positive) heating anomaly during El Niño (La Nina) years. This suggests that deep convection is favoured (suppressed) by El Niño (La Nina) condition east of the 85$^{o}$E longitude, whereas an opposite effect is observed

west of this line.

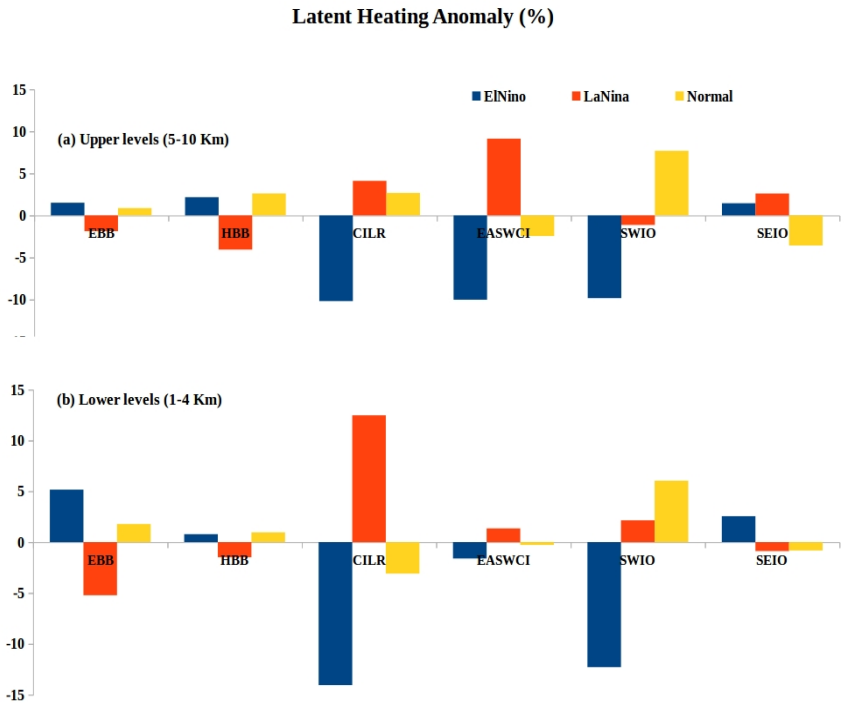


Figure 6.7. Percentage deviation from climatology of latent heating in the lower (1-4 Km) (below) and upper (5-10 Km) (above) levels in the six boxes considered for the analysis.

The most El Nino-depleted box is CILR with about 14%. That region also has the maximum positive anomaly (+12%) during La Niña years. On the other hand, while there is considerable negative anomaly (-10%) in upper level heating in CILR during El Niño years, the positive anomaly during La Niña years is low (+4%). This suggests that the rain contribution from low level convective type of rainfall is most decisive of the rainfall availability in Indian land mass which leads to deficient or surplus situations during El Niño and La Niña.

Another interesting result from this analysis is that there is only meagre

deviation in lower level latent heating in the EASWCI region. This confirms that the convective type of rainfall in the region is governed almost entirely by the orographic effect of the Western Ghats. However, on the upper level heating in the same region, there is considerable negative anomaly (-10%) during El Niño years and positive anomaly (+9 %) during La Niña years.

South west Indian Ocean region exhibits large negative anomaly during El Niño years with the lower and upper level heating reduced by about 12% and 10% respectively but the anomalies during La Niña years are negligible. However, it may be noticed that lower level heating is slightly positive and upper level heating slightly negative in the region during La Niña.

As discussed earlier, the three sub regions considered east of longitude 85º E, namely the Head Bay of Bengal, Eastern Bay of Bengal and the South east Indian Ocean region, all have typically a reverse pattern with respect to the El Niño, La Niña years. Even though the departure from climatology in percentage is comparatively low (magnitude less than 5% in general), the signal is significant. These regions have positive anomalies during El Niño years and negative anomalies during La Niña years.

Figure 6.8 provides latent heating anomaly during El Niño and La Niña years in different latitude belts for the period Jun-Sep averaged. It may be noted that the opposing anomalous behaviour during El Niño and La Niña years are present in all latitude belts east of 60ºE longitude. It is interesting to note the phase change occurring east of roughly 85ºE, the El Niño anomalies from negative to positive and La Niña anomalies from positive to negative. However, this assumes a second reversal further east in some cases. In the northern belt (15-25ºN), the anomalies at upper and lower levels assume a significant phase change east of 85º E longitude with respect to El Niño and

La Niña years. Further eastward, a narrow strip of longitude band between 100 -110º E has positive La Niña - negative El Niño anomalies. In the middle belt (5-15ºN), the phase shifts from positive La Niña - negative El Niño anomalies to positive El Niño – negative La Niña anomalies are observed both in lower and upper levels in a further eastward longitude (95ºE). In southern belt (10-0ºS) however, such a phase reversal is not evident in upper levels, but occurs at nearly 75ºE in the lower levels, and reversal of phase occurs again further eastward. The positive La Niña – negative El Niño anomalies reappear east of roughly 100º E both in the lower and upper levels in the southern belt.

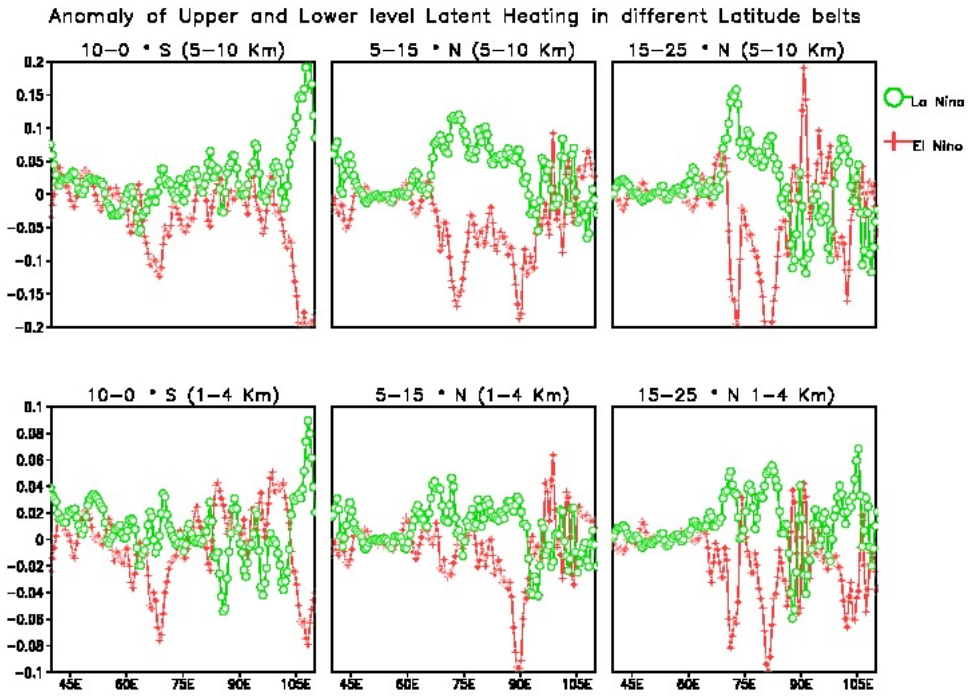


Figure 6.8. Latent heating anomaly during El Niño and La Niña years in different latitude belts for the period Jun-Sep averaged. Upper panel gives upper level (5-10 Km) and lower panel gives lower level (1-4 Km) latent heating anomalies for 10-0ºS (left panel), 5-15ºN (middle panel), and 15-25ºN (right panel)

Among all the regions under consideration, The Indian land region is found to have the maximum negative (positive) anomaly during the El Niño

(La Niña) years. This leads one to identify the eastern border of negative (positive) impact of El Niño (La Niña) over the South Asian region. To be exact, if one draws an imaginary line parallel to 85ºE longitudes near the Head Bay of Bengal, taking an eastward bend in the central Bay to about 95ºE and again taking a westward bend southward to roughly 75ºE at 10ºS, this line will have El Niño and La Niña having opposing influences east and west of it.

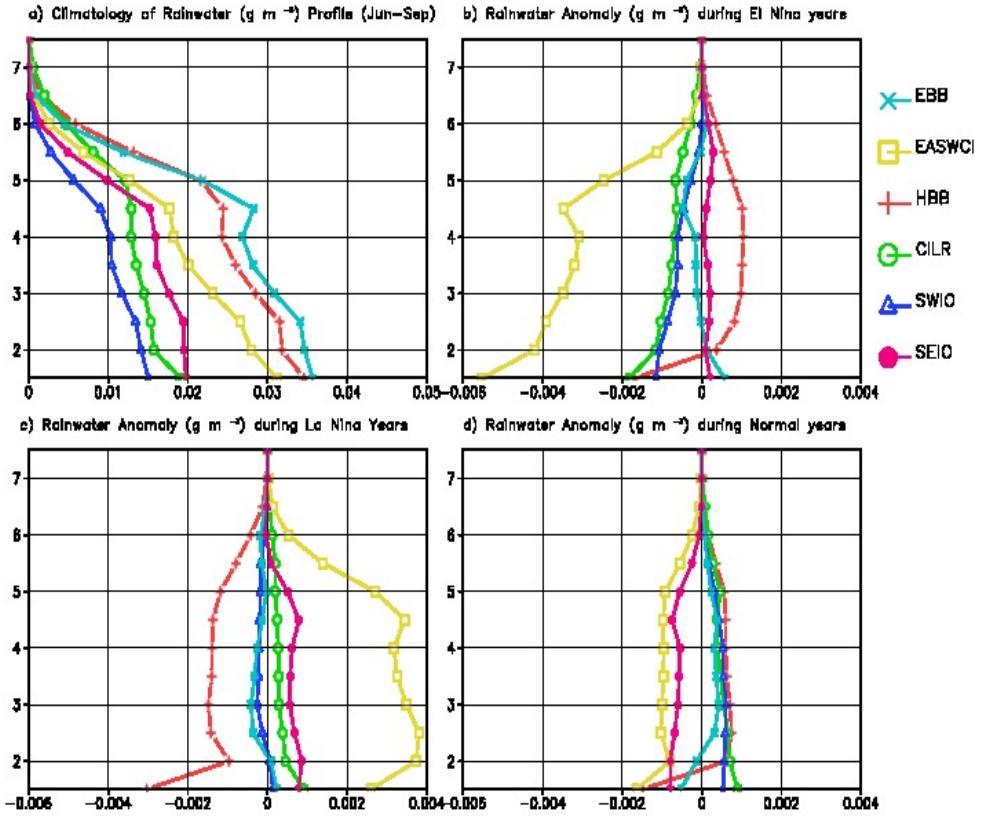


Figure 6.9. Climatology of Rainwater at different levels from 1-8 Km averaged for Jun-Sep for the period 1998-2014 (a), anomalies (Jun-Sep) in rainwater profile during (b) El Niño, (c) La Niña and (d) Normal years.

It is evident that water molecules can take a variety of physical forms in a cloud. The various forms of water and ice co-exist and interact within the overall cloud ensemble. Obviously, it is the overall properties of the cloud

ensemble that is of primary interest in cloud dynamics. At the same time, it is also impossible to ignore the microphysical processes, which is important for the overall behaviour of the clouds (Abhilash *et al.,* 2008). Figure 6.9 (a) provides the climatology of rainwater at different levels in atmosphere. In general, there are two peaks, roughly in between 2 and 3 Km and in between 4 and 5 Km. It is likely that the lower peak results from the convective type clouds having maximum presence at 3-4 Km height and the upper peak in rainwater results from the stratiform type of clouds present at higher altitudes (>6Km). The largest value of rain water is for the EBB followed by HBB, EASWCI, SEIO, CILR and SWIO regions. Kumar *et al.,* (2014) have observed that warm rain process is dominant near the Western Ghats and cold rain from mixed phase processes is dominant near the Myanmar Coast. Much deeper clouds develop over the Myanmar Coast because of dynamical and latent heating response of the air column hits the tropopause and forms bigger cloud anvils. So, more than half of the rain comes from melting of snow and graupel present in the large scale and anvils of cloud. The prominent peak at higher altitudes (4-5 Km) in the rain water profiles for EBB and HBB boxes which coincide with the study area of Kumar *et al.,* (2013) may be attributable to the cold process rain. Values comparable to the same over the EASWCI box occurs at lower altitudes (2-3 Km) indicating warm rain process.

Figure 6.9 (b), (c) and (d) provides anomalies during El Niño, La Niña and Normal years respectively. In tune with the heating anomalies shown in Figure 6.6, the HBB and the SEIO regions have positive anomalies in rain water at all levels during the El Niño years and negative anomaly during La Niña years. However, for the Eastern bay region, positive anomaly in rain water during the El Niño period is absent. This reveals that the El Niño largely affects the higher altitudes in the region in a positive manner. Largest

anomalies are present in the Eastern Arabian Sea and West coast of India region, negative during El Niño and positive during La Niña. Central Indian land region has positive anomaly in rainwater during La Niña years and negative anomaly during El Niño years at all levels.

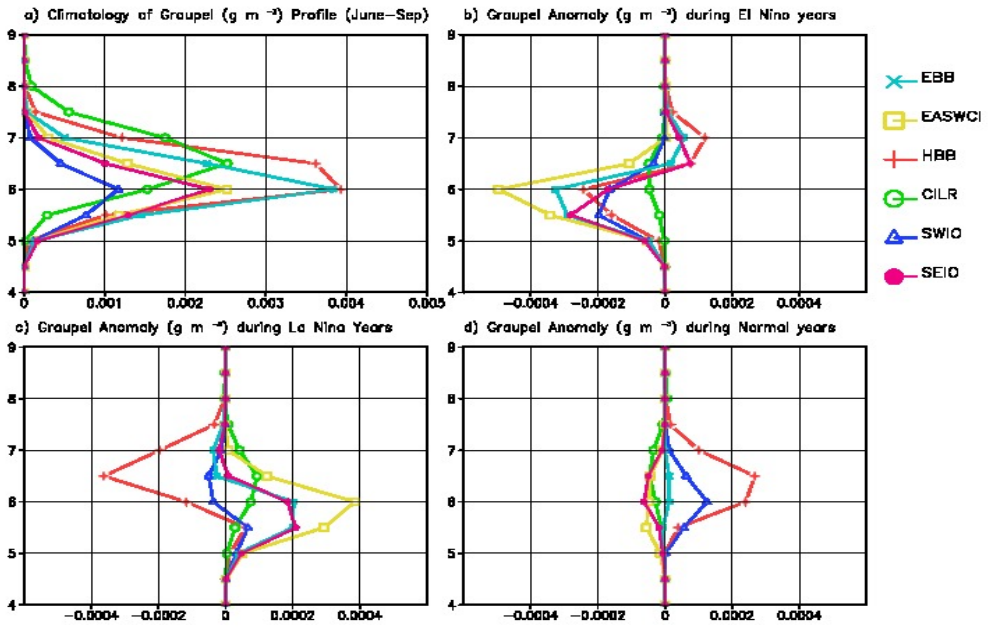


Figure 6.10. Climatology of graupel at different levels from 4-9 Km averaged for Jun-Sep for the period 1998-2014 (a), anomalies (Jun-Sep) in graupel profile during (b) El Niño, (c) La Niña and (d) Normal years.

Figure 6.10(a) provides the climatological (1998-2014) profiles of graupel in the six sub regions. The maximum value of graupel in CILR and HBB region are located at a little higher level compared to the same in other sub regions. Graupel is having higher values in the HBB and EBB regions. In CILR, EASWCI and SEIO regions, the climatological graupel is having comparable magnitudes. Presence of graupel is low over the SEIO region. Figure 6.10(b) gives anomalies during El Niño years. It may be noticed that in HBB, EBB and SEIO there exists a reverse relationship above and below 6 Km. There is positive anomaly above and negative anomaly below 6 Km line.

During La Niña years, graupel anomaly is negative over the HBB but positive over the CILR. Over the EASWCI, graupel anomaly is negative during El Niño years but positive during La Niña years at all levels.

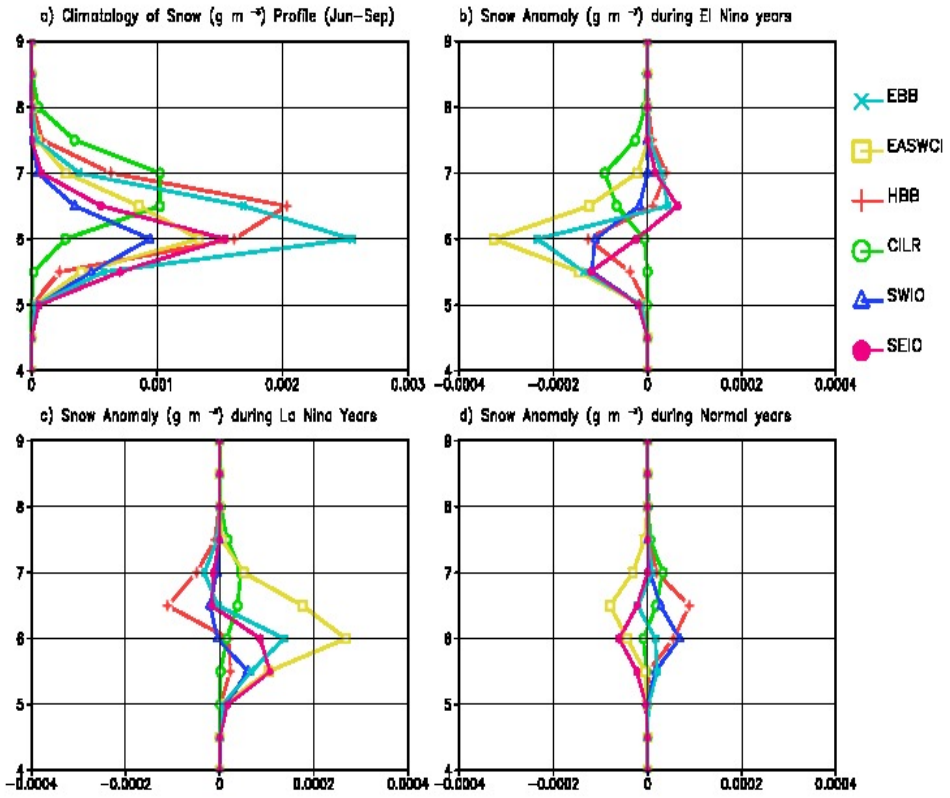


Figure 6.11. Climatology of snow at different levels from 4-9 Km averaged for Jun-Sep for the period 1998-2014 (a), anomalies (Jun-Sep) in snow profile during (b) El Niño, (c) La Niña and (d) Normal years.

Similar as in the case of graupel, maximum of snow (Figure 6.11 a-d) in the HBB and CILR region occur at slightly higher altitudes as compared to the other sub regions. While the maximum values are present in EBB and HBB region, SEIO and EASWCI regions have moderate occurrence of snow presence. Only less than half of the amount of snow present in HBB and EBB is available at CILR and SWIO region. There is positive anomaly in snow

amounts over HBB, EBB and SEIO and negative anomaly over EASWCI, CILR and SWIO during El Niño years. The reverse is the case with La Niña.

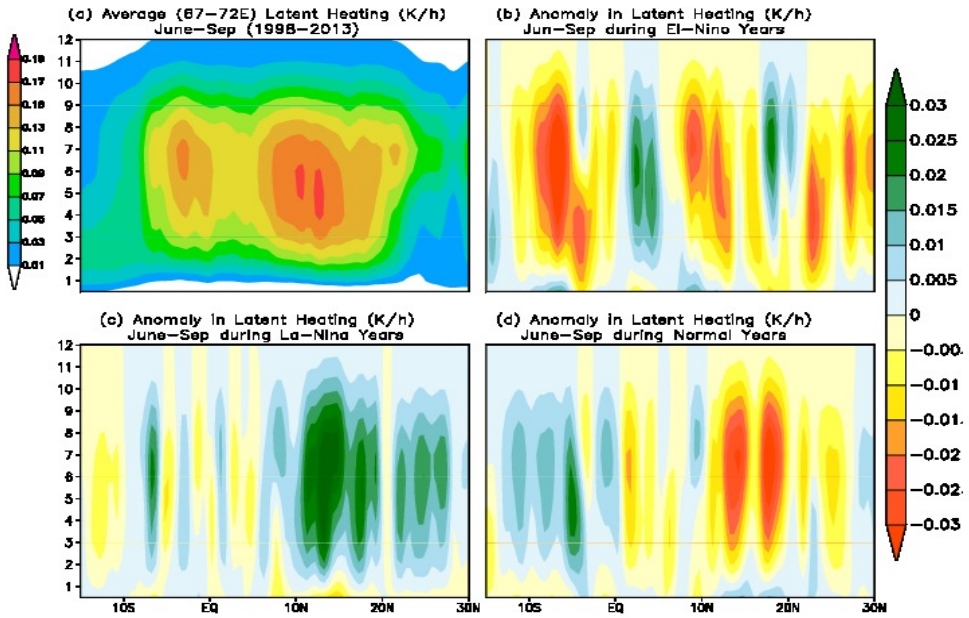


Figure 6.12. (a) Latent Heating averaged for the longitudes 67-72 E representing the Arabian Sea for Jun-Sep for the period 1998-2014, anomalies during El Niño (b), La Niña(c) and Normal years (d).

Figure 6.12 (a) gives the latent heating at vertical levels averaged between longitudes 67-72$^{o}$E representing the Arabian Sea. The two hotspots are one between 5-0$^{o}$S and the other between 10-20$^{o}$N. The core of the northern hotspot is at lower levels, between 4 and 6 Km whereas the core of the southern hotspot is a little higher nearly around 7 Km. Anomaly during La Niña (c) is interestingly positive in the latitudes between 10 and 20$^{o}$N, corresponding to enhanced convective activity in the region during La Niña years as compared to the El Niño and normal years. Figure 6.13 (a) gives the vertical pressure velocity ($\omega$) averaged for longitude 67-72$^{o}$E for the period 1998 to 2014. Negative $\omega$ anomalies occur at regions of large rain accumulations. It may be noted that the reversal in sign of $\omega$ anomaly with

respect to El Niño and La Niña is evident in the region especially between equator to 30°N.

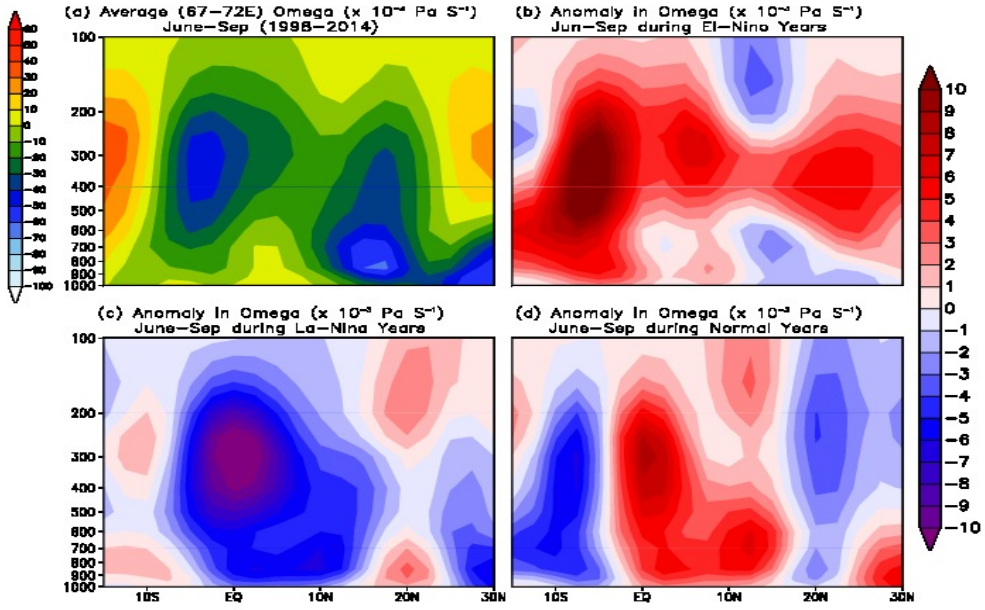


Figure 6.13 (a) Vertical pressure velocity ($\omega$) averaged for the longitudes 67-72°E representing the Arabian Sea for Jun-Sep for the period 1998-2014, anomalies in $\omega$ during El Niño (b), La Niña(c) and Normal years (d).

The location of largest negative $\omega$ values occur at higher altitudes south of the equator in this Arabian Sea longitudes whereas a peak is observed in the latitudes between 10-20°N at lower levels corresponding to the orographic ascent due to the Western Ghats. However, its influence is extended to higher altitudes considerably. The anomaly in $\omega$ during El Niño years is positive corresponding to the large values present in climatology at higher altitudes south of the equator, indicating reduced rising motion. However, the anomalies during El Niño are insignificant at lower levels of the Western Ghats region but considerably positive at higher altitudes. This reveals that the stratiform cloud formation is suppressed during the El Niño years. On the contrary, during the La Niña period, there is a large negative

anomaly in $\omega$ at all levels from almost 10°S to 20°N latitudes indicating favourable ascending of air mass producing enhanced rainfall. During normal years, the anomaly in $\omega$ values is negative at all levels between latitudes 5°S to 15°N.

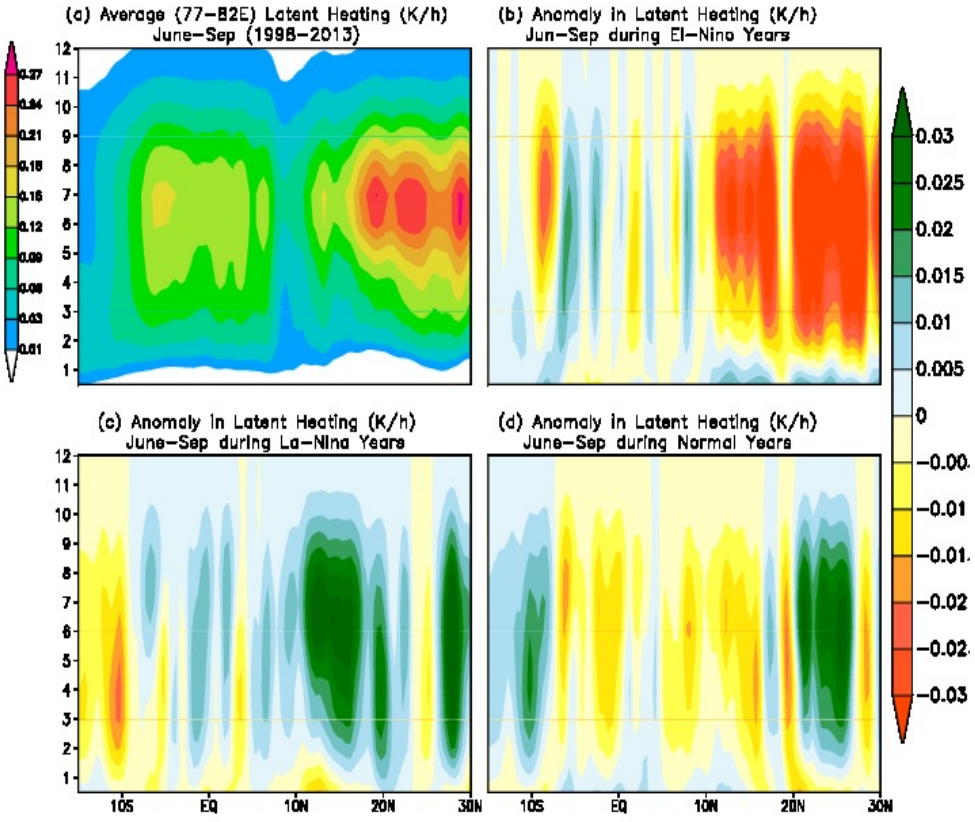


F

Figure 6. 14. (a) Latent Heating averaged for the longitudes 77-82°E representing the Indian mainland for Jun-Sep for the period 1998-2014, anomalies during El Niño (b), La Niña (c) and Normal years (d).

Figure 6.14 (a) shows that in the longitudes representing the Indian mainland, the maximum heating is confined between 15 and 30°N at altitude 6 and 8 Km. There is strong negative anomaly in the region during the El Niño years and positive anomaly during La Niña years. During normal years north of 20°N, and south of 8°S there is positive anomaly in latent heating (b-d).

The $\omega$ values in Figure 6.15 (a) shows that the location of the maximum negative values is present at a little lower altitudes in the oceanic region south of Indian mainland as compared to the Arabian Sea longitudes. However, in the region 10°N and 25°N, which is over the Indian mainland, the extent of negative $\omega$ values reach very high altitudes indicating deep convection. However, the average low level values of $\omega$ between the equator and 15°N latitudes are positive indicating reduced possibility for low level convection. This reveals the reason why the stratiform cloudiness has an upper hand in producing the overall rain in the region. These findings are in tune with the observations of Vijaykumar *et al.,* (2017) that rain producing clouds prefer to occur at lower altitudes over the south West Indian Ocean region and at higher altitudes over the central India.

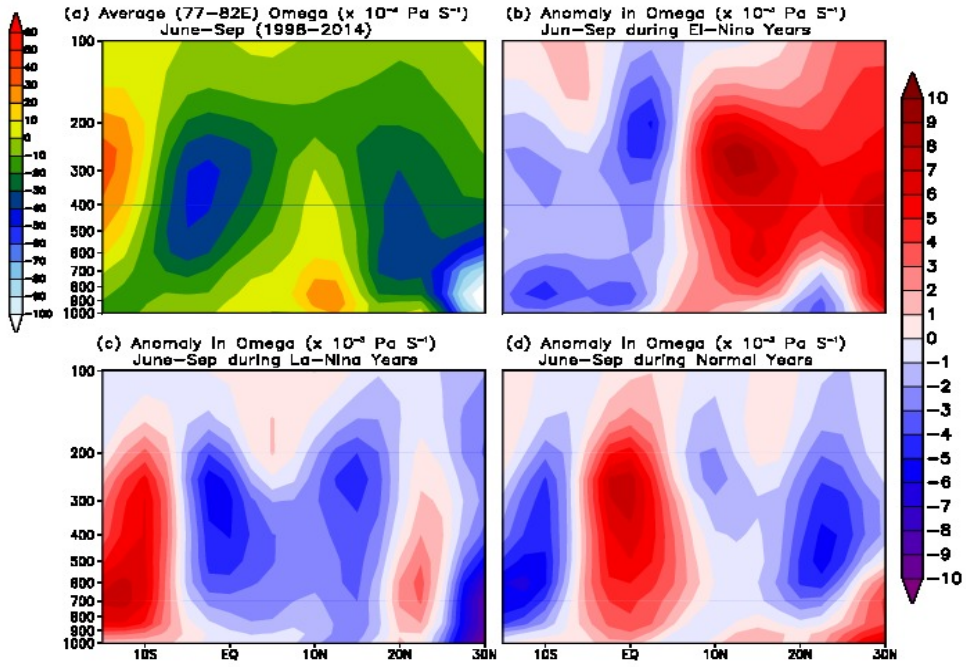


Figure 6.15 (a) Vertical pressure velocity ($\omega$) averaged for the longitudes 77-82°E representing the Indian mainland for Jun-Sep for the period 1998-2014, anomalies in $\omega$ during El Niño (b), La Niña (c) and Normal years (d).

From Figure 6.15 (b-d) the $\omega$ anomaly during El Niño years is positive at all levels north of 5$^{o}$N latitudes, indicating reduced rains both from lower level convective and higher level stratiform types. On the contrary, during the La Niña years, both at lower and higher altitudes between 5$^{o}$S to 20$^{o}$N, the $\omega$ anomaly is negative indicating enhancement in both the convective and stratiform type rain activity over the Indian mainland producing surplus surface rainfall. During normal years, there is a positive anomaly in $\omega$ values centred on the equator, but over the Indian mainland, by and large, the anomaly is slightly negative. This observation indicates that both El Niño and La Niña favours convection in the southern tip of India, leading to above normal rainfall but during normal years, convection remains suppressed. This could be one of the reasons why the southernmost State of Kerala on the western edge of India receives below normal rainfall even when the rest of the mainland receive normal rainfalls as happened during certain normal rainfall monsoons. The abnormal negative values north of 25$^{o}$N at lower levels in Figure 6.15 (a) may be an error in data sampling due to undesirable influence of the Himalayan orography.

In the Bay of Bengal region, the hotspot of heating is confined between 15$^{o}$ and 25$^{o}$ N at altitudes 6 to 8 Km (Figure 6.16 a). Positive anomaly is observed during El Niño years and negative anomaly during La Niña years in the hotspot regions. During normal years, the pattern is mixed (Figure 6.16 b-d). The corresponding vertical pressure velocity given in Figure 6.16 a, indicates that large negative $\omega$ values are present in the Head Bay of Bengal region at higher altitudes. The counterpart of it in the Southeast Indian Ocean is located at comparatively lower altitudes. Further, there is negative $\omega$ anomaly in the head bay region during El Niño years, explaining why the El Niño has an influence of enhanced rainfall in the region. During La Niña years

and normal years, the anomalies in $\omega$ are positive. South of the equator, the anomaly has opposite pattern during El Niño and La Niña as compared to the north of the equator region. The anomaly is strongly positive (negative) in the southern part during El Niño (La Nina) years.

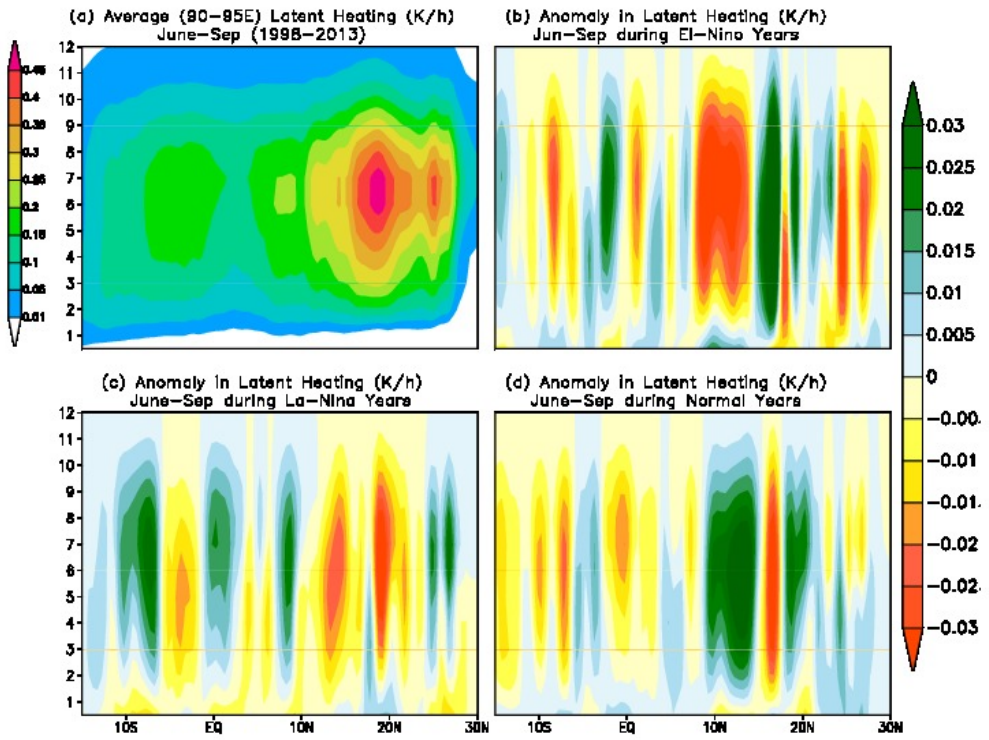


Figure 6.16 (a) Latent Heating averaged for the longitudes 90-95°E representing the Bay of Bengal for Jun-Sep for the period 1998-2014, anomalies during El Niño (b), La Niña (c) and Normal years (d).

It is widely believed that El Niño's impact on the Indian monsoon is through the east-west displacement of the ascending and descending branches of the Walker circulation that link Indo-Pacific climates (Shukla *et al.,* 1987; Ropelewski and Halpert, 1987). Unusually warm waters during El Niño cause an increased ascent associated with increased rainfall. Air mass continuity requires increased descent broadly over Southeast Asia, suppressing monsoon

rains (Krishnakumar *et al.,* 2006). However, as discussed earlier, this influence of El Niño and La Niña is found to be having significant regional differences over the South Asian monsoon region.

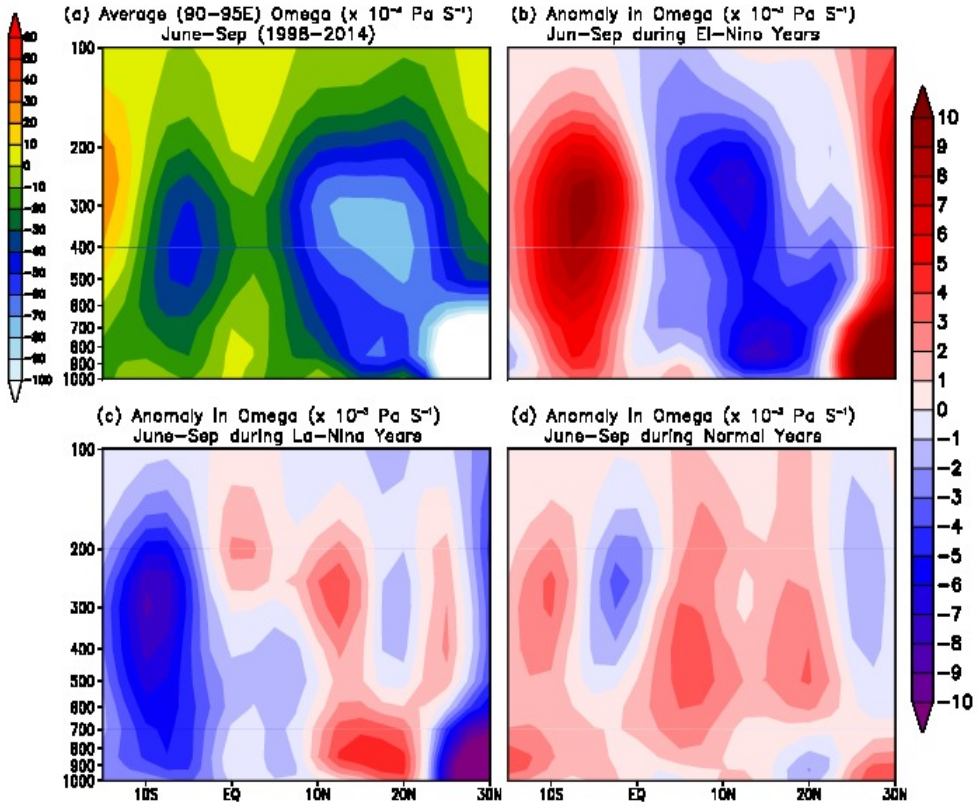


Figure 6.17 (a) Vertical pressure velocity ($\omega$) averaged for the longitudes 90-95°E representing the Bay of Bengal for Jun-Sep for the period 1998-2014, anomalies in $\omega$ during El Niño (b), La Niña(c) and Normal years (d).

There are no strong El Niño or La Niña events in the period of this analysis as details given in Table-1. Hence, presently witnessed reversal of El Niño and La Niña effect nearly parallel to 85°E longitude may differ when years with strong El Niño or La Niña cases are included in the analysis.

### 6.4. Conclusions

Patterns of the vertical profiles of latent heating and the hydrometeors

in the six sub regions of interest over the Indian mainland and surrounding Ocean for the El Niño, La Niña and normal years during one and a half decade are revealed. The major finding of the present analysis is the distinctly different responses to the El Niño and La Niña in the sub regions considered. East and west of roughly 85ºE line, contradictory influence of El Niño and La Niña is observed. To be exact, if one draws an imaginary line parallel to 85ºE longitudes near the Head Bay of Bengal, taking an eastward bend in the central Bay to about 95ºE and again taking a westward bend southward to roughly 75ºE at 10ºS, this line will have El Niño and La Niña having opposing influences east and west of it. The anomalies are most pronounced east of 60ºE longitude. The negative impact of El Niño in terms of reduced rain availability is suffered mostly by the central Indian mainland. La Niña period is witnessed with enhanced convective activity over the Indian mainland at all altitudes leading to more stratiform and convective type rainfall. The major limitation of the study is the absence of representative cases of strong El Niño or La Niña during the study period, available cases are moderate and weak El Niño and La Niña years.

**Chapter-7**

# 7.1. Summary and Conclusions

The focus of present study is on the characteristics of cloudiness in the Asian monsoon region during different seasons in general and summer monsoon season in particular. In the first part of the thesis, an attempt is made to understand the relationship between rain intensity and infrared brightness temperature (BT). For the purpose, Cloud Top Brightness Temperature (CTBT) derived from INSAT three hourly IR radiances was compared with corresponding TRMM PR Rain Rate (TPRR) during Indian Summer Monsoon periods of 2007 and 2008. BT value ranges corresponding to events of various intensities of rain in the four major raining sub regions identified in Indian subcontinent and surrounding ocean are compared. The sub regions identified are (1) Head Bay of Bengal, (2) Central Indian land region, (3) Eastern Arabians Sea and West coast of India and (4) South West Indian Ocean. BT values are grouped into classes of 10 K bin width between 270 and 180$^{O}$K. Number of occurrence of three classes of rain (light - > 4.5 mm, moderate - 4.5-9 mm and heavy 9.0 mm and above cumulative for 3 hours) belonging in each BT classes is calculated. It is observed that the three classes of rainfall have distinct characteristic BT ranges. This rain category - BT range relation has geographical (spatial) variability. This could be due to the variation in

types of clouds prevalent in the sub regions considered. The study improves the understanding of the structure and spatial variability of cloudiness and rainfall in and around Indian region during monsoon season.

The Seasonal and Intraseasonal Variability of Cloudiness and Rainfall over Indian mainland and adjacent Oceans during different pre, summer and post monsoon seasons were studied and presented. Prominent cloud features over the Asian monsoon regions during different seasons was explored using INSAT brightness temperature data for a period of 5 years. Frequency of occurence of different types of clouds was studied in detail. In general deepest of clouds occur over the north and central Bay of Bengal during the pre and summer monsoon seasons. During the post monsoon season, deepest clouds are found over the east equatorial Indian Ocean and over Sumatra Island. The height of clouds in the Bay of Bengal during the post monsoon season were found to be a little lower compared to the other two seasons. The Indian mainland is largely covered by clouds during the summer monsoon season. The highest of clouds over the Indian mainland during the summer monsoon season are present in the latitude belt 15-25$^{O}$N. Over the Arabian Sea and off west of west coast of India, prominent rain producing clouds are shallow to high rather than deep. Rain producing clouds in the western equatorial Indian Ocean are mostly shallow during all seasons. Analysis of seasonal variation of

extreme rainfall events revealed that such events are more frequent over the land as compared to ocean. West central and central states of India experience frequent extreme rain incidents during the summer monsoon season. Northeast states of India receive extreme rainfall during both the pre and summer monsoon seasons. During all three seasons, extreme rain events occur over the southwest tip of India. Southeast coastal states of the country are prone to extreme rain events during the post monsoon season. Extreme rainfall significantly contributes to the total rain obtained in a season over the northeast and northwest states of India and some regions of central India. Spatio temporal evolution of active and break events are studied for the first time using brightness temperature data. The most significant inference from the analysis is the differential behaviour of very deep and shallow to high clouds during the Active phase of Indian summer monsoon. Deep convective clouds move west to north-westward whereas shallow to high clouds mostly propagates northward. These two cloud types and their distinct propagation characteristics are together contributing to the Active spell over Indian region.

The diurnal variation (DV) of convection over the Indian monsoon region is studied using Kalpana-1 IR Brightness Temperature and TRMM 3B42RT datasets were studied in detail. Over Indian mainland and surrounding Oceanic regions significant diurnal variation of convective

activity is observed during all three seasons under study. In general, the amplitude of DV is high over land as compared to ocean. Among the different classes of convection studied, deep (<220$^{O}$K) convection exhibits the most distinct spatial patterns of DV. During the pre-monsoon season, the preferable time of occurrence of deep convection in a day over regions like the north-eastern states and southwest tip of India and Bangladesh is roughly between 11:00 and 20:00 GMT, with the peaking between 18:00-19:00 GMT hours. Oceanic convection remains weak during 11:00 to 17:00 GMT and suddenly peaks afterwards and continues to sustain longer. During the summer monsoon season, deep convection over the Bay of Bengal and Indian mainland are observed to be in opposing phases. A northwest march of deep convection over ocean and land is evidently seen. From 17:00 GMT onwards, intensification of convection over the east central Bay of Bengal is observed. Deep convection spreads westward and north-westward and intensifies further by 23:00 GMT. Organised deep convection in an area close to the east coast of India in the head Bay is prominent by 08:00 GMT. From 08:00 GMT onwards, location of convection starts to shift from the ocean to the land across the east coast of India. During 10:00-11:00 GMT hours, two distinct patches of apparently independent organised convection co-exists, one over the north west Bay of Bengal and the other over the inland close to the east central coast

of India. The Oceanic convective region then starts to subside whereas the land convection spreads further west north-westward. Off west coast of India, very deep clouds preferably appear during 20:00-04:00 GMT hours during the summer monsoon season. The spatial pattern of post monsoon season is largely similar to that of the pre monsoon but the oceanic convection is present more prevalent and prolonged. Along the Southeast coastal regions of India, deep convection is present around the clock whereas over the southwest tip of India, convection peaks during 12:00-17:00 GMT hours. There are considerable diurnal variations in the average rainfall, contribution to the total rain by different rain intensity classes and the fractional contribution of different category of clouds associated with the rain in the sub regions chosen for the study. In regions where the rainfall is largely modulated by the orography, light to moderate type rain has a prominent role to play. In north central India, East coast of India and northwest Bay of Bengal, intense rain class contributes the most to the total rainfall. Over the central Bay of Bengal, light, moderate and heavy rain types have more or less equal share in producing total rainfall.

The relation between the Indian summer monsoon rainfall and the sea surface temperatures over the Pacific Ocean is complex and eludes complete understanding. An attempt is made in the final working chapter of this thesis

to shed light by analysing high resolution TRMM satellite derived multilevel products over the Indian subcontinent and surrounding oceanic region during El Niño, La Niña and normal years from 1998 to 2014. Rainfall anomaly of rainfall patterns, contribution of rainfall by convective and stratiform cloud types, tropospheric heating characteristics, hydrometeor distribution profile during El Niño, La Niña and normal years reveals contradictory influences of El Niño and La Niña over Bay of Bengal longitudes vs. Indian mainland and the Arabian Sea (that is, across 85° E longitude). The impact of El Niño is not uniform over Southeast Asia but has significant regional dependency. The influence of El Niño and La Niña is most prominent over the Indian mainland as compared to the Oceanic regions.

## 7.2. Scope for future studies

A number of results discussed in this study could be investigated further to reveal more on the features of cloudiness and their impact on the energetic of the earth atmosphere system. Extending the study by examining dynamical aspects of convection, oceanic influence on cloud characteristics and topographic modulations of cloudiness may help understand better the feedback mechanisms that are significant in the phenomenal monsoon system over the Asian continent. Investigation of the role of Land and Sea breezes and moisture influx in determining cloud properties along the coastal regions is

highly prospective. Characteristics of the enhanced cloud zone over the equatorial Indian Ocean remain as one of the prominent aspect to be investigated further. Over the monsoon trough region where very deep convection is generally observed during the monsoon season there are pockets of intensely sustained and concentrated convection. The influence of topography is suspected for this feature and provides scope for detailed investigation.

# References


1. Abhilash S, Mohankumar K, Das S. 2008. Simulation of microphysical structure associated with tropical cloud clusters using mesoscale model and comparison with TRMM observations. Int J Remote Sens. 29:2411–2432.
2. Adler RF, Huffman GJ, Bolvin DT, Curtis S, Nelkin EJ. 2000. Tropical Rainfall Distributions Determined Using TRMM Combined with Other Satellite and Rain Gauge Information. J Appl Meteorol. 39:2007–2023.
3. Ahrens CD. 2008. Essentials of meteorology : an invitation to the atmosphere / C. Donald Ahrens. Brooks/Cole, Cengage Learning.
4. Alexander G, Keshavamurty R, De U, Chellappa R, Das K, Pillai P. 1978. Fluctuations of monsoon Activity. Indian J Meteorol Geophys. 29:76–87.
5. Annamalai H, Slingo JM. 2001. Active/break cycles: diagnosis of the intraseasonal variability of the Asian Summer Monsoon. Clim Dyn. 18:85–102.
6. Arkin PA, Joyce R, Janowiak JE. 1994. The estimation of global monthly mean rainfall using infrared satellite data: The GOES precipitation index (GPI). Remote Sens Rev. 11:107–124.
7. Arkin PA, Krishna Rao AVR, Kelkar RR. 1989. Large-Scale Precipitation and Outgoing Longwave Radiation from INSAT-1B during the 1986 Southwest Monsoon Season. J Clim. 2:619–628.
8. Basu BK. 2007. Diurnal Variation in Precipitation over India during the Summer Monsoon Season: Observed and Model Predicted. Mon Weather Rev. 135:2155–2167.
9. Bergman JW, Salby ML, Bergman JW, Salby ML. 1997. The Role of

Cloud Diurnal Variations in the Time-Mean Energy Budget. J Clim. 10:1114–1124.

10. Bhattacharya PK and Bhattacharya SG. 1980. Diurnal variation of rainfall in the upper catchments of north Bengal Rivers. Mausam. 31:51–54.
11. Bony S, Collins WD, Fillmore DW, Bony S, Collins WD, Fillmore DW. 2000. Indian Ocean Low Clouds during the Winter Monsoon. J Clim. 13:2028–2043.
12. Chattopadhyay R, Goswami BN, Sahai AK, Fraedrich K. 2009. Role of stratiform rainfall in modifying the northward propagation of monsoon intraseasonal oscillation. J Geophys Res. 114:D19114.
13. Chen SS, Houze RA. 1997. Diurnal variation and life-cycle of deep convective systems over the tropical Pacific warm pool. Q J R Meteorol Soc. 123:357–388.
14. Chen T-C, Chen J-M, Chen T-C, Chen J-M. 1993. The 10–20-Day Mode of the 1979 Indian Monsoon: Its Relation with the Time Variation of Monsoon Rainfall. Mon Weather Rev. 121:2465–2482.
15. Crutcher, HL and Meserve JM. 1970. Selected-Level Heights, Temperatures and Dew Point Temperatures for the Northern Hemisphere. :U.S. Naval Weather Service, 16 plus 243 maps.
16. De US, Mukhopadhyay RK. 2002. Breaks in monsoon and related precursors. Mausam. 53:309–318.
17. Devasthale A, Grassl H. 2009. A daytime climatological distribution of high opaque ice cloud classes over the Indian summer monsoon region observed from 25-year AVHRR data. Atmos Chem Phys Atmos Chem Phys. 9:4185–4196.
18. Donald Shepard. 1968. A two dimensional interpolation function for

irregularly spaced data. In: Proc - 1968 ACM Natl Conf.; p. 517–524.

19. Frank WM, McBride JL, Frank WM, McBride JL. 1989. The Vertical Distribution of Heating in AMEX and GATE Cloud Clusters. J Atmos Sci. 46:3464–3478.
20. Gadgil S, Joseph P V. 2003. On breaks of the Indian monsoon. J Earth Syst Sci. 112:529–558.
21. Gadgil S, Joseph P V., Joshi N V. 1984. Ocean–atmosphere coupling over monsoon regions. Nature. 312:141–143.
22. Gadgil S, Vinayachandran PN, Francis PA, Gadgil S. 2004. Extremes of the Indian summer monsoon rainfall, ENSO and equatorial Indian Ocean oscillation. Geophys Res Lett. 31:L12213.
23. Gambheer A V., Bhat GS. 2001. Diurnal variation of deep cloud systems over the Indian region using INSAT-1B pixel data. Meteorol Atmos Phys. 78:215–225.
24. Gambheer A V, Bhat GS. 2000. Life Cycle Characteristics of Deep Cloud Systems over the Indian Region Using INSAT-1B Pixel Data. Mon Weather Rev. 128:4071–4083.
25. Goswami BN, Mohan RSA. 2001. Intraseasonal Oscillations and Interannual Variability of the Indian Summer Monsoon. J Clim. 14:1180–1198.
26. Goswami BN, Venugopal V, Sengupta D, Madhusoodanan MS, Xavier PK. 2006. Increasing Trend of Extreme Rain Events Over India in a Warming Environment. Science (80- ). 314:1442–1445.
27. Goswami BN, Xavier PK. 2003. Potential Predictability and Extended Range Prediction of Indian Summer Monsoon Breaks. Geophys Res Lett. 30:1966.
28. Goswami BN, Xavier PK. 2005. ENSO control on the south Asian

monsoon through the length of the rainy season. Geophys Res Lett. 32:L18717.

29. Gray WM, Jacobson RW. 1977. Diurnal Variation of Deep Cumulus Convection. Mon Weather Rev. 105:1171–1188.
30. Grossman RL, Durran DR. 1984. Interaction of Low-Level Flow with the Western Ghat Mountains and Offshore Convection in the Summer Monsoon. Mon Weather Rev. 112:652–672.
31. Grossman RL, Garcia O. 1990. The Distribution of Deep Convection over Ocean and Land during the Asian Summer Monsoon. J Clim. 3:1032–1044.
32. Haldar, G. C., Sud, A. M. and Marathe, S. D. 1991. Diurnal variation of monsoon rainfall in central India. Mausam, 42: 37–40.
33. Hall TJ, Vonder Haar TH. 1999. The Diurnal Cycle of West Pacific Deep Convection and Its Relation to the Spatial and Temporal Variation of Tropical MCSs. J Atmos Sci. 56:3401–3415.
34. Harrison EF, Minnis P, Barkstrom BR, Ramanathan V, Cess RD, Gibson GG. 1990. Seasonal variation of cloud radiative forcing derived from the Earth Radiation Budget Experiment. J Geophys Res. 95:18687.
35. Haynes JM, Stephens GL. 2007. Tropical oceanic cloudiness and the incidence of precipitation: Early results from CloudSat. Geophys Res Lett. 34:L09811.
36. Hendon HH, Woodberry K. 1993. The diurnal cycle of tropical convection. J Geophys Res. 98:16623.
37. Hirose M, Nakamura K. 2005. Spatial and diurnal variation of precipitation systems over Asia observed by the TRMM Precipitation Radar. J Geophys Res. 110:D05106.
38. Hou AY, Kakar RK, Neeck S, Azarbarzin AA, Kummerow CD, Kojima

M, Oki R, Nakamura K, Iguchi T. 2014. The Global Precipitation Measurement Mission. Bull Am Meteorol Soc. 95:701–722.

39. Houze RA. 1982. Cloud Clusters and Large-Scale Vertical Motions in the Tropics. J Meteorol Soc Japan. 60.
40. Houze RA. 1989. Observed structure of mesoscale convective systems and implications for large-scale heating. Q J R Meteorol Soc. 115:425–461.
41. Houze RA, Wilton DC, Smull BF. 2007. Monsoon convection in the Himalayan region as seen by the TRMM Precipitation Radar. Q J R Meteorol Soc. 133:1389–1411.
42. Hoyos CD, Webster PJ. 2007. The Role of Intraseasonal Variability in the Nature of Asian Monsoon Precipitation. J Clim. 20:4402–4424.
43. Huffman GJ. 2016. The Transition in Multi-Satellite Products from TRMM to GPM (TMPA to IMERG). available at: https://pmm.nasa.gov/sites/default/files/document_files/ TMPA-to-IMERG_transition.pdf.
44. Huffman GJ, Adler RF, Bolvin DT, Gu G, Nelkin EJ, Bowman KP, Hong Y, Stocker EF, Wolff DB. 2007. The TRMM Multisatellite Precipitation Analysis (TMPA): Quasi-Global, Multiyear, Combined-Sensor Precipitation Estimates at Fine Scales. J Hydrometeorol. 8:38–55.
45. Imaoka K, Spencer RW. 2000. Diurnal Variation of Precipitation over the Tropical Oceans Observed by TRMM/TMI Combined with SSM/I. J Clim. 13:4149–4158.
46. Janowiak JE, Arkin PA, Morrissey M. 1994. An Examination of the Diurnal Cycle in Oceanic Tropical Rainfall Using Satellite and In Situ Data. Mon Weather Rev. 122:2296–2311.
47. Jiang X, Li T, Wang B. 2004. Structures and Mechanisms of the

Northward Propagating Boreal Summer Intraseasonal Oscillation. J Clim. 17:1022–1039.

48. Joshi UR, Rajeevan M. 2006. Trends in precipitation extremes over India. National Climate Centre (NCC) Research Report No. 3. Tech Rep 3, Natl Clim Centre, India Met Dep Pune.:1–25.
49. Kaila VK, Kirankumar AS, Sundaramurthy TK, Ramakrishnan S, Prasad MYS, Desai PS, Jayaraman V, Manikiam B. 2002. METSAT – a unique mission for weather and climate. Curr Sci. 83:1081–1088.
50. Kalnay E, Kanamitsu M, Kistler R, Collins W, Deaven D, Gandin L, Iredell M, Saha S, White G, Woollen J, et al. 1996. The NCEP/NCAR 40-Year Reanalysis Project. Bull Am Meteorol Soc. 77:437–471.
51. Kang I-S, Ho C-H, Lim Y-K, Lau K-M. 1999. Principal Modes of Climatological Seasonal and Intraseasonal Variations of the Asian Summer Monsoon. Mon Weather Rev. 127:322–340.
52. Kidd C, Levizzani V, Bauer P. 2009. A review of satellite meteorology and climatology at the start of the twenty-first century. Prog Phys Geogr. 33:474–489.
53. Kidder SQ, Vonder Haar TH. 1995. Satellite meteorology : an introduction. Academic Press.
54. Kiehl JT, Trenberth KE. 1997. Earth's Annual Global Mean Energy Budget. Bull Am Meteorol Soc. 78:197–208.
55. King MD, Platnick S, Menzel WP, Ackerman SA, Hubanks PA. 2013. Spatial and Temporal Distribution of Clouds Observed by MODIS Onboard the Terra and Aqua Satellites. IEEE Trans Geosci Remote Sens. 51:3826–3852.
56. Kripalani RH, Kulkarni A, Sabade SS, Revadekar J V., Patwardhan SK, Kulkarni JR. 2004. Intra-seasonal oscillations during monsoon 2002 and

2003. Curr Sci. 87:325–331.

57. Krishnamurthy CKB, Lall U, Kwon H-H. 2009. Changing Frequency and Intensity of Rainfall Extremes over India from 1951 to 2003. J Clim. 22:4737–4746.
58. Krishnamurthy V, Kirtman BP. 2003. Variability of the Indian Ocean: Relation to monsoon and ENSO. Q J R Meteorol Soc. 129:1623–1646.
59. Krishnamurthy V, Shukla J. 2000. Intraseasonal and Interannual Variability of Rainfall over India. J Clim. 13:4366–4377.
60. Krishnamurthy V, Shukla J. 2007. Intraseasonal and Seasonally Persisting Patterns of Indian Monsoon Rainfall. J Clim. 20:3–20.
61. Krishnamurthy V, Shukla J. 2008. Targeted Training Activity: Seasonal Predictability in Tropical Regions to be followed by Workshop on Multi-scale Predictions of the Asian and African Summer Monsoon Seasonal persistence and propagation of intraseasonal patterns over the Indian monsoon re. Clim Dyn. 30.
62. Krishnamurti TN, Ardanuy P. 1980. The 10 to 20-day westward propagating mode and "Breaks in the Monsoons." Tellus. 32:15–26.
63. Krishnamurti TN, Bhalme HN. 1976. Oscillations of a Monsoon System. Part I. Observational Aspects. J Atmos Sci. 33:1937–1954.
64. Krishnamurti TN, Kishtawal CM. 2000. A Pronounced Continental-Scale Diurnal Mode of the Asian Summer Monsoon. Mon Weather Rev. 128:462.
65. Krishnamurti TN, Subrahmanyam D. 1982. The 30–50 Day Mode at 850 mb During MONEX. J Atmos Sci. 39:2088–2095.
66. Krishnan R, Zhang C, Sugi M. 2000. Dynamics of Breaks in the Indian Summer Monsoon. J Atmos Sci. 57:1354–1372.
67. Kulkarni, P. L., Talwalkar, D. R., Nair, S., Rajamani S. 1993. Estimation

of divergent wind from OLR data for use in objective analysis over the Indian region. Mausam. 44:77–84.

68. Kulkarni PL, Mitra AK, Narkhedkar SG, Bohra AK, Rajamani S. 1997. On the impact of divergent part of the wind computed from INSAT OLR data on global analysis and forecast fields. Meteorol Atmos Phys. 64:61–82.
69. Kumar KK, Rajagopalan B, Cane MA. 1999. On the weakening relationship between the Indian monsoon and ENSO. Science. 284:2156–9.
70. Kumar KK, Rajagopalan B, Hoerling M, Bates G, Cane M. 2006. Unraveling the Mystery of Indian Monsoon Failure during El Nino. Science (80- ). 314:115–119.
71. Kumar MRR, Devasthale A, Levy G, Sankar S, Bakan S, Grassl H. 2012. A multi-sensor climatological view of double ITCZs over the Indian Ocean. Int J Remote Sens. 33:2925–2936.
72. Kumar S, Hazra A, Goswami BN. 2014. Role of interaction between dynamics, thermodynamics and cloud microphysics on summer monsoon precipitating clouds over the Myanmar Coast and the Western Ghats. Clim Dyn. 43:911–924.
73. Kummerow C, Barnes W, Kozu T, Shiue J, Simpson J. 1998. The Tropical Rainfall Measuring Mission (TRMM) Sensor Package. J Atmos Ocean Technol. 15:809–817.
74. Lau K-H, Lau N-C. 1992. The Energetics and Propagation Dynamics of Tropical Summertime Synoptic-Scale Disturbances. Mon Weather Rev. 120:2523–2539.
75. Lau K-M, Yang GJ, Shen SH. 1988. Seasonal and Intraseasonal Climatology of Summer Monsoon Rainfall over Eeat Asia. Mon

Weather Rev. 116:18–37.

76. Lawrence DM, Webster PJ. 2001. Interannual Variations of the Intraseasonal Oscillation in the South Asian Summer Monsoon Region. J Clim. 14:2910–2922.
77. Lawrence DM, Webster PJ. 2002. The Boreal Summer Intraseasonal Oscillation: Relationship between Northward and Eastward Movement of Convection. J Atmos Sci. 59:1593–1606.
78. Linho, Wang B. 2002. The Time–Space Structure of the Asian–Pacific Summer Monsoon: A Fast Annual Cycle View. J Clim. 15:2001–2019.
79. Machado LAT, Desbois M, Duvel J-P. 1992. Structural Characteristics of Deep Convective Systems over Tropical Africa and the Atlantic Ocean. Mon Weather Rev. 120:392–406.
80. Machado LAT, Rossow WB, Guedes RL, Walker AW. 1998. Life Cycle Variations of Mesoscale Convective Systems over the Americas. Mon Weather Rev. 126:1630–1654.
81. Magagi R, Barros AP. 2004. Estimation of Latent Heating of Rainfall during the Onset of the Indian Monsoon Using TRMM PR and Radiosonde Data. J Appl Meteorol. 43:328–349.
82. Mahakur M, Prabhu A, Sharma AK, Rao VR, Senroy S, Singh R, Goswami BN. 2013. A high-resolution outgoing longwave radiation dataset from Kalpana-1 satellite during 2004–2012. Curr Sci. 105:1124–1133.
83. Mandke SK, Sahai AK, Shinde MA, Joseph S, Chattopadhyay R. 2007. Simulated changes in active/break spells during the Indian summer monsoon due to enhanced CO2 concentrations: assessment from selected coupled atmosphere–ocean global climate models. Int J Climatol. 27:837–859.

84. Mao J, Wu G. 2012. Diurnal variations of summer precipitation over the Asian monsoon region as revealed by TRMM satellite data. Sci China Earth Sci. 55:554–566.

85. Mapes BE, Houze RA. 1993. Cloud Clusters and Superclusters over the Oceanic Warm Pool. Mon Weather Rev. 121:1398–1416.

86. McGarry MM, Reed RJ. 1978. Diurnal Variations in Convective Activity and Precipitation during Phases II and III of GATE. Mon Weather Rev. 106:101–113.

87. Meenu S, Parameswaran K, Rajeev K. 2012. Role of sea surface temperature and wind convergence in regulating convection over the tropical Indian Ocean. J Geophys Res Atmos. 117: D14102, doi:10.1029/2011JD016947.

88. Meenu S, Rajeev K, Parameswaran K, Kumar A, Nair M, Nair AKM. 2010. Regional distribution of deep clouds and cloud top altitudes over the Indian subcontinent and the surrounding oceans. J Geophys Res. 115:D05205, doi:10.1029/2009JD011802.

89. Meenu S, Rajeev K, Parameswaran K, Suresh Raju C. 2007. Characteristics of the double intertropical convergence zone over the tropical Indian Ocean. J Geophys Res. 112:D11106, doi:10.1029/2006JD007950.

90. Murakami M. 1983. Analysis of the Deep Convective Activity over the Western Pacific and Southeast Asia Part I: Diurnal Variation. J Meteorol Soc Japan. 61: 60-76.

91. Nair AKM, Rajeev K, Sijikumar S, Meenu S. 2011. Characteristics of a persistent pool of inhibited cloudiness and its genesis over the Bay of Bengal associated with the Asian summer monsoon. Ann Geophys. 29:1247–1252.

92. Nesbitt SW, Zipser EJ. 2003. The Diurnal Cycle of Rainfall and Convective Intensity according to Three Years of TRMM Measurements. J Clim. 16:1456–1475.
93. Nio T, Saito S, Stocker EF, Pawloski JH, Murayama Y, Ohata T. 2015. Tropical Rainfall Measurement Mission (TRMM) Operation Summary. Technical Report: https://ntrs.nasa.gov/archive/nasa/casi.ntrs.nasa.gov/20150022471.pdf.
94. Nitta T, Sekine S. 1994. Diurnal Variation of Convective Activity over the Tropical Western Pacific. J Meteorol Soc Japan Ser II. 72:627–641.
95. Ohsawa T, Ueda H, Hayashi T, Watanabe A, Matsumoto J. 2001. Diurnal Variations of Convective Activity and Rainfall in Tropical Asia. J Meteorol Soc Japan. 79:333–352.
96. Pai DS, Rajeevan M. 1998. Clouds and cloud radiative forcing over tropical Indian Ocean and their relationship with sea surface temperature. Curr Sci. 75:372–381.
97. Pai DS, Sridhar L, Rajeevan M, Sreejith OP, Satbhai NS, Mukhopadhyay B. 2014. Development of a new high spatial resolution (0.25° × 0.25°) long period (1901-2010) daily gridded rainfall data set over India and its comparison with existing data sets over the region. Mausam. 65:1–18.
98. Pant GB, Parthasarathy B. 1981. Some aspects of an association between the southern oscillation and Indian summer monsoon. Arch Meteorol Geophys Bioclimatol Ser B. 29:245–252.
99. Patil SD, Yadav RK. 2005. Large-scale changes in the cloud radiative forcing over the Indian region. Atmos Environ. 39:4609–4618.
100. Pokhrel S, Sikka DR. 2013. Variability of the TRMM-PR total and convective and stratiform rain fractions over the Indian region during

the summer monsoon. Clim Dyn. 41:21–44.

101. Prasad B. 1970. Diurnal variation of rainfall in India. Indian J Meteorol Geophys. 21:443–450.
102. Prasad B. 1974. Diurnal variation of rainfall in Bhrahmaputhra valley. Indian J Meteorol Geophys. 25:245–250.
103. Pruppacher HR and Klett JD. 1980. Microphysics of Clouds and Precipitation. Book: D Reidel Publishing Company, ISBN: 978-90-277-1106-9., springer.com. doi: 10.1007/978-94-009-9905-3.
104. Puranik DM, Karekar RN, Puranik DM, Karekar RN. 2006. Precursors to Convection over Peninsular India during March–May in AMSU-B Data. Weather Forecast. 21:781–801.
105. Raghavan K. 1973. Break-Monsoon over India. Mon Weather Rev. 101:33–43.
106. Rajeevan M, Bhate J. 2009. A high resolution daily gridded rainfall dataset (1971–2005) for mesoscale meteorological studies. Curr Sci. 96:558–562.
107. Rajeevan M, Bhate J, Jaswal AK. 2008. Analysis of variability and trends of extreme rainfall events over India using 104 years of gridded daily rainfall data. Geophys Res Lett. 35:L18707.
108. Rajeevan M, Bhate J, Kale JD, Lal B. 2006. High resolution daily gridded rainfall data for the Indian region: Analysis of break and active monsoon spells. Curr Sci. 91:296–306.
109. Rajeevan M, Gadgil S, Bhate J. 2010. Active and break spells of the Indian summer monsoon. J Earth Syst Sci. 119:229–247.
110. Rajeevan M, Rohini P, Niranjan Kumar K, Srinivasan J, Unnikrishnan CK. 2013. A study of vertical cloud structure of the Indian summer monsoon using CloudSat data. Clim Dyn. 40:637–650.

111. Rajeevan M, Srinivasan J. 2000. Net Cloud Radiative Forcing at the Top of the Atmosphere in the Asian Monsoon Region. J Clim. 13:650–657.
112. Ramage C. 1971. Monsoon Meteorology, in International Geophysical Series. Vol 15: 296. Academic Press, San Diego, California.
113. Ramamurthy K. 1969. Monsoons of India : Some Aspects of the Break in the Indian Southwest Monsoon during July and August. Forecast Manual 1-57, No. IV 18.3, India Met Dept 1969.
114. Ramanathan V, Cess RD, Harrison EF, Minnis P, Barkstrom BR, Ahmad E, Hartmann D. 1989. Cloud-Radiative Forcing and Climate: Results from the Earth Radiation Budget Experiment. Science (80- ). 243:57–63.
115. Rao YP. 1976. Meteorological Monograph Synoptic Meteorology No. 1 /1976 Southwest Monsoon. 1–365.
116. Rao AVRK, Rao VR. 1992. Diurnal variation of cloudiness during south-west monsoon season using INSAT-1B radiance data. Mausam. 4:127–134.
117. Rasmusson EM, Carpenter TH. 1982. Variations in Tropical Sea Surface Temperature and Surface Wind Fields Associated with the Southern Oscillation/El Niño. Mon Weather Rev. 110:354–384.
118. Rickenbach TM, Rutledge SA. 1998. Convection in TOGA COARE: Horizontal Scale, Morphology, and Rainfall Production. J Atmos Sci. 55:2715–2729.
119. Roca R, Louvet S, Picon L, Desbois M. 2005. A study of convective systems, water vapor and top of the atmosphere cloud radiative forcing over the Indian Ocean using INSAT-1B and ERBE data. Meteorol Atmos Phys. 90:49–65.
120. Roca R, Ramanathan V. 2000. Scale Dependence of Monsoonal

Convective Systems over the Indian Ocean. J Clim. 13:1286–1298.

121. Roca R, Viollier M, Picon L, Desbois M. 2002. A multisatellite analysis of deep convection and its moist environment over the Indian Ocean during the winter monsoon. J Geophys Res. 107:8012.
122. Rodwell MJ. 1997. Breaks in the Asian Monsoon: The Influence of Southern Hemisphere Weather Systems. J Atmos Sci. 54:2597–2611.
123. Rogers R, Yau M. 1979. A short course in cloud physics. Butterworth-Heinemann, Oxford UK.
124. Ropelewski CF, Halpert MS. 1987. Global and Regional Scale Precipitation Patterns Associated with the El Niño/Southern Oscillation. Mon Weather Rev.
125. Rossow, W. B., Schiffer, R. A. 1999. Advances in Understanding Clouds from ISCCP. Bull Am Meteorol Soc. 80:2261–2287.
126. Rossow WB, Dueñas EN. 2004. The International Satellite Cloud Climatology Project (ISCCP) Web Site An Online Resource for Research. Bull Am Meteorol Soc. 85:167–176.
127. Rossow WB, Garder LC. 1993. Cloud Detection Using Satellite Measurements of Infrared and Visible Radiances for ISCCP. J Clim. 6:2341–2369.
128. Rossow WB, Schiffer RA. 1991. ISCCP Cloud Data Products. Bull Am Meteorol Soc. 72:2–20.
129. Sabin TP, Babu CA, Joseph P V. 2013. SST-convection relation over tropical oceans. Int J Climatol. 33:1424–1435.
130. Sadler JC. 1975. The Monsoon Circulation and Cloudiness over the GATE Area. Mon Weather Rev. 103:369–387.
131. Saha K. 1972. Double intertropical convergence zone in the Indian ocean : act or fiction? J Mar Biol Assoc India. 14:758–766.

132. Saha K. 1971. Mean cloud distributions over tropical oceans. Tellus. 23:183–195.
133. Sahany S, Venugopal V, Nanjundiah RS. 2010. Diurnal-scale signatures of monsoon rainfall over the Indian region from TRMM satellite observations. J Geophys Res. 115:D02103.
134. Samala BK, Krishnan R. 2008. Cloud-radiative impacts on the tropical Indian Ocean associated with the evolution of “monsoon breaks.” Int J Climatol. 28:205–217.
135. Sathiyamoorthy V, Pal PK, Joshi PC. 2004. Influence of the Upper-Tropospheric Wind Shear upon Cloud Radiative Forcing in the Asian Monsoon Region. J Clim. 17:2725–2735.
136. Schiffer RA, Rossow WB. 1983. The International Satellite Cloud Climatology Project (ISCCP): The First Project of the World Climate Research Programme. Bull Am Meteorol Soc. 64:779–784.
137. Schumacher C, Houze RA. 2003. Stratiform Rain in the Tropics as Seen by the TRMM Precipitation Radar. J Clim. 16:1739–1756.
138. Sengupta D, Ravichandran M. 2001. Oscillations of Bay of Bengal sea surface temperature during the 1998 summer monsoon. Geophys Res Lett. 28:2033–2036.
139. Shah S, Rao BM, Kumar P, Pal PK. 2010. Verification of cloud cover forecast with INSAT observation over western India. J Earth Syst Sci. 119:775–781.
140. Shin K-S, North GR, Ahn Y-S, Arkin PA. 1990. Time Scales and Variability of Area-Averaged Tropical Oceanic Rainfall. Mon Weather Rev. 118:1507–1516.
141. Short DA, Nakamura K. 2000. TRMM Radar Observations of Shallow Precipitation over the Tropical Oceans. J Clim. 13:4107–4124.

142. Shukla J. 1987. Interannual Variability of Monsoons. In: Jay S Fein and Pamela L Stephens, editor. MONSOONS. John Wiley and Sons; p. 399–464.
143. Sikka DR. 1980. Some aspects of the large scale fluctuations of summer monsoon rainfall over India in relation to fluctuations in the planetary and regional scale circulation parameters. J Earth Syst Sci. 89:179–195.
144. Sikka DR, Gadgil S. 1980. On the Maximum Cloud Zone and the ITCZ over Indian, Longitudes during the Southwest Monsoon. Mon Weather Rev. 108:1840–1853.
145. Singh D, Gopalakrishnan V, Singh RP, Kamra AK, Singh S, Pant V, Singh R, Singh AK. 2007. The atmospheric global electric circuit: An overview. Atmos Res. 84:91–110.
146. Smith GL, Green RN, Raschke E, Avis LM, Suttles JT, Wielicki BA, Davies R. 1986. Inversion methods for satellite studies of the Earth's Radiation Budget: Development of algorithms for the ERBE Mission. Rev Geophys. 24:407.
147. Sorooshian S, Gao X, Hsu K, Maddox RA, Hong Y, Gupta H V. 2002. Diurnal Variability of Tropical Rainfall Retrieved from Combined GOES and TRMM Satellite Information. J Clim. 15:983–1001.
148. Srinivasan, J. ; Joshi PC. 2007. What have we learned about the Indian monsoon from satellite data? Curr Sci. 93:165–172.
149. Srinivasan V. 1968. Some aspects of broad scale cloud distribution over the Indian Ocean during the Indian south west monsoon. Indian J Meteorol Geophys. 19:39–54.
150. Stano G, Krishnamurti TN, Kumar TSVV, Chakraborthy A. 2002. Hydrometeor structure of a composite monsoon depression using the TRMM radar. Tellus A. 54:370–381.

151. Stubenrauch, C. J., S. Kinne, and GEWEX Cloud Assessment Team, 2009. Evaluation of global cloud data products, *Global Energy and Water Cycle Experiment News*, 19(1), 6–7.
152. Stubenrauch, C. J., W. B. Rossow and Kinne S. 2012. Assessment of global cloud datasets from satellites: A project of the World Climate Research Programme Global Energy and Water Cycle Experiment (GEWEX) Radiation Panel. WCRP Rep 23.:176.
153. Suhas E, Neena J M, Goswami B N. 2013. An Indian monsoon intraseasonal oscillations (MISO) index for real time monitoring and forecast verification. Clim Dyn. 40:2605–2616.
154. Sui C-H, Lau K-M, Takayabu YN, Short DA. 1997. Diurnal Variations in Tropical Oceanic Cumulus Convection during TOGA COARE. J Atmos Sci. 54:639–655.
155. Sunilkumar SV, Parameswaran K, Rajeev K, Krishna Murthy BV, Meenu S, Mehta SK, Babu A. 2010. Semitransparent cirrus clouds in the tropical tropopause layer during two contrasting seasons. J Atmos Solar-Terrestrial Phys. 72:745–762.
156. Tao W-K, Lang S, Olson WS, Meneghini R, Yang S, Simpson J, Kummerow C, Smith E, Halverson J. 2001. Retrieved Vertical Profiles of Latent Heat Release Using TRMM Rainfall Products for February 1988. J Appl Meteorol. 40:957–982.
157. Tao W-K, Lang S, Simpson J, Sui C-H, Ferrier B, Chou M-D, Tao W-K, Lang S, Simpson J, Sui C-H, et al. 1996. Mechanisms of Cloud-Radiation Interaction in the Tropics and Mid latitudes. J Atmos Sci. 53:2624–2651.
158. Tao W-K, Smith EA, Adler RF, Haddad ZS, Hou AY, Iguchi T, Kakar R, Krishnamurti TN, Kummerow CD, Lang S, et al. 2006. Retrieval of

Latent Heating from TRMM Measurements. Bull Am Meteorol Soc. 87:1555–1572.

159. Thies B, Bendix J. 2011. Review Satellite based remote sensing of weather and climate: recent achievements and future perspectives. Meteorol Appl. 18:262–295.
160. Thompson RM, Payne SW, Recker EE, Reed RJ. 1979. Structure and Properties of Synoptic-Scale Wave Disturbances in the Intertropical Convergence Zone of the Eastern Atlantic. J Atmos Sci. 36:53–72.
161. Tian B, Soden BJ, Wu X. 2004. Diurnal cycle of convection, clouds, and water vapor in the tropical upper troposphere: Satellites versus a general circulation model. J Geophys Res. 109:D10101.
162. Trenberth KE, Fasullo JT, Kiehl J. 2009. Earth's Global Energy Budget. Bull Am Meteorol Soc. 90:311–324.
163. Varikoden H, Samah AA, Babu CA. 2010. Spatial and temporal characteristics of rain intensity in the peninsular Malaysia using TRMM rain rate. J Hydrol. 387:312–319.
164. Vijaykumar P, Abhilash S, Santhosh KR, Mapes BE, Suvarchal Kumar C, Hu I-K. 2017. Distribution of cloudiness and categorization of rainfall types based on INSAT IR brightness temperatures over Indian subcontinent and adjoining oceanic region during south west monsoon season. J Atmos Solar-Terrestrial Phys. 161:76–82.
165. Waliser DE, Lau KM, Stern W, Jones C. 2003. Potential Predictability of the Madden–Julian Oscillation. Bull Am Meteorol Soc. 84:33–50.
166. Wang B, Webster PJ, Teng H. 2005. Antecedents and self-induction of active-break south Asian monsoon. Geophys Res Lett. 32:L04704.
167. Wang B, Xie X. 1997. A Model for the Boreal Summer Intraseasonal Oscillation. J Atmos Sci. 54:72–86.

168. Webster PJ, Magaña VO, Palmer TN, Shukla J, Tomas RA, Yanai M, Yasunari T. 1998. Monsoons: Processes, predictability, and the prospects for prediction. J Geophys Res Ocean. 103:14451–14510.
169. Webster PJ. 1983. Mechanisms of Monsoon Low-Frequency Variability: Surface Hydrological Effects. J Atmos Sci. 40:2110–2124.
170. Wonsick MM, Pinker RT, Govaerts Y. 2009. Cloud Variability over the Indian Monsoon Region as Observed from Satellites. J Appl Meteorol Climatol. 48:1803–1821.
171. Xie S-P, Xu H, Saji NH, Wang Y, Liu WT. 2006. Role of Narrow Mountains in Large-Scale Organization of Asian Monsoon Convection. J Clim. 19:3420–3429.
172. Yang G-Y, Slingo J. 2001. The Diurnal Cycle in the Tropics. Mon Weather Rev. 129:784–801.
173. Yang J, Gong P, Fu R, Zhang M, Chen J, Liang S, Xu B, Shi J, Dickinson R. 2013. The role of satellite remote sensing in climate change studies. Nat Clim Chang. 3:875–883.
174. Yang S, Smith EA. 2006. Mechanisms for Diurnal Variability of Global Tropical Rainfall Observed from TRMM. J Clim. 19:5190–5226.
175. Yasunari T. 1979. Cloudiness fluctuations associated with the northern hemisphere summer monsoon. J meteorlogical Soc Japan. 57:227–242.
176. Zuidema P. 2003. Convective Clouds over the Bay of Bengal. Mon Weather Rev. 131:780–798.
177. Zuluaga MD, Hoyos CD, Webster PJ. 2009. Spatial and Temporal Distribution of Latent Heating in the South Asian Monsoon Region. J Clim. 23:2010–2029.